

Aus dem

Universitätsklinikum Düsseldorf

Institut für Diagnostische und Interventionelle Radiologie

(Direktor: Univ.-Prof. Dr. med. Gerald Antoch)

**Automatisierte Erfassung, Analyse und Optimierung von Untersuchungs- und
Dosisparametern der Computertomographie im Hinblick auf die
Patientenkonstitution sowie diagnostische Referenzwerte**

Habilitationsschrift zur Erlangung der venia legendi für

das Fach Radiologie des Fachbereichs Medizin

der Heinrich-Heine Universität Düsseldorf

vorgelegt von

Dr. med. Johannes Boos

Juni 2018

Inhaltsverzeichnis

1. Kurze Zusammenfassung	5
2. Literaturangaben der zugrunde liegenden Forschungsarbeiten.....	11
3. Ausführliche Zusammenfassung und Diskussion	13
a. Einleitung	13
b. Untersuchungen und Ergebnisse	19
c. Diskussion.....	35
d. Ausblick.....	44
e. Literaturverzeichnis	45
4. Danksagung.....	58
5. Zugrunde liegende Forschungsarbeiten	60

Abkürzungen

AAPM	American Association of Physicists in Medicine
ACR	American College of Radiologists
ALARA	„as low as reasonably achievable“
BfS	Bundesamt für Strahlenschutz
BMI	Body Mass Index
CNR	Kontrast zu Rausch Verhältnis
CT	Computertomographie
CTDIvol	volumetrischer Computertomographie Dosisindex
Deff	effektiver Durchmesser
DICOM	Digital Imaging and Communications in Medicine
DICOM-RDSR	Digital Imaging and Communications in Medicine Radiation Dose Structured Report
DLP	Dosislängenprodukt
DMS	Dosismanagementsystem
DRW	Diagnostische Referenzwerte
Dw	Wasseräquivalenter Durchmesser
EUCLID	European Study on Clinical Diagnostic Reference Levels
ESR	Europäische Röntgengesellschaft
MPPS	Modality Performed Procedure Steps

OSDR	Organspezifische Dosisreduktion
SimDS	Simultane Dual-source CT
SNR	Signal zu Rausch Verhältnis
SpiralDs	Dual-source CT im Spiral Modus
SSDE	Größenspezifische Dosisabschätzungen

1. Kurze Zusammenfassung

Die vorliegende Habilitationsschrift zeigt neue Ansätze zur Erfassung und systematischen Auswertung von Dosisdaten in der Computertomographie (CT) auf und untersucht verschiedene Techniken, die zur Dosisoptimierung von CT Untersuchungen genutzt werden können.

Die CT hat eine große Bedeutung in der modernen Medizin und dient als diagnostische Methode der ersten Wahl zur Beantwortung einer großen Anzahl an Fragestellungen. Hierzu gehört die Evaluation der Lungen, der parenchymatösen Abdominalorgane, der Gefäße und der ableitenden Harnwege. Auch in der Notfalldiagnostik spielt die CT eine große Rolle, so z.B. zur Beurteilung von Traumafolgen und im Rahmen der Schlaganfalldiagnostik. Die Bildgebung mittels CT macht lediglich 8% der diagnostischen medizinischen Untersuchungen mit Röntgenstrahlen in Deutschland aus, ist jedoch für 60% der medizinischen Strahlenexposition verantwortlich (1).

Grundlage der CT ist die Röntgenstrahlung, welche das menschliche Erbgut schädigen und so das Tumorrisiko erhöhen kann (2). Deshalb ist neben einer Überprüfung und genauen Indikationsstellung von CT Untersuchungen eine Optimierung der Strahlendosis jeder einzelnen CT Untersuchung von großer Bedeutung. Hierbei können automatische und semiautomatische technische Hilfsmittel verwendet werden. Neuartige Möglichkeiten der automatischen Erfassung und Auswertung von CT Dosisdaten ermöglichen weiterhin das Erkennen von Dosisoptimierungspotenzial.

Im Rahmen der ersten Studie wurde eine organspezifische Dosisreduktionstechnik (OSDR; XCare, Siemens, Forchheim) bei der Thorax CT von Kindern untersucht (1.

Arbeit). Bei der Spiral CT wird durch die OSDR Technik ventral die Dosis reduziert und entsprechend dorsal erhöht. Da die radiosensiblen Organe wie die Schilddrüse, die Augenlinsen und das Brustdrüsenparenchym ventral im Körper liegen, führt diese Modulation zu einer geringeren Organdosis, die Gesamtdosis der Untersuchung verändert sich nicht. In der vorgelegten ersten Arbeit konnte demonstriert werden, dass die Dosismodulation der OSDR Technik bei Thorax CT Untersuchungen von pädiatrischen Patienten keinen negativen Einfluss auf die Bildqualität hat.

Neben der Lage der radiosensiblen Organe im Körper hat auch der Körperhabitus eine große Bedeutung für die Dosis von CT Untersuchungen. Zur dezidierten Beurteilung der Dosisparameter von CT Untersuchungen im Rahmen einer Qualitätssicherung sind zunächst eine vollständige Erfassung der CT Dosisdaten sowie eine umfangreiche Auswertung notwendig.

In der 2. vorgelegten Arbeit wurde ein neuartiger strukturierter Dosisbericht aus dem Digital Imaging and Communications in Medicine (DICOM) Standard (DICOM-structured radiation dose report, DICOM-RDSR) genutzt, um die CT Strahlenexposition bei Untersuchungen des Abdomens von erwachsenen Patienten auszuwerten und die Abhängigkeit der Dosisexposition vom Body Mass Index (BMI) der Patienten zu evaluieren. Hier konnte gezeigt werden, dass eine automatische Erfassung sowie eine umfangreiche Auswertung großer Dosisdaten mit dem DICOM-RDSR möglich ist. Weiterhin wurde nachgewiesen, dass die Dosis der CT Untersuchungen des Abdomens mit steigendem BMI deutlich zunimmt.

In der 3. Arbeit wurde eine automatisierte Methode basierend auf dem DICOM-RDSR zur Erfassung und Auswertung von CT Dosisdaten anhand der aktuellen deutschen diagnostischen Referenzwerte des Bundesamtes für Strahlenschutz (BfS) evaluiert. Die Entwicklung und Evaluation dieser cloud-basierten Methode erfolgte in

Zusammenarbeit mit der Firma Pulmokard (Herdecke). Es konnte anhand der Auswertung der Dosisparameter von 36523 Untersuchungen gezeigt werden, dass die CT Dosisexposition im Institut für Diagnostische und Interventionelle Radiologie des Uniklinikums Düsseldorf 52,8% des volumetrischen Computertomographie Dosisindex (CTDIvol) Referenzwertes und 51,3% des Dosislängenprodukts (DLP) Referenzwertes betrug.

Die traditionell zur Dokumentation und Auswertung der CT Dosis verwendeten Werte des CTDIvol und DLP basieren auf Phantommessungen. Die verwendeten Phantome haben einen Durchmesser von 16 und 32 cm. Bei einer Abweichung der Patientengröße von der Phantomgröße sind die angezeigten Dosiswerte inakkurat. Deshalb wurde von der American Association of Physicists in Medicine (AAPM) das Konzept der Größenspezifischen Dosisabschätzungen („size-specific dose estimates“, SSDE) eingeführt. Hierbei wird der Patientendurchmesser für die Berechnung des SSDE Wertes herangezogen.

In der 4. Arbeit wurde die Genauigkeit des Körpergewichts und des BMIs als Surrogatparameter für den Patientendurchmesser zur Berechnung der SSDE untersucht. Es konnte gezeigt werden, dass der BMI und das Körpergewicht zur SSDE Berechnung genutzt werden können und die mittlere Differenz zur Verwendung des Patientendurchmessers 4,2% beträgt. Zusätzlich wurde gezeigt, dass die Verwendung des BMI in der Abdominal CT zu einer höheren Genauigkeit des SSDE Wertes führt als das Körpergewicht.

Die Bildqualität und die Dosis von CT Untersuchungen werden durch verschiedene Faktoren beeinflusst, hierzu zählen die Röhrenspannung, das Röhrenstrom-Zeit-Produkt, der Bildrekonstruktionsalgorithmus und die Kontrastmittelmenge. Zur Dosisoptimierung können diese Faktoren an die Patientenkonstitution angepasst

werden. Insbesondere der Reduktion der Röhrenspannung bei Kontrastmittelgestützten Untersuchungen kommt auf Grund der k-Kante von Iod eine große Bedeutung zu (3).

Die 5. vorgelegte Arbeit evaluiert ein neuartiges Niedrigdosis CT Angiographie Protokoll zur Beurteilung der Aorta bei Patienten mit einem BMI unter 32 kg/m^2 . Während traditionell CT Angiographie Untersuchungen der Aorta mit einer Röhrenspannung von 120 kVp oder 100 kVp untersucht wurden, verwendet das neuartige Protokoll eine Röhrenspannung von 80 kVp in Kombination mit automatischer Röhrenstrommodulation und iterativer Bildrekonstruktion. Das 80 kVp Protokoll wurde mit einem 100 kVp Protokoll verglichen und führte zu einer diagnostischen Bildqualität bei gleichzeitiger Reduktion des Dosislängenproduktes um bis zu 50%.

Neben den oben genannten Untersuchungsparametern bietet die dual-source CT weitere Möglichkeiten zur Dosisoptimierung. Dual-source CT Geräte besitzen zwei Röntgenröhren und zwei Detektoren. Diese können parallel betrieben werden, wodurch die Röhrenspannung und damit auch die Kontrastmittelmenge weiter reduziert werden kann. Eine Dosisoptimierung der Untersuchungen ist so möglich.

In der 6. vorgelegten Arbeit wurde der simultane dual-source CT Modus bei Patienten mit Verdacht auf Lungenarterienembolie untersucht. Die Machbarkeit und Bildqualität des neuartigen CT Protokolls mit 70 kVp und einer reduzierten Kontrastmittelmenge von 40 ml wurde untersucht und mit einem dual-source Spiral-CT mit hohem Pitchfaktor und 70 ml Kontrastmittel verglichen. Es konnte gezeigt werden, dass der neuartige Modus mit nur 40 ml Kontrastmittel bei Patienten mit einem BMI von unter 35 kg/m^2 durchgeführt werden kann und zu diagnostisch

verwendbaren Bildern führt. Das Dosislängenprodukt der Untersuchung kann so um bis zu 50% reduziert werden.

Die Anwendung der untersuchten Dosisoptimierungsmethoden muss immer auf die Patientenkonstitution abgestimmt sein damit eine diagnostische Bildqualität gewährleistet werden kann. Zwar ist die Verwendung des BMI oder des Patientengewichts zur Berechnung des SSDE Wertes möglich, die akkurateste Methode zur Ermittlung ist jedoch die Messung des wasseräquivalenten Patientendurchmessers (Dw). Hierzu muss zunächst in jeder Schicht des CT Untersuchungsvolumens der Dw ermittelt werden. Anschließend wird der SSDE Wert jeder Schicht ermittelt und dann der Mittelwert des Untersuchungsvolumens gebildet. Diese Berechnung ist aufwendig und rechenintensiv.

In der 7. Arbeit wurde deshalb untersucht, ob die Verwendung des Dw der mittleren Schicht des Untersuchungsvolumens zusammen mit dem mittleren CTDIvol der Gesamtuntersuchung zu einer ausreichenden Genauigkeit der SSDE Berechnung führt. Hierfür wurde zunächst ein Programm entwickelt, welches den Dw und die SSDE jeder Untersuchungsschicht automatisch berechnet. Anhand der Evaluation von 1812 CT Serien des Thorax und Abdomens konnte gezeigt werden, dass der mittlere Fehler dieser Methode bei 2 – 5% liegt. Jedoch ist die Genauigkeit abhängig von der Patientengröße mit Dosisunterschätzung bei übergewichtigen und Dosisunterschätzung bei schlanken Patienten. Um systematische Fehler zu vermeiden sollten daher Dw und SSDE, falls möglich und trotz höherem Rechenaufwand, aus allen Schichten des Untersuchungsvolumens berechnet werden.

Um Dosisoptimierungsprozesse durchzuführen sowie zur Einschätzung der CT Dosisanwendungen sind diagnostische Referenzwerte (DRW) hilfreich. Die vom BfS

bereitgestellten Referenzwerte basieren auf einem Standardpatienten mit 70 kg. Für diesen Standardpatienten werden für verschiedenen diagnostische CT Untersuchungen Referenzwerte als CTDIvol und DLP bereitgestellt. Der Einsatz dieser Referenzwerte bei unter- oder übergewichtigen Patienten ist limitiert.

In der 8. Arbeit wurden daraufhin institutionelle diagnostische Referenzwerte basierend auf dem wasseräquivalenten Durchmesser der Patienten und dem SSDE Konzept entwickelt. Es konnte gezeigt werden, dass die Implementierung von DRWs basierend auf dem Dw und SSDE in der CT des Thorax und des Abdomens machbar ist und es einen linearen Zusammenhang zwischen dem Dw und dem SSDE der Patienten gibt. Anhand der gewonnenen Daten kann eine automatische, genauere Einordnung der Dosisparameter von CT Untersuchungen unter Berücksichtigung des Dw jedes Patienten erfolgen.

2. Literaturangaben der zugrunde liegenden Forschungsarbeiten

1. **Boos J**, Kröpil P, Klee D, Heusch P, Schimmöller L, Schaper J, Antoch G, Lanzman RS. Evaluation of the impact of organ-specific dose reduction on image quality in pediatric chest computed tomography. *Pediatr Radiol*. 2014 Sep;44(9):1065-9.

Impact Faktor (IF): 1,5

2. **Boos J**, Lanzman RS, Meineke A, Heusch P, Sawicki LM, Antoch G, Kröpil P. Dose monitoring using the DICOM structured report: assessment of the relationship between cumulative radiation exposure and BMI in abdominal CT. *Clin Radiol*. 2015 Feb;70(2):176-82.

Impact Faktor (IF): 2,1

3. **Boos J**, Meineke A, Rubbert C, Heusch P, Lanzman RS, Aissa J, Antoch G, Kröpil P. Cloud-Based CT Dose Monitoring using the DICOM-Structured Report: Fully Automated Analysis in Regard to National Diagnostic Reference Levels. *Rofo*. 2016 Mar;188(3):288-94.

Impact Faktor (IF): 1,6

4. **Boos J**, Lanzman RS, Heusch P, Aissa J, Schleich C, Thomas C, Sawicki LM, Antoch G, Kröpil P. Does body mass index outperform body weight as a surrogate parameter in the calculation of size-specific dose estimates in adult body CT? *Br J Radiol*. 2016;89(1059):20150734.

Impact Faktor (IF): 2,1

5. **Boos J**, Aissa J, Lanzman RS, Heusch P, Schimmöller L, Schleich C, Thomas C, Antoch G, Kröpil P. CT angiography of the aorta using 80 kVp in combination with sinogram-affirmed iterative reconstruction and automated tube current modulation: Effects on image quality and radiation dose. *J Med Imaging Radiat Oncol.* 2016 Apr;60(2):187-93.

Impact Faktor (IF): 1,2

6. **Boos J**, Kröpil P, Lanzman RS, Aissa J, Schleich C, Heusch P, Sawicki LM, Antoch G, Thomas C. CT pulmonary angiography: simultaneous low-pitch dual-source acquisition mode with 70 kVp and 40 ml of contrast medium and comparison with high-pitch spiral dual-source acquisition with automated tube potential selection. *Br J Radiol.* 2016 Jun;89(1062):20151059.

Impact Faktor (IF): 2,1

7. **Boos J**, Kröpil P, Bethge OT, Aissa J, Schleich C, Sawicki LM, Heinzler N, Antoch G, Thomas C. Accuracy of size-specific dose estimate calculation from center slice in computed tomography. *Radiat Prot Dosimetry.* 2017 May 25:1-12.

Impact Faktor (IF): 0,9

8. **Boos J**, Thomas C, Appel E, Klosterkemper Y, Schleich C, Aissa J, Bethge O, Antoch G, Kröpil P. Institutional computed tomography diagnostic reference levels based on water-equivalent diameter and size-specific dose estimates. *J Radiol Prot.* 2017 Dec 20, Epub.ahead of print

Impact Faktor (IF): 1,7

3. Ausführliche Zusammenfassung und Diskussion

3. a. Einleitung

Zur Bilderzeugung mittels Computertomographie (CT) werden Röntgenstrahlen verwendet. Diese können im Rahmen des stochastischen Strahlungsrisikos die DNA schädigen und das Tumorrisiko erhöhen (2). Die Anzahl der CT Untersuchungen hat in den letzten Jahrzehnten weltweit kontinuierlich zugenommen (4). CT Geräte sind heutzutage in breiter Masse verfügbar und die fortschreitende technische Entwicklung ermöglicht die Abklärung vielfältiger klinischer Fragestellung mittels CT. So ist die CT ein grundlegender Bestandteil der Notfalldiagnostik und ist wichtiger Bestandteil der Diagnostik bei verschiedenen onkologischen Fragestellungen wie z.B. dem Lungenkarzinom oder dem Pankreaskarzinom (5–7). Die inzwischen verfügbare hohe temporale Auflösung moderner CT Geräte ermöglicht die Untersuchung des Herzens (8). Die hohe räumliche Auflösung kann z.B. zur Darstellung von interstitiellen Lungenerkrankungen genutzt werden (9). Obwohl die Computertomographie in Deutschland nur 8% aller medizinischen Untersuchungen mit ionisierender Strahlung ausmacht ist sie für 60% der kollektiven Strahlendosis verantwortlich (1,10,11).

Im Sinne des „as low as reasonably achievable“ („ALARA“) Prinzips ist eine gewissenhafte Prüfung und Indikationsstellung von CT Untersuchungen durch den Radiologen von großer Bedeutung (12). Dies bedeutet weiterhin, dass jede einzelne CT Untersuchung, unter Berücksichtigung der jeweiligen Indikation im Hinblick auf die Strahlendosis optimiert werden muss. Hierbei können automatische und semiautomatische technische Hilfsmittel eingesetzt werden. Zusätzlich führen der technische Fortschritt und die fortwährende Entwicklungsarbeit zu immer

effizienteren CT Geräten. Während initiale CT Geräte lediglich eine Detektorzeile besaßen, enthalten moderne Geräte teilweise zwei Detektoren mit jeweils 256 Zeilen. Neben einer höheren räumlichen und zeitlichen Auflösung ermöglichen diese modernen Geräte kürzere Untersuchungszeiten und eine Strahlendosisoptimierung (13). Zusätzlich werden fortwährend neue Programme und Techniken zur Dosisoptimierung in moderne CT Geräte integriert, so sind beispielhaft zu nennen der „z-Springfokus“ (14), die Zinnfilterung (15), organspezifische Dosisreduktion (16), automatische Röhrenstrommodulation (17), automatische Röhrenspannungselektion (18) und die iterative Rekonstruktion (19).

Technische Hilfsmittel zur Dosisoptimierung

Die automatische Röhrenstrommodulation adaptiert das Röhrenstrom-Zeit-Produkt entlang der z-Achse des Untersuchungsvolumens. Die Anpassung erfolgt anhand von Dichtewerten, welche dem Planungsbild entnommen werden. So kann der Röhrenstrom bei Abschnitten mit niedriger Dichte, z.B. in der luftgefüllten Lunge, reduziert werden, ohne dass die Bildqualität beeinträchtigt wird (17,20).

Die automatische Röhrenspannungselektion ermittelt automatisch die optimale Röhrenspannung der Untersuchung. Hierzu wird ebenfalls das Planungsbild des Patienten analysiert und in Abhängigkeit der Untersuchungsindikation und der Patientenkonstitution eine optimale Röhrenspannung ausgewählt. Eine Reduktion der Röhrenspannung führt ebenfalls zu einer Dosisreduktion der Untersuchung, geht allerdings bei fehlenden weiteren Anpassungen mit einer Verschlechterung der Bildqualität einher (18). Auf Grund der k-Kante von Jod, welches Hauptbestandteil des CT-Kontrastmittels ist, führt eine geringere Röhrenspannung jedoch zu einer stärkeren photoelektrischen Absorption des Kontrastmittels und damit zu einem

höheren Kontrast (3). Dies kann insbesondere bei Gefäßdarstellungen genutzt werden (21).

Die organspezifische Dosisreduktion reduziert die Strahlendosis von ventral und gleicht dies kompensatorisch durch eine leicht erhöhte Dosis von dorsal aus (16). So wird die Gesamtdosis nicht reduziert, die Umverteilung reduziert jedoch die Strahlendosis der ventral gelegenen radiosensitiven Organe wie Augenlinse, Schilddrüse und Brustparenchym.

CT Bilder wurden seit den 1970er Jahren traditionell mit gefilterter Rückprojektion rekonstruiert. Die zunehmende Verfügbarkeit von Rechenkapazität durch moderne Computer hat die Einführung immer effektiverer iterative Rekonstruktionsalgorithmen ermöglicht (19,22). Durch die verbesserte Rekonstruktion kann die Strahlendosis von Untersuchungen um bis zu 50% reduziert werden (22).

Diagnostische Referenzwerte

Das Bundesamt für Strahlenschutz (BfS) veröffentlicht Referenzwerte für diagnostische und interventionelle radiologische Untersuchungen mit Röntgenstrahlung (23). Es werden verschiedene Referenzwerte für die unterschiedlichen Körperregionen bereitgestellt. Für jede Körperregion wird nur ein Referenzwert veröffentlicht, dieser gilt für einen normalgewichtigen Patienten. Normalgewichtig wird in der Veröffentlichung des BfS als 70 ± 3 kg definiert (23). Der veröffentlichte volumetrische Computertomographie Dosisindex (CTDIvol) und das Dosis-Längen-Produkt (DLP) werden von modernen CT Geräten für jede Untersuchung bereitgestellt und können mit den Referenzwerten verglichen werden. Bei den Referenzwerten des BfS handelt es sich nicht um Grenzwerte.

Überschreitungen der Referenzwerte für einzelne Patienten sind zulässig, z.B. damit bei übergewichtigen Patienten eine diagnostische Bildqualität erreicht werden kann (23).

Wie oben beschrieben stellt das BfS die Referenzwerte in Form eines CTDIvol und DLP zur Verfügung. Das CTDIvol gibt die Dosis pro Untersuchungsschicht wieder und wird in mGy angegeben. Das DLP errechnet sich aus dem CTDIvol multipliziert mit der Länge der Untersuchung und wird in mGy x cm angegeben. Zwar werden beide Werte von modernen CT Geräten regelhaft für jede Untersuchung bereitgestellt, es handelt sich jedoch nicht um gemessene Werte. Stattdessen wird das CTDIvol auf der Basis eines runden Standardphantoms mit dem Durchmesser von 32 cm berechnet. Somit handelt es sich lediglich um eine Abschätzung der Patientendosis.

Zur genaueren Abschätzung der Patientendosis hat die American Association of Physicists in Medicine (AAPM) das Konzept der Größenspezifischen Dosisabschätzungen („size-specific dose estimates“, SSDE) vorgestellt (24,25).

Durch die Verwendung des Phantoms zur Berechnung des CTDIvol ist dieser Wert bei kleinen Patienten zu niedrig und bei großen Patienten zu hoch. Deshalb ermittelte die AAPM Korrekturfaktoren für das CTDIvol. Diese richten sich nach der Patientenkonstitution.

Zur Ermittlung der Korrekturfaktoren können verschiedene Messwerte der Patientengröße verwendet werden. Hierzu zählen der laterale und der anterior-posterior Durchmesser aus dem Planungsbild, der effektive Durchmesser ermittelt in einem axialen CT Bild und der wasseräquivalente Patientendurchmesser (24,25). Zur Berechnung des wasseräquivalenten Durchmessers werden die gemessenen Dichtewerte aus einer axialen Schicht des Patienten auf die Dichte von Wasser

normiert und so der wasseräquivalente Patientendurchmesser bestimmt (25). Mit dieser Methode ist laut AAPM die genaueste Berechnung der größenspezifischen Dosisabschätzungen möglich (25)

Erfassung und Auswertung von CT Dosisdaten

Zur Erfassung und Auswertung von dosisrelevanten CT-Daten gibt es verschiedene Möglichkeiten (10). Ein Bild mit den Dosisdaten wird zu jeder Untersuchung gespeichert und in das Picture Archiving and Communications System (PACS) versendet. Dies kann manuell oder mittels optischer Bilderkennung ausgelesen werden. Ein Nachteil ist der große Aufwand, da jede Untersuchung einzeln geöffnet werden muss. Neuere Verfahren zur Auswertung von dosisrelevanten CT-Daten sind die im Digital Imaging and Communications Standard (DICOM-Standard (26)) verankerten Modality performed procedure steps (MPPS) und der strukturierte Strahlendosis Report (DICOM radiation dose structured report, DICOM-RDSR). Diese können automatisch erfasst, weiterverarbeitet und ausgewertet werden. So wird eine Erfassung und Auswertung von großen Datenmengen möglich. Hierfür sind jedoch dezidierte Softwarelösungen (sogenannte Dosismanagement oder Dosismonitoring Systeme, DMS) notwendig, welche aktuell zunehmend verfügbar werden (10).

Eine CT Dosisoptimierung muss somit immer aus zwei Bausteinen bestehen. Zum einen müssen die Bildakquisitionsparameter optimiert werden. Der Einsatz neuer Techniken kann hier auch in Zukunft zu einer weiteren Dosisoptimierung führen. Hierzu müssen neue Verfahren jedoch im Rahmen von wissenschaftlichen Studien validiert werden, so dass ein Einsatz in der klinischen Routine ermöglicht wird. Als zweites müssen die dosisrelevanten Daten der durchgeführten CT Untersuchungen

systematisch erfasst und ausgewertet werden. Obwohl inzwischen eine Vielzahl an Dosismanagement Systemen (DMS) entwickelt wurden, ist eine Weiterentwicklung und Anpassung an die jeweilige Institution und Fragestellung notwendig. So können in Zukunft fehlerhafte Dosisanwendungen und Potenziale zu einer weiteren Dosisoptimierung erkannt werden.

3. b. Untersuchungen und Ergebnisse

1. Arbeit

Boos J, Kröpil P, Klee D, Heusch P, Schimmöller L, Schaper J, Antoch G, Lanzman RS. Evaluation of the impact of organ-specific dose reduction on image quality in pediatric chest computed tomography. *Pediatr Radiol.* 2014 Sep;44(9):1065-9.

In der Thorax CT liegen radiosensitive Organe wie die Schilddrüse oder das Brustdrüsenparenchym im Untersuchungsvolumen. Dies macht eine Optimierung der Dosis bei Thorax CT Untersuchungen unabdingbar. Hierzu wurden organspezifische Dosisreduktionsalgorithmen (OSDR) eingeführt, welche die Dosis ventral verringern und kompensatorisch dorsal erhöhen. Es konnte gezeigt werden, dass so die Dosis auf die radiosensitiven Organe im ventralen Thorax reduziert werden kann (27). Der Einfluss auf die Bildqualität bei CT-Thorax Untersuchungen von pädiatrischen Patienten wurde in bisherigen Studien nicht untersucht.

Ziel der Studie war es, den Einfluss eines neuartigen OSDR auf die Bildqualität von pädiatrischen Thorax CT-Untersuchungen zu ermitteln.

Es wurden CT Untersuchungen des Thorax von 28 Kindern (mittleres Alter $10,9 \pm 4,8$ Jahre, Spannweite 3 – 18 Jahre) in diese retrospektive Studie eingeschlossen. Die kontrastmittelgestützten Untersuchungen wurden an einem 128-Zeilen CT Gerät durchgeführt. Die Durchführung erfolgte mit einer Röhrenspannung von 100 kVp, automatischer Röhrenstrommodulation und einem neuartigen organspezifischen Dosisreduktionsalgorithmus (XCare, Siemens, Forchheim, Deutschland). Sieben Kinder hatten Voruntersuchungen ohne organspezifische Dosisreduktion an einem

64-Zeilen CT mit einer Röhrenspannung von 100 kVp und automatischer Röhrenstrommodulation. Die subjektive Bildqualität wurde auf einer 5-Punkte Skala bewertet (1: nicht diagnostisch, 5: exzellent). Das Kontrast-zu-Rausch Verhältnis (CNR) und das Signal-zu-Rausch Verhältnis (SNR) der deszendierenden thorakalen Aorta wurden ermittelt.

Insgesamt betrug die mittlere subjektive Bildqualität $4,1 \pm 0,6$. In der Subgruppe der Kinder, die mit und ohne OSDR untersucht wurden, war die subjektive Bildqualität vergleichbar ($4,4 \pm 0,5$ mit OSDR vs. $4,4 \pm 0,7$ ohne OSDR). Es gab keinen signifikanten Unterschied zwischen dem mittleren SNR und CNR (mit OSDR: $38,3 \pm 10,1$ und $28,5 \pm 8,7$ vs. $35,5 \pm 8,5$ und $26,5 \pm 7,8$) ($p > 0,05$). Der volumetrische Computertomographie Dosisindex (CTDIvol) und die größenspezifischen Dosisabschätzungen (SSDE) zeigten keinen Unterschied zwischen den beiden Akquisitionsarten ($1,7 \pm 0,8$ mGy vs. $1,7 \pm 0,8$ mGy; $p > 0,05$).

Zusammenfassend konnte gezeigt werden, dass der OSDR Algorithmus keinen Einfluss auf die Bildqualität von pädiatrischen Thorax-CT Untersuchungen hat. OSDR kann deshalb in der klinischen Routine zur Reduktion der Strahlendosis eingesetzt werden und ermöglicht hier insbesondere eine Dosisreduktion der ventral gelegenen radiosensitiven Organe wie des Brustdrüsenparenchyms und der Schilddrüse.

2. Arbeit

Boos J, Lanzman RS, Meineke A, Heusch P, Sawicki LM, Antoch G, Kröpil P. Dose monitoring using the DICOM structured report: assessment of the relationship between cumulative radiation exposure and BMI in abdominal CT. Clin Radiol. 2015 Feb;70(2):176-82.

Dosisauswertungen von CT Untersuchungen wurden in der Vergangenheit häufig mittels des im PACS gespeicherten Dosisberichtes, dem DICOM-header oder den modality performed procedure steps (MPPS) durchgeführt. Die manuelle Auswertung der Dosisberichte ist aufwändig, insbesondere bei großen Untersuchungskollektiven. Der DICOM-header und insbesondere die MPPS weisen eine große Variabilität auf, so dass eine Auswertung erschwert ist (28–30). Der strukturierte DICOM Dosisreport (DICOM-RDSR) ist Teil des DICOM Standards und wird von modernen CT Geräten automatisch ausgegeben. Dosisrelevante Daten werden hier gespeichert und können ausgewertet werden. Die Struktur des DICOM-RDSR ist jedoch komplex und kann zwischen verschiedenen Modalitäten, Herstellern und CT Geräten variieren.

Die Dosis von CT Untersuchungen wird mit modernen technischen Mitteln an die Patientenkonstitution angepasst, so z.B. bei der automatischen Röhrenstrommodulation oder der automatischen Röhrenspannungsselektion. Zur Quantifizierung der Konstitution wird häufig das Patientengewicht und der Body Mass Index (BMI) genutzt (31,32).

Ziel der Studie war es, den strukturierten DICOM-RDSR zu nutzen, um eine groß angelegte Analyse zum Verhältnis der kumulativen Strahlendosis zu dem BMI in der Abdomen CT durchzuführen.

In diese retrospektive Studie wurden die DICOM-SR von 3121 Abdomen CTs ausgewertet, welche zwischen April 2013 und März 2014 durchgeführt wurden. Alle Untersuchungen wurden an einem 128-Zeilen CT Gerät durchgeführt. Die Patienten (mittleres Alter 61 ± 15 Jahre) wurden in fünf Subgruppen eingeteilt: Gruppe A: BMI < 20 kg/m^2 ; B: $20 - 25 \text{ kg/m}^2$; C: $25 - 30 \text{ kg/m}^2$; D: $30 - 35 \text{ kg/m}^2$; E: $> 35 \text{ kg/m}^2$. Der volumetrische CT Dosis Index (CTDIvol) und das Dosislängenprodukt (DLP) der Gruppen wurden mit den nationalen Referenzwerten verglichen.

Das mittlere CTDIvol und DLP betrug $5,4 \pm 2,9 \text{ mGy}$ und $243 \pm 153 \text{ mGy*cm}$ in Gruppe A, $6 \pm 3,6 \text{ mGy}$ und $264 \pm 179 \text{ mGy*cm}$ in Gruppe B, $7 \pm 3,6 \text{ mGy}$ und $320 \pm 180 \text{ mGy*cm}$ in Gruppe C, $8,1 \pm 5,2 \text{ mGy}$ und $375 \pm 306 \text{ mGy*cm}$ in Gruppe D, und $10 \pm 8 \text{ mGy}$ und $476 \pm 403 \text{ mGy*cm}$ in Gruppe E. CTDIvol und DLP unterschieden sich signifikant zwischen sämtlichen Gruppen ($p < 0,05$), mit Ausnahme von Gruppe A und Gruppe B. Es kam zu signifikant mehr Überschreitungen der nationalen Referenzwerte in den Gruppen D und E ($2,1\%$ und $6,3\%$) verglichen mit Gruppe B ($0,5\%$, $p < 0,05$).

Zusammenfassend konnte gezeigt werden, dass der strukturierte DICOM Dosisreport als eine umfassende und effiziente Methode zur Analyse von CT Dosisdaten genutzt werden kann. Der strukturierte DICOM Report ermöglicht insbesondere die Auswertung von CT Dosisdaten großer Kollektive. Die CT Dosis in der Abdomen CT steigt mit steigendem BMI der Patienten und ist bei stark übergewichtigen Patienten um bis zu 96% gegenüber normalgewichtigen erhöht.

3. Arbeit

Boos J, Meineke A, Rubbert C, Heusch P, Lanzman RS, Aissa J, Antoch G, Kröpil P. Cloud-Based CT Dose Monitoring using the DICOM-Structured Report: Fully Automated Analysis in Regard to National Diagnostic Reference Levels. *Rofo*. 2016 Mar;188(3):288-94.

Im Rahmen der Qualitätssicherung ist eine automatische Erfassung sowie ein Abgleich der lokalen Dosisparameter mit den diagnostischen Referenzwerten des BfS unabdingbar. Hierfür sind die Implementierung eines automatischen DMS sowie die Integration der nationalen diagnostischen Referenzwerte in dieses System notwendig. Während lokale DMS die Auswertung der eigenen Dosisparameter ermöglichen, bieten dezentrale („cloud-basierte“) Systeme zusätzlich die Möglichkeit des Vergleiches zwischen Institutionen.

Ziel dieser Studie war die Implementierung eines dezentralen cloud-basierten CT-DMS basierend auf dem DICOM-radiation dose structured report (DICOM-RDSR) zur automatischen Überwachung der lokalen Dosisexposition im Hinblick auf die nationalen diagnostischen Referenzwerte (DRW).

Zur automatischen Erfassung und Überwachung der CT-Dosisdaten wurde eine neuartige, in Kooperation mitentwickelte Software basierend auf dem DICOM-RDSR eingesetzt. Der DICOM-RDSR aller CT-Untersuchungen unserer Einrichtung zwischen 09/2011 und 03/2015 wurde automatisch anonymisiert und an einen Cloud-Server verschickt. Die Daten wurden automatisch im Hinblick auf die Körperregion, das Patientenalter und den korrespondierenden DRW für den volumetrischen

Computertomografie-Dosis-Index (CTDIvol) sowie für das Dosislängenprodukt (DLP) analysiert.

Datensätze von 36523 CT-Untersuchungen (131527 Untersuchungsserien) von drei verschiedenen CT-Geräten und einem PET-CT wurden analysiert. Insgesamt betrug der mittlere CTDIvol 51,3% und das mittlere DLP 52,8% der nationalen DRW. Bezogen auf die nationalen DRW betrugen CTDIvol und DLP für die Abdomen-CT 43,8% und 43,1% (n=10590 Untersuchungsserien), für die Schädel-CT 66,6% und 69,6% (n=16098 Untersuchungsserien) und für die Thorax-CT 37,8% und 44,0% (n=10387 Untersuchungsserien). Insgesamt überschritten 1,9% der CT-Untersuchungen den CTDIvol und 2,9% der Untersuchungen das DLP der nationalen DRW. Zwischen unterschiedlichen CT-Protokollen, die dem gleichen nationalen DRW zugeordnet wurden, variierte die Strahlenexposition um bis zu 50%.

Zusammenfassend ermöglichte das implementierte, cloud-basierte CT-DMS basierend auf dem DICOM-RDSR eine automatische, umfassende Analyse im Hinblick auf die nationalen DRW. Insgesamt betrug die Dosisexposition der CT ungefähr 50% der DRW bei deutlicher Variabilität zwischen den unterschiedlichen CT-Protokollen. Dies deutet darauf hin, dass eine Aktualisierung der DRW sowie die Implementierung von Protokoll-spezifischen DRW wünschenswert sind. Der cloud-basierte Ansatz ermöglicht einen potentiellen Vergleich der Dosisdaten zwischen angeschlossenen Institutionen und bietet großes Potenzial, die Strahlenexposition der CT in radiologischen Abteilungen weiter zu optimieren.

4. Arbeit

Boos J, Lanzman RS, Heusch P, Aissa J, Schleich C, Thomas C, Sawicki LM, Antoch G, Kröpil P. Does body mass index outperform body weight as a surrogate parameter in the calculation of size-specific dose estimates in adult body CT? Br J Radiol. 2016;89(1059):20150734.

Zur Korrektur des CTDI_{vol} Wertes auf Basis der Patientenkonstitution wurde durch die AAPM das SSDE Konzept entwickelt (24,25). Zur Berechnung der SSDE Werte wird der Patientendurchmesser benötigt. Khawara et al. konnten zeigen, dass bei pädiatrischen Patienten auch das Gewicht zur Berechnung des SSDE Wertes verwendet werden kann (33).

Ziel der Studie war es, den Wert des Body Mass Index (BMI) im Vergleich zum Körpergewicht als Surrogatparameter in der Berechnung von größenspezifischen Dosisabschätzungen (SSDE) in der CT des Thorax und Abdomens von Erwachsenen zu ermitteln.

401 CT Untersuchungen von 235 Patienten (194 Thorax CT Untersuchungen, 205 Abdomen CT Untersuchungen, 95 weiblich, 140 männlich, Alter $62,5 \pm 15,0$ Jahre) wurden eingeschlossen und das Gewicht, die Größe und der BMI (kg/m^2) analysiert. Der effektive Durchmesser (Deff, cm) wurde aus den axialen CT Bildern ermittelt. Die Korrelation zwischen BMI, Gewicht und Deff wurde berechnet. SSDE wurden jeweils basierend auf Deff (Referenzstandard), Gewicht und BMI berechnet und Tabellen zur Berechnung von SSDE aus dem BMI und dem Körpergewicht wurden erstellt.

Durchschnittlich ergaben sich für Größe, Gewicht, BMI und Deff $172,5 \pm 9,9$ cm, $79,5 \pm 19,1$ kg, $26,6 \pm 5,6$ kg/m^2 und $30,1 \pm 4,3$ cm. Es gab eine signifikante

Korrelation zwischen Deff und dem BMI sowie Deff und dem Gewicht ($r=0,85$ vs. $R=0,84$; jeweils $p < 0,05$). Die Korrelation war signifikant besser für den BMI in der Abdominal CT ($r=0,89$ vs. $r=0,84$; $p < 0,05$) und besser für das Gewicht in der Thorax CT ($r=0,87$ vs. $r=0,81$; $p < 0,05$). SSDE basierend auf dem Referenzstandard (Deff) und dem BMI waren nicht signifikant unterschiedlich mit einer mittleren absoluten Differenz von 4,2 % pro Patient (Interquartilsabstand 25-75: 3,1 – 7,9; Spannweite 0 – 25,3%).

Zusammenfassend zeigten sowohl der BMI als auch das Körpergewicht eine signifikante Korrelation mit dem Deff bei erwachsenen Patienten. Beide können somit als Surrogatparameter zur Berechnung der SSDE genutzt werden. Die in dieser Studie entwickelten Nachschlagetabellen können genutzt werden, um den SSDE Wert basierend auf dem Körpergewicht oder dem BMI der Patienten zu berechnen.

5. Arbeit

Boos J, Aissa J, Lanzman RS, Heusch P, Schimmöller L, Schleich C, Thomas C, Antoch G, Kröpil P. CT angiography of the aorta using 80 kVp in combination with sinogram-affirmed iterative reconstruction and automated tube current modulation: Effects on image quality and radiation dose. *J Med Imaging Radiat Oncol.* 2016 Apr;60(2):187-93.

CT Protokolle mit reduzierter Röhrenspannung sind auf Grund der k-Kante von Iod insbesondere zur CT Angiographie geeignet. Initiale CT Angiographie Protokolle wurden mit 120 kVp oder 100 kVp durchgeführt (34–36).

Ziel dieser Studie war die Evaluation der Bildqualität und der Strahlendosis eines Computertomographie Angiographie (CTA) Untersuchungsprotokolls mit 80 kVp in Kombination mit iterativer Bildrekonstruktion und automatischer Röhrenstrommodulation.

95 CTA Untersuchungen der Aorta wurden in die Studie eingeschlossen. Ein neuartiges CTA Protokoll mit einer Röhrenspannung von 80 kVp mit iterativer Bildrekonstruktion und automatischer Röhrenstrommodulation wurde in unserem Institut im März 2012 für Patienten mit einem Body mass index (BMI) unter 32 kg/m² eingeführt. Die ersten 72 konsekutiven Untersuchungen wurden retrospektiv ausgewertet und der Gruppe A zugeteilt (56 Patienten, 52 männlich, 14 weiblich, mittleres Alter 69,6 ± 10,7 Jahre, BMI Spannweite 19,7 – 31,1 kg/m²). Zum Vergleich wurden die letzten 23 konsekutiven Untersuchungen, welche mit dem vorherigen CTA Protokoll mit einer Röhrenspannung von 100 kVp durchgeführt wurden, eingeschlossen und der Gruppe B zugeordnet (21 Patienten, 13 männlich, 8

weiblich, mittleres Alter $67,4 \pm 11,1$ Jahre, BMI Spannweite: $19,7 - 31,9$ kg/m²). Thorakal und abdominal wurde das Kontrast-zu-Rauschen (CNR) und das Signal-zu-Rauschen (SNR) Verhältnis ermittelt. Die Bildqualität wurde subjektiv mittels einer Fünfpunkteskala (1= nicht diagnostisch, 5= exzellent) beurteilt. Weiterhin wurde das Dosislängenprodukt (DLP) und der volumetrische Computertomographie Dosisindex (CTDIvol) analysiert.

Die Bildqualität aller Untersuchungen war diagnostisch verwertbar. Die Dichte der Aorta war in Gruppe A signifikant höher als in Gruppe B (Thorax: $443,5 \pm 90,5$ Hounsfield Einheiten (HE) vs. $296,0 \pm 61,0$ HE; Abdomen: $426,3 \pm 94,2$ HE vs. $283,9 \pm 60,5$ HE; jeweils $p < 0,05$). CNR, SNR und die subjektive Bildqualität waren zwischen beiden Gruppen vergleichbar (CNR: $12,8 \pm 3,7$ vs. $13,0 \pm 7,4$; SNR $14,4 \pm 3,9$ vs. $14,9 \pm 8,2$; subjektive Bildqualität: $4,3 \pm 0,6$ vs. $4,5 \pm 0,6$; jeweils $p > 0,05$). CTDIvol und DLP waren in Gruppe A signifikant niedriger als in Gruppe B ($1,9 \pm 0,5$ mGy; $139,2 \pm 41,1$ mGy*cm vs. $4,2 \pm 1,4$ mGy; $292,1 \pm 91,5$ mGy*cm; jeweils $p < 0,001$).

Zusammenfassend ermöglichte die Niedrigdosis-CTA der Aorta mit einer Röhrenspannung von 80 kVp und iterativer Bildrekonstruktion bei Patienten mit einem BMI unter 32 kg/m² eine diagnostisch verwertbare Bildqualität und führte zu einer signifikanten Dosisreduktion um bis zu 50% verglichen mit einem 100 kVp CTA Protokoll.

6. Arbeit

Boos J, Kröpil P, Lanzman RS, Aissa J, Schleich C, Heusch P, Sawicki LM, Antoch G, Thomas C. CT pulmonary angiography: simultaneous low-pitch dual-source acquisition mode with 70 kVp and 40 ml of contrast medium and comparison with high-pitch spiral dual-source acquisition with automated tube potential selection. *Br J Radiol.* 2016 Jun;89(1062):20151059.

Die Reduktion der Röhrenspannung mit Annäherung an die k-Kante von Iod ermöglicht bei CT Angiographie Untersuchungen zusätzlich auch eine Reduktion der Kontrastmittelmenge (36–39).

Ziel dieser Studie war die Evaluation eines neuartigen Lungenarterien CTA Protokolls mit 70 kVp und dem simultanen dual-source Modus (SimDS) mit 40 ml Kontrastmittel sowie Vergleich mit einer spiralen dual-source Akquisition mit hohem Pitch Faktor (SpiralDS), automatischer Röhrenspannungsselektion und 70 ml Kontrastmittel.

Nach der Einführung des neuartigen SimDS Protokolls im Dezember 2014 für alle Patienten mit einem Body Mass Index (BMI) unter 35 kg/m² wurden die ersten 35 konsekutiven Patienten in die Studie eingeschlossen (Gruppe A, BMI 27 ± 4 kg/m²; Alter 66 ± 15 Jahre). Die letzten 35 Patienten mit einem BMI unter 35 kg/m², die eine Untersuchung mit dem vorherigen SpiralDS Protokoll erhalten hatten, wurden zum Vergleich eingeschlossen (Gruppe B, BMI 27 ± 4 kg/m², Alter 68 ± 16 Jahre). Die subjektive Bildqualität wurde durch zwei Radiologen ermittelt (1=nicht diagnostisch, 4=exzellent). Das Signal-zu-Rauschen (SNR) und das Kontrast-zu Rauschen (CNR) Verhältnis wurden gemessen. Der volumetrische Computertomographie Dosisindex

(CTDIvol), das Dosislängenprodukt (DLP) und die effektive Dosis wurden ausgewertet.

Die Bildqualität aller Untersuchungen war diagnostisch verwertbar. Die subjektive Bildqualität, SNR und CNR waren zwischen der Gruppe A und der Gruppe B vergleichbar ($3,7 \pm 0,6$ vs $3,7 \pm 0,5$, $14,6 \pm 6,0$ vs $13,9 \pm 3,7$ und $12,4 \pm 5,7$ vs $11,6 \pm 3,3$, jeweils $p > 0,05$). CTDIvol, DLP und die effektive Dosis waren in Gruppe A signifikant niedriger als in Gruppe B ($4,5 \pm 1,6$ vs $7,5 \pm 2,1$ mGy, $143,3 \pm 44,8$ vs $278,3 \pm 79,4$ mGy*cm und $2,0 \pm 0,6$ vs $3,9 \pm 1,1$ mSv, jeweils $p < 0,05$).

Zusammenfassend kann die SimDS-CT mit einer Kontrastmittelmenge von 40 ml zur Detektion von Lungenarterienembolien verwendet werden und führt zu einer diagnostisch verwertbaren Bildqualität. Im Vergleich zur SpiralDS-CT mit automatischer Röhrenspannungsselektion kann die Strahlendosis und die Kontrastmittelmenge um 50% bzw. 40% reduziert werden.

7. Arbeit

Boos J, Kröpil P, Bethge OT, Aissa J, Schleich C, Sawicki LM, Heinzler N, Antoch G, Thomas C. Accuracy of size-specific dose estimate calculation from center slice in computed tomography. *Radiat Prot Dosimetry*. 2017 May 25:1-12.

Zur optimalen Berechnung der Größenspezifischen Dosisabschätzungen muss der wasseräquivalente Patientendurchmesser jeder Untersuchungsschicht bestimmt werden. Der Mittelwert sämtlicher Schichten kann dann zur Berechnung des SSDE Wertes genutzt werden (24,25,40,41). In einer initialen Arbeit konnte in einem kleinen Kollektiv von erwachsenen Patienten gezeigt werden, dass auch der wasseräquivalente Durchmesser der mittleren Schicht des Untersuchungsvolumens zur SSDE Berechnung genutzt werden kann.

In der hier vorgelegten Studie sollte in einem großen Kollektiv aus pädiatrischen und erwachsenen Patienten mit unterschiedlicher Konstitution ermittelt werden, ob der wasseräquivalente Durchmesser (D_w) der Mittelschicht des Computertomographie (CT) Volumens für die Berechnung von größenspezifischen Dosisabschätzungen ausreichend ist.

1812 CT Serien (1583 Erwachsene: 1195 Abdominal, 388 Thorax, $61,5 \pm 15,7$ Jahre, Body Mass Index [BMI] $26,0 \pm 5,6$ kg/m²; 229 Kinder: 26 Abdominal, 203 Thorax, $9,3 \pm 5,0$ Jahre, BMI $17,6 \pm 4,3$ kg/m²) wurden in diese retrospektive Studie eingeschlossen. Der D_w der mittleren Schicht jedes CT Volumens wurden automatisch mit einer selbst entwickelten Matlab-Anwendung ermittelt (The Mathworks, Natick, MA). SSDE wurden berechnet: 1. Basierend auf D_w von der Mittelschicht und dem CTDI_{vol} der Untersuchung; und 2. Basierend auf D_w und

CTDIvol von jeder einzelnen Schicht des Scanvolumens, dies diene als Referenzstandard. Der Einfluss von Patientengewicht, Größe und BMI auf die Genauigkeit der SSDE wurden ermittelt.

Die mittlere Differenz zwischen beiden Methoden betrug $3,9 \pm 3,4\%$ (Spannweite 0 - 30,5%) für Erwachsene in der Abdominal-CT, $5,0 \pm 3,2\%$ (0 - 17,2%) für Erwachsene in der Thorax-CT, $3,1 \pm 2,6\%$ (0 - 9,2%) für die pädiatrische Abdominal-CT und $2,0 \pm 1,7\%$ (0 - 15,5%) für die pädiatrische Thorax-CT. Die Genauigkeit bei Verwendung der Mittelschicht korrelierte mit dem BMI und dem Gewicht der Patienten (BMI: $r = 0,15$ in der pädiatrischen Thorax-CT bis $r = 0,43$ in der Abdominal-CT von Erwachsenen; Gewicht: $r = 0,26$ in der pädiatrischen Thorax-CT bis $r = 0,49$ in der pädiatrischen Abdominal-CT). Es bestand eine Tendenz zur Dosisüberschätzung bei schlanken und Dosisunterschätzung bei übergewichtigen Patienten.

Zusammenfassend führt die SSDE Berechnung mittels der Volumenmittelschicht zu einem mittleren Fehler von 2 – 5% verglichen mit der Berechnung aus allen Schichten des Scanvolumens. Die Genauigkeit ist abhängig vom BMI und dem Gewicht der Patienten mit einer Dosisunterschätzung bei übergewichtigen und - Dosisüberschätzung bei schlanken Patienten.

8. Arbeit

Boos J, Thomas C, Appel E, Klosterkemper Y, Schleich C, Aissa J, Bethge O, Antoch G, Kroepil P. Institutional computed tomography diagnostic reference levels based on water-equivalent diameter and size-specific dose estimates. *J Radiol Prot.* 2018 Jun;38(2):536-548.

Ziel der Studie war die Entwicklung von lokalen größenspezifischen diagnostischen Referenzwerten für die Computertomographie (CT) des Thorax und des Abdomens basierend auf dem wasseräquivalenten Durchmesser (Dw) der Patienten und größenspezifischen Dosisabschätzungen (SSDE).

1690 CT Untersuchungen des Thorax, des Oberbauches und des Abdomens, durchgeführt zwischen 07/2016 und 11/2016 wurden in diese retrospektive Studie eingeschlossen (mittleres Patientenalter: $62,8 \pm 14,7$ Jahre, 618 männlich, 1072 weiblich). Der mittlere Dw des Untersuchungsvolumens sowie der SSDE jeder Untersuchung wurden mittels einer selbst entwickelten Software anhand der Bild- und Dosisdaten jeder Untersuchung automatisch berechnet. Anhand der 75% Perzentile der Dosisdaten wurden institutionelle größenspezifische diagnostische Referenzwerte (DRW) entwickelt. CTDIvol von durchschnittlich großen Patienten wurde mit den nationalen deutschen DRW verglichen.

Der mittlere CTDIvol, Dw und SSDE betrug $7,2 \pm 4,0$ mGy (0,8 - 47,9 mGy), $29,0 \pm 3,4$ cm and $8,5 \pm 3,8$ mGy (1,2 - 37,7 mGy). Insgesamt waren die SSDE-Werte im Thorax und im Abdomen höher als der CTDIvol (jeweils $p < 0,001$). Die Analyse ergab eine starke Korrelation zwischen Dw und SSDE in der Thorax-CT ($R^2 = 0,66$), in der Oberbauch-CT ($R^2 = 0,96$) und in der Abdomen-CT ($R^2 = 0,98$), so dass

größenspezifische DRWs entwickelt werden konnten. Für einen durchschnittlich großen Patienten in unserem Kollektiv ($D_w = 29 \text{ cm}$) betrug der CTDIvol $52,2 \pm 27,7\%$ der nationalen DRW in der Thorax-CT, $40,9 \pm 9,7\%$ in der Oberbauch-CT und $53,2 \pm 13\%$ in der Abdomen-CT.

Zusammenfassend ist die Entwicklung von größenspezifischen DRW basierend auf dem D_w und SSDE möglich und erlaubt eine dezidierte Auswertung der Dosisdaten in Abhängigkeit von der Patientengröße. Der CTDIvol von mittels D_w ermittelten durchschnittlich großen Patienten war in unseren Untersuchungen deutlich niedriger als die deutschen DRWs.

3. c. Diskussion

In den im Rahmen dieser Habilitationsschrift dargelegten Arbeiten wurden einerseits verschiedene Techniken untersucht, die bei modernen CT Geräten zur Dosisoptimierung zur Verfügung stehen und helfen können eine Strahlendosisoptimierung sowie eine Optimierung der Bildqualität bei gleichzeitiger Reduktion der Kontrastmittelmenge durchzuführen. Zum anderen wurden eine genauere und automatisierte Erfassung, Weiterverarbeitung und Auswertung von CT Dosisdaten entwickelt, implementiert und evaluiert. Die verbesserten Auswertungsmöglichkeiten wurden genutzt, um die institutionellen Dosiswerte im Hinblick auf die diagnostischen Referenzwerte des BfS auszuwerten. Darüber hinaus wurden neuartige institutionelle größenspezifische diagnostische Referenzwerte entwickelt und implementiert.

In der 1., der 5. und der 6. Arbeit wurden die Optimierung von CT Akquisitionsparametern zur Verbesserung der Bildqualität und Reduktion der Strahlendosis in der CT untersucht. Hierbei wurden vielfältige Dosisoptimierungstechniken kombiniert. Diese beinhalten die Verwendung von dezidierten Protokollen mit niedriger Röhrenspannung, die organspezifische Dosisreduktion, die iterative Rekonstruktion, die automatische Röhrenspannungsselektion und die automatische Röhrenstrommodulation.

Die hier in der ersten, fünften und sechsten Studie dargelegte Verwendung der adaptiven statistischen iterativen Rekonstruktion ermöglicht die Reduktion der Strahlendosis um bis zu 50% gegenüber der gefilterten Rückprojektion bei erhaltener Bildqualität. Die Stärke der iterativen Rekonstruktion kann stufenweise ausgewählt

werden. Während höhere Stufen der iterativen Rekonstruktion theoretisch eine stärkere Dosisreduktion ermöglichen, wurde in klinischen Studien gezeigt, dass sich hier auch der Bildeindruck verändert (42). Die optimale Dosisreduktion bei erhaltenem Bildeindruck wurde für mittlere Stufen der iterativen Rekonstruktion nachgewiesen (42–44). Neuartige Modell-basierte iterative Rekonstruktionsalgorithmen (22) ermöglichen inzwischen eine Dosisreduktion von über 90% verglichen mit der traditionellen gefilterten Rückprojektion. Statistische iterative Rekonstruktionsverfahren sind heute vielfach wissenschaftlich evaluiert und werden in der klinischen Routine verwendet (45–49). Die zunehmende Rechenleistung moderner Computer ermöglicht die Verwendung von Modell-basierten iterative Rekonstruktionsalgorithmen, die vor kurzer Zeit noch bis zu 40 min pro Rekonstruktion benötigten (50). Eine Überlegenheit gegenüber der statistischen iterativen Bildrekonstruktion wurde bereits nachgewiesen, so dass in Zukunft eine weitere Dosisreduktion in der CT möglich erscheint (49).

Zusätzlich wurde in den dargelegten Arbeiten 1, 5 und 6 eine automatische Röhrenstrommodulation verwendet und die Kombination mit anderen Dosisoptimierungsverfahren untersucht. Die automatische Röhrenstrommodulation adaptiert das Röhrenstrom-Zeit-Produkt entlang der z-Achse des Patienten. Die Reduktion des Röhrenstroms ist linear zur abgegebenen Strahlendosis. Somit ist die Reduktion des Röhrenstrom-Zeit-Produktes ein einfacher Weg die Strahlendosis zu reduzieren, geht jedoch mit einer Verschlechterung der Bildqualität einher. Die Anpassung durch die automatische Röhrenstrommodulation erfolgt anhand von Dichtewerten, welche dem Planungsbild entnommen werden. So kann der Röhrenstrom bei Abschnitten mit niedriger Dichte (exemplarisch in der Lunge) reduziert werden, ohne dass es zu einer Verschlechterung der Bildqualität kommt. Es

konnte gezeigt werden, dass die automatische Röhrenstrommodulation zu einer signifikanten Reduktion der CT Dosis führt, ohne dass die Bildqualität negativ beeinflusst wird (20,51–53). Inzwischen hat diese Technik Einzug in die klinische Routine erhalten und wird regelhaft bei CT Untersuchungen verwendet. Wie in den Arbeiten 5 und 6 gezeigt, ist eine Kombination mit anderen Dosisreduktionstechniken möglich und wird vielfach angewandt (54–56).

Die automatische Röhrenspannungsselektion, welche in der ersten Arbeit verwendet wurde, ermittelt anhand des Planungsbildes der CT Untersuchung die optimale Röhrenspannung für die jeweilige Untersuchung. Hierbei wird sowohl die Patientenkonstitution als auch die Untersuchungsart berücksichtigt. Mittels eines Referenz Röhrenstrom-Zeit-Produktes kann die spätere Bildqualität im Vorfeld festgelegt werden.

Eine Reduktion der Röhrenspannung führt zu einer Dosisreduktion der Untersuchung, diese ist jedoch nicht linear sondern verhält sich exponentiell. Eine Reduktion der Röhrenspannung geht bei unverändertem Röhrenstrom-Zeit-Produkt allerdings mit einer Verschlechterung der Bildqualität einher. Die Kontrastmittel in der CT Diagnostik basieren auf Iod. Auf Grund der k-Kante von Jod bei 33,2 keV führt eine Reduktion der Röhrenspannung jedoch zu einer Annäherung an die k-Kante und damit zu einer stärkeren Absorption des Kontrastmittels. Somit bietet das Kontrastmittel in Untersuchungen mit niedrigerer Röhrenspannung einen höheren Kontrast (3). Dies kann insbesondere bei Gefäßdarstellungen genutzt werden, um die Dosis zu reduzieren. Trotz der reduzierten Strahlendosis kann so sogar eine Verbesserung des Signal-zu-Rauschen (SNR) und Kontrast-zu-Rauschen Verhältnis (CNR) erreicht werden (57) .

In Abhängigkeit von der Patientengröße muss eine Reduktion der Röhrenspannung durch eine Anpassung bzw. Erhöhung des Röhrenstrom-Zeit-Produktes ausgeglichen werden. Hierfür wird eine sehr leistungsfähige Röntgenröhre benötigt. Der technische Fortschritt mit immer effizienteren Röntgenröhren ermöglicht eine zunehmende Ausdehnung der Untersuchungen mit niedriger Röhrenspannung. Einschränkungen dieser Technik können bei übergewichtigen Patienten auftreten, da hier selbst moderne Röntgenröhren das zum Erreichen einer diagnostischen Bildqualität benötigte Röhrenstrom-Zeit-Produkt nicht mehr erzeugen können. Deshalb muss die Röhrenspannung teilweise an die Patientenkonstitution angepasst werden. Dies konnte auch in der vorgelegten zweiten Arbeit bestätigt werden.

Neben der automatischen Röhrenspannungsselektion gewinnen dezidierte Protokolle mit niedriger Röhrenspannung zunehmend an Bedeutung, insbesondere in der Gefäßdarstellung mittels CT (57–60). Diese Protokolle wurden in den Arbeiten 5 und 6 untersucht. Während initiale Arbeiten die Röhrenspannung auf 100 kVp reduzierten (61), wurden durch die fortwährende technische Entwicklung CT Protokolle (wie in Studie 5) mit 80 kVp und anschließend (wie in Studie 6) mit 70 kVp eingeführt und evaluiert (57,58,62–66). Die hier dargelegte Studie 5. demonstriert die Machbarkeit einer Verwendung von 80 kVp in Kombination mit iterativer Rekonstruktion zur Darstellung der gesamten Aorta. In initialen Studien wurde eine Röhrenspannung von 80 kVp nur in der Thorax CT Angiographie untersucht (62). Dies war durch die technischen Limitationen begründet. Eine reduzierte Röhrenspannung muss durch ein höheres Röhrenstrom-Zeit-Produkt kompensiert werden. Aufgrund der generell niedrigeren Dosis bei Thorax Untersuchungen ist es hier einfacher das benötigte Röhrenstrom-Zeit-Produkt zu erreichen. In mehreren weiteren Studien wurden CT Protokolle mit einer Röhrenspannung von 80 kVp zur Untersuchung der thorakalen

Aorta, der Gefäße der unteren Extremitäten, bei Schädel CT Untersuchungen bei Kindern und bei Untersuchungen der Nasennebenhöhlen eingeführt und es konnte eine diagnostische Bildqualität bei gleichzeitig signifikanter Dosisreduktion nachgewiesen werden (57,67–69). Zwischenzeitlich ermöglicht die weitere Verbesserung der Röntgenröhren auch für die Aorta eine Verwendung einer Röhrenspannung von lediglich 70 kVp bei erhaltener diagnostischer Bildqualität (70). Neben dem in der vorgelegten sechsten Studie untersuchten CT Protokoll mit einer Röhrenspannung von 70 kVp zur Beurteilung von Lungenarterienembolien wurden zwischenzeitlich CT Protokolle mit einer Röhrenspannung von 70 kVp sowohl für die Herz-CT als auch für die CT des Halses untersucht (60,71).

Die Arbeiten 2 und 3 beschäftigen sich mit der automatisierten Erfassung und Verarbeitung von CT Dosisdaten. Das Bundesamt für Strahlenschutz stellt Referenzwerte für verschiedene CT Untersuchungen zur Verfügung (23). Eine Auswertung der institutsinternen Dosisdaten in Bezug auf diese Referenzwerte ist ein wichtiger Bestandteil der Qualitätssicherung. In den durchgeführten Arbeiten wurde eine neuartige Erfassung basierend auf dem strukturierten Dosisreport aus dem DICOM-Standard implementiert und untersucht. Es konnte gezeigt werden, dass sich hiermit zuverlässig und in großen Maßstab CT Dosisdaten erfassen lassen. Die Erfassung mittels des DICOM-Standards ermöglicht eine deutlich einfachere Auswertung von Dosisdaten. Vorher verwendete Methoden wie die manuelle Auswertung mittels Excel Tabelle, das optische Auslesen des Patientenprotokolls aus dem Picture Archiving and Communication System (PACS), die Verwendung der Modality performed procedure steps (MPPS) oder des DICOM headers sind nicht mehr notwendig (28,72–75). DMS basierend auf dem DICOM-RDSR wurden

zwischenzeitlich von verschiedenen Hersteller entwickelt. Neben dem Einsatz in der klinischen Routine wurden viele DMS zwischenzeitlich auch für wissenschaftliche Auswertungen verwendet (28,76–79) . Der Trend zur automatisierten und umfassenden Dosiserfassung von CT Untersuchungen spiegelt sich auch in der Euratom 2013/59 Richtlinie wider, welche aktuell in nationales Gesetz der Mitgliedsstaaten übernommen wird.

Die Dosisauswertung in großem Maßstab mit Hilfe des DICOM-RDSR wurde in der vorgelegten zweiten Arbeit genutzt, um den Zusammenhang zwischen der Dosis von abdominellen CT Untersuchungen und der Patientenkonstitution zu ermitteln. Hier konnte unter Verwendung der klassischen CT Dosisparameter CTDIvol und DLP gezeigt werden, dass zur Untersuchung des Abdomens bei übergewichtigen Patienten eine deutlich höhere Strahlendosis verwendet wird.

Bei den von modernen CT Geräten ausgegebenen Dosisparametern CTDIvol und DLP handelt es sich nicht um gemessene Werte. Stattdessen basiert die angegebene Dosis auf Phantommessungen, die mit Hilfe eines 16 cm oder 32 cm Phantoms durchgeführt werden (80). Damit geben sie lediglich an, wieviel Dosis das CT bei einer spezifischen Untersuchung abgegeben hat. Die Wirksamkeit der Dosis ist jedoch abhängig von der Konstitution des Patienten. Bei einem übergewichtigen Patienten ist die wahre Dosis niedriger, bei einem sehr schlanken Patienten oder einem Kind teilweise sehr viel höher.

Die vorgelegte vierte, siebte und achte Arbeit beschäftigen sich mit der genaueren Berechnung der applizierten Dosis unter Berücksichtigung der Patientenkonstitution. In Arbeit 4 und 7 wurden verschiedene Möglichkeiten der Berechnung von größenspezifischen Dosisabschätzungen untersucht. Es konnte gezeigt werden, dass auch das Patientengewicht und der BMI der Patienten zur Berechnung der SSDE Werte genutzt werden können. Dies konnte auch in weiteren Studien bestätigt werden (33,81,82).

Die Verwendung des Patientengewichts oder des BMI kann in Fällen nützlich sein, in denen der Patientendurchmesser nicht bestimmt wurde. Die Verwendung des Durchmessers der Mittelschicht des Untersuchungsvolumens kann die Berechnung der SSDE Werte deutlich vereinfachen und ggf. auch manuell durchgeführt werden. Allerdings hängt die Genauigkeit dieser Methode von der Patientenkonstitution ab, so dass die Verwendung des Patientendurchmessers und insbesondere des mittleren wasseräquivalenten Patientendurchmessers aus allen Schichten des Untersuchungsvolumens als Referenzstandard anzusehen ist (41,83).

In der achten Arbeit wurden institutsinterne diagnostische Referenzwerte basierend auf größenspezifischen Dosisabschätzungen ermittelt und implementiert. Die Implementierung von größenspezifischen diagnostischen Referenzwerten ist aktuell nur durch das American College of Radiology (ACR) in den Vereinigten Staaten von Amerika erfolgt (84–86). Die aktuellen deutschen Referenzwerte des BfS werden hingegen lediglich als singulärer Wert bereitgestellt. Dieser wird aus Abfragen der aktuell in Deutschland applizierten Dosis ermittelt (23). Der Vorteil von größenspezifischen diagnostischen Referenzwerten ergibt sich durch eine vereinfachte und genauere Auswertung der Dosisdaten im Rahmen der

Qualitätssicherung (84,86,87). Während das ACR größenspezifisch diagnostische Referenzwerte veröffentlicht hat, arbeitet die Europäische Gesellschaft für Radiologie (ESR) im Rahmen des „Eurosafe“ Projektes an diagnostischen Referenzwerten basierend auf klinischen Indikationen (88). Diese können eine dezidiere Auswertung ermöglichen als diagnostische Referenzwerte basierend auf anatomischen Regionen. Beispielhaft sind die Untersuchungsparameter und Dosiswerte eines CT Abdomens im Rahmen der Abklärung einer Urolithiasis nicht zu vergleichen mit einer CT des Abdomen im Rahmen eines Tumorstaging, so dass hier separate diagnostische Referenzwerte sinnvoll erscheinen (84). Allerdings führt diese Auftrennung auch zu einer Zunahme der Anzahl an diagnostischen Referenzwerten und somit zu einer umfangreicheren und komplizierteren Auswertung. Die genaue Anzahl an sinnvollen klinischen Indikationen für diagnostische Referenzwerte wird aktuell im Rahmen des „European Study on Clinical Diagnostic Reference Levels“ („EUCLID“) Projektes erarbeitet (89). Sowohl für die größenspezifische Auswertung als auch für die Auswertung einer großen Anzahl an diagnostischen Referenzwerten basierend auf klinischen Indikationen ist ein DMS sinnvoll (10). Wie in der achten Arbeit gezeigt kann ein DMS auch genutzt werden um lokale diagnostische Referenzwerte zu erstellen. Diese ermöglichen eine genauere Qualitätssicherung im Hinblick auf die institutsinterne Gerätestruktur und das lokale Patientenkollektiv, welche über die Auswertung im Hinblick auf die nationalen diagnostischen Referenzwerte hinausgeht. Dies spiegelt sich auch in den Anforderungen der Eurosafe Zertifizierung wider, welche eine Auswertung anhand von lokalen diagnostischen Referenzwerten fordert (88).

Abschließend lässt sich schlussfolgern, dass eine Dosisoptimierung in der CT auf Grund der zunehmenden Anzahl an Indikationen von CT Untersuchungen und

der hierdurch bedingten Zunahme der Anzahl von CT Untersuchungen eine wichtige Rolle spielt. Durch eine automatische Dosiserfassung und eine systematische Auswertung im Rahmen der Qualitätssicherung kann ein Potenzial zur weiteren Dosisoptimierung erkannt werden. Zusätzlich können fehlerhafte Dosisapplikationen nachgewiesen und analysiert werden. Durch eine intelligente Kombination von neuartigen Dosisoptimierungsalgorithmen lässt sich die Dosisapplikation in der CT weiter optimieren, ohne dass hierbei die Bildqualität und damit die diagnostische Wertigkeit der Untersuchungen negativ beeinflusst wird. Eine Kombination aus einer Verbesserung der Untersuchungsparameter und eine umfangreiche Auswertung im Rahmen der Qualitätssicherung führen im Endeffekt zu einer Erhöhung der Patientensicherheit und einer Verbesserung der Patientenversorgung.

3. d. Ausblick

Die in dieser Habilitationsschrift dargelegten Arbeiten zeigen die Bedeutung und das Potenzial einer automatischen Erfassung, einer systematischen Auswertung sowie einer gezielten Optimierung der Dosis von CT Untersuchungen. Die Überführung der Euratom 2013/59 Richtlinie in nationales Recht erfolgt aktuell. Hierbei wird der systematischen Auswertung von Dosisdaten eine große Bedeutung zugeschrieben. Zusätzlich wird die Stellung von Medizinphysik-Experten als Teil des Dosismonitorings gestärkt. Eine Weiterentwicklung und flächendeckende Implementierung von diagnostischen Referenzwerten im Rahmen des Eurosafe Projektes der ESR ist aktuell im Gange. Es bleibt abzuwarten, ob hier die Patientenkonstitution als Parameter für diagnostische Referenzwerte in Zukunft implementiert wird. Die fortwährende Entwicklung mit Verbesserung der CT Geräte und verbesserten Nachverarbeitungsalgorithmen wird in Zukunft eine weitere Optimierung der Dosis von CT Untersuchungen erlauben.

3. e. Literaturverzeichnis

1. Bundesamt für Strahlenschutz (BfS). Jahresbericht 2010. 2011.<http://doris.bfs.de/jspui/handle/urn:nbn:de:0221-201109056248>. Accessed August 15, 2015.
2. Brenner DJ, Hall EJ. Computed tomography--an increasing source of radiation exposure. *N Engl J Med*. 2007;357(22):2277–2284.
3. Megyeri B, Christe A, Schindera ST, et al. Diagnostic confidence and image quality of CT pulmonary angiography at 100 kVp in overweight and obese patients. *Clin Radiol*. 2015;70(1):54–61.
4. United Nations Scientific Committee on the Effects of Atomic Radiation. United Nations Scientific Committee on the Effects of Atomic Radiation UNSCEAR 2008 Report to the General Assembly, with scientific annexes Volume I: Report to the General Assembly, Scientific Annexes A and B. http://www.unscear.org/unscear/en/publications/2008_1.html. Accessed August 15, 2015.
5. Hicketier T, Mammadov K, Baeßler B, et al. Whole-body computed tomography in trauma patients: optimization of the patient scanning position significantly shortens examination time while maintaining diagnostic image quality. *Ther Clin Risk Manag*. 2018;14:849–859.
6. Smith NJ, Bees N, Barbachano Y, Norman AR, Swift RI, Brown G. Preoperative computed tomography staging of nonmetastatic colon cancer predicts outcome: implications for clinical trials. *British Journal of Cancer*. 2007;96(7):1030–1036.

7. Brook OR, Brook A, Vollmer CM, Kent TS, Sanchez N, Pedrosa I. Structured reporting of multiphasic CT for pancreatic cancer: potential effect on staging and surgical planning. *Radiology*. 2015;274(2):464–472.
8. Zhao R-P, Hao Z-R, Song Z-J. Diagnostic value of Flash dual-source CT coronary artery imaging combined with dual-energy myocardial perfusion imaging for coronary heart disease. *Exp Ther Med*. 2014;7(4):865–868.
9. Mueller-Mang C, Grosse C, Schmid K, Stiebellehner L, Bankier AA. What Every Radiologist Should Know about Idiopathic Interstitial Pneumonias. *RadioGraphics*. 2007;27(3):595–615.
10. Boos J, Meineke A, Bethge OT, Antoch G, Kröpil P. Dose Monitoring in Radiology Departments: Status Quo and Future Perspectives. *Rofo*. 2016;188(5):443–450.
11. Smith-Bindman R, Miglioretti DL, Johnson E, et al. Use of diagnostic imaging studies and associated radiation exposure for patients enrolled in large integrated health care systems, 1996-2010. *JAMA*. 2012;307(22):2400–2409.
12. The Council of the European Union. Council Directive 97/43/Euratom of 30 June 1997 on health protection of individuals against the dangers of ionizing radiation in relation to medical exposure, and repealing Directive Euratom, 1997,. <https://publications.europa.eu/en/publication-detail/-/publication/aa7564fa-fd07-4872-943c-66df8f4f1099/language-en>. Accessed May 15, 2018.
13. Guberina N, Lechel U, Forsting M, Ringelstein A. Efficacy of high-pitch CT protocols for radiation dose reduction. *J Radiol Prot*. 2016;36(4):N57–N66.

14. Kyriakou Y, Kachelriess M, Knaup M, Krause JU, Kalender WA. Impact of the z-flying focal spot on resolution and artifact behavior for a 64-slice spiral CT scanner. *Eur Radiol.* 2006;16(6):1206–1215.
15. Seuss H, Janka R, Hammon M, Cavallaro A, Uder M, Dankerl P. Virtual Computed Tomography Colonography: Evaluation of 2D and Virtual 3D Image Quality of Sub-mSv Examinations Enabled by Third-generation Dual Source Scanner Featuring Tin Filtering. *Acad Radiol.* 2018;
16. Boos J, Kröpil P, Klee D, et al. Evaluation of the impact of organ-specific dose reduction on image quality in pediatric chest computed tomography. *Pediatr Radiol.* 2014;44(9):1065–1069.
17. Kalra MK, Maher MM, Toth TL, et al. Techniques and applications of automatic tube current modulation for CT. *Radiology.* 2004;233(3):649–657.
18. Lurz M, Lell MM, Wuest W, et al. Automated tube voltage selection in thoracoabdominal computed tomography at high pitch using a third-generation dual-source scanner: image quality and radiation dose performance. *Invest Radiol.* 2015;50(5):352–360.
19. Lee SH, Kim M-J, Yoon C-S, Lee M-J. Radiation dose reduction with the adaptive statistical iterative reconstruction (ASIR) technique for chest CT in children: an intra-individual comparison. *Eur J Radiol.* 2012;81(9):e938-943.
20. Kalra MK, Maher MM, Toth TL, Kamath RS, Halpern EF, Saini S. Comparison of Z-axis automatic tube current modulation technique with fixed tube current CT scanning of abdomen and pelvis. *Radiology.* 2004;232(2):347–353.

21. Boos J, Aissa J, Lanzman RS, et al. CT angiography of the aorta using 80 kVp in combination with sinogram-affirmed iterative reconstruction and automated tube current modulation: Effects on image quality and radiation dose. *J Med Imaging Radiat Oncol.* 2016;60(2):187–193.
22. Kataria B, Althén JN, Smedby Ö, Persson A, Sökjer H, Sandborg M. Assessment of image quality in abdominal CT: potential dose reduction with model-based iterative reconstruction. *Eur Radiol.* 2018;28(6):2464–2473.
23. BfS - Diagnostische Referenzwerte.
http://www.bfs.de/DE/themen/ion/anwendung-mezizin/diagnostik/referenzwerte/referenzwerte_node.html. Accessed February 26, 2018.
24. The Report of AAPM Taks Group 204. Size-Specific Dose Estimates (SSDE) in Pediatric and Adult Body CT Examinations.
https://www.aapm.org/pubs/reports/RPT_204.pdf. Accessed August 30, 2015.
25. The Report of AAPM Task Group 220. Use of Water Equivalent Diameter for Calculating Patient Size and Size-Specific Dose Estimates (SSDE) in CT.
https://www.aapm.org/pubs/reports/RPT_220.pdf. Accessed August 15, 2015.
26. National Electrical Manufacturers Association. Digital Imaging and Communications in Medicine, ISO 12052,. Digital Imaging and Communications in Medicine, ISO 12052,. <http://medical.nema.org/Dicom/about-DICOM.html>. Accessed August 15, 2015.
27. Duan X, Wang J, Christner JA, Leng S, Grant KL, McCollough CH. Dose reduction to anterior surfaces with organ-based tube-current modulation:

- evaluation of performance in a phantom study. *AJR Am J Roentgenol.* 2011;197(3):689–695.
28. Cook TS, Zimmerman SL, Steingall SR, Maidment ADA, Kim W, Boonn WW. RADIANCE: An automated, enterprise-wide solution for archiving and reporting CT radiation dose estimates. *Radiographics.* 2011;31(7):1833–1846.
 29. Treichel T, Liebmann P, Burgert O, Gessat M. Applicability of DICOM structured reporting for the standardized exchange of implantation plans. *Int J Comput Assist Radiol Surg.* 2010;5(1):1–9.
 30. Treichel T, Gessat M, Prietzel T, Burgert O. DICOM for implantations--overview and application. *J Digit Imaging.* 2012;25(3):352–358.
 31. WHO | Obesity: preventing and managing the global epidemic. WHO. http://www.who.int/entity/nutrition/publications/obesity/WHO_TRS_894/en/index.html. Accessed June 12, 2018.
 32. Szucs-Farkas Z, Strautz T, Patak MA, Kurmann L, Vock P, Schindera ST. Is body weight the most appropriate criterion to select patients eligible for low-dose pulmonary CT angiography? Analysis of objective and subjective image quality at 80 kVp in 100 patients. *Eur Radiol.* 2009;19(8):1914–1922.
 33. Khawaja RDA, Singh S, Vettiyil B, et al. Simplifying size-specific radiation dose estimates in pediatric CT. *AJR Am J Roentgenol.* 2015;204(1):167–176.
 34. Krissak R, Henzler T, Prechel A, et al. Triple-rule-out dual-source CT angiography of patients with acute chest pain: dose reduction potential of 100 kV scanning. *Eur J Radiol.* 2012;81(12):3691–3696.

35. Horiguchi J, Fujioka C, Kiguchi M, Yamamoto H, Shen Y, Kihara Y. In vitro measurement of CT density and estimation of stenosis related to coronary soft plaque at 100 kV and 120 kV on ECG-triggered scan. *Eur J Radiol.* 2011;77(2):294–298.
36. Szucs-Farkas Z, Schibler F, Cullmann J, et al. Diagnostic accuracy of pulmonary CT angiography at low tube voltage: intraindividual comparison of a normal-dose protocol at 120 kVp and a low-dose protocol at 80 kVp using reduced amount of contrast medium in a simulation study. *AJR Am J Roentgenol.* 2011;197(5):W852-859.
37. Kanematsu M, Goshima S, Miyoshi T, et al. Whole-body CT angiography with low tube voltage and low-concentration contrast material to reduce radiation dose and iodine load. *AJR Am J Roentgenol.* 2014;202(1):W106-116.
38. Kidoh M, Nakaura T, Nakamura S, et al. Contrast material and radiation dose reduction strategy for triple-rule-out cardiac CT angiography: feasibility study of non-ECG-gated low kVp scan of the whole chest following coronary CT angiography. *Acta Radiol.* 2014;55(10):1186–1196.
39. Xia W, Wu J-T, Yin X-R, Wang Z-J, Wu H-T. CT angiography of the neck: value of contrast medium dose reduction with low tube voltage and high tube current in a 64-detector row CT. *Clin Radiol.* 2014;69(4):e183-189.
40. Christner JA, Braun NN, Jacobsen MC, Carter RE, Kofler JM, McCollough CH. Size-specific dose estimates for adult patients at CT of the torso. *Radiology.* 2012;265(3):841–847.

41. Leng S, Shiung M, Duan X, Yu L, Zhang Y, McCollough CH. Size-specific Dose Estimates for Chest, Abdominal, and Pelvic CT: Effect of Inpatient Variability in Water-equivalent Diameter. *Radiology*. 2015;276(1):184–190.
42. Kröpil P, Bigdeli AH, Nagel HD, Antoch G, Cohnen M. Impact of increasing levels of advanced iterative reconstruction on image quality in low-dose cardiac CT angiography. *Rofo*. 2014;186(6):567–575.
43. Greffier J, Macri F, Larbi A, et al. Dose reduction with iterative reconstruction in multi-detector CT: What is the impact on deformation of circular structures in phantom study? *Diagnostic and Interventional Imaging*. 2016;97(2):187–196.
44. Bodelle B, Wichmann JL, Scholtz J-E, et al. Iterative Reconstruction Leads to Increased Subjective and Objective Image Quality in Cranial CT in Patients With Stroke. *American Journal of Roentgenology*. 2015;205(3):618–622.
45. Li X, Shu H, Zhang Y, et al. Low-dose CT with adaptive statistical iterative reconstruction for evaluation of urinary stone. *Oncotarget*. 2018;9(28):20103–20111.
46. Feng C, Zhu D, Zou X, et al. The combination of a reduction in contrast agent dose with low tube voltage and an adaptive statistical iterative reconstruction algorithm in CT enterography: Effects on image quality and radiation dose. *Medicine (Baltimore)*. 2018;97(12):e0151.
47. Precht H, Thygesen J, Gerke O, Egstrup K, Waaler D, Lambrechtsen J. Influence of adaptive statistical iterative reconstruction algorithm on image quality in coronary computed tomography angiography. *Acta Radiol Open*. 2016;5(12):2058460116684884.

48. Noda Y, Goshima S, Koyasu H, et al. Renovascular CT: comparison between adaptive statistical iterative reconstruction and model-based iterative reconstruction. *Clin Radiol*. 2017;72(10):901.e13-901.e19.
49. Katsura M, Sato J, Akahane M, Mise Y, Sumida K, Abe O. Effects of pure and hybrid iterative reconstruction algorithms on high-resolution computed tomography in the evaluation of interstitial lung disease. *Eur J Radiol*. 2017;93:243–251.
50. Fontarensky M, Alfidja A, Perignon R, et al. Reduced Radiation Dose with Model-based Iterative Reconstruction versus Standard Dose with Adaptive Statistical Iterative Reconstruction in Abdominal CT for Diagnosis of Acute Renal Colic. *Radiology*. 2015;276(1):156–166.
51. Greess H, Nömayr A, Wolf H, et al. Dose reduction in CT examination of children by an attenuation-based on-line modulation of tube current (CARE Dose). *Eur Radiol*. 2002;12(6):1571–1576.
52. Greess H, Wolf H, Baum U, et al. Dose reduction in computed tomography by attenuation-based on-line modulation of tube current: evaluation of six anatomical regions. *Eur Radiol*. 2000;10(2):391–394.
53. Greess H, Wolf H, Baum U, Kalender WA, Bautz W. [Dosage reduction in computed tomography by anatomy-oriented attenuation-based tube-current modulation: the first clinical results]. *Rofo*. 1999;170(3):246–250.
54. Tang Y-C, Liu Y-C, Hsu M-Y, Tsai H-Y, Chen C-M. Adaptive Iterative Dose Reduction 3D Integrated with Automatic Tube Current Modulation for CT Coronary Artery Calcium Quantification: Comparison to Traditional Filtered Back

- Projection in an Anthropomorphic Phantom and Patients. *Acad Radiol.* 2018;([Epub ahead of print]).
55. Gang GJ, Siewerdsen JH, Webster Stayman J. Task-driven optimization of CT tube current modulation and regularization in model-based iterative reconstruction. *Phys Med Biol.* 2017;62(12):4777–4797.
 56. O’Hora L, Foley SJ. Iterative reconstruction and automatic tube voltage selection reduce clinical CT radiation doses and image noise. *Radiography (Lond).* 2018;24(1):28–32.
 57. Liu B, Gao S, Chang Z, Wang C, Liu Z, Zheng J. Lower extremity CT angiography at 80 kVp using iterative model reconstruction. *Diagn Interv Imaging.* 2018;[Epub ahead of print].
 58. Leithner D, Wichmann JL, Mahmoudi S, et al. Diagnostic yield of 90-kVp low-tube-voltage carotid and intracerebral CT-angiography: effects on radiation dose, image quality and diagnostic performance for the detection of carotid stenosis. *Br J Radiol.* 2018;20170927.
 59. Gräni C, Vontobel J, Benz DC, et al. Ultra-low-dose coronary artery calcium scoring using novel scoring thresholds for low tube voltage protocols-a pilot study. *Eur Heart J Cardiovasc Imaging.* 2018;[Epub ahead of print].
 60. Gnannt R, Winklehner A, Goetti R, Schmidt B, Kollias S, Alkadhi H. Low kilovoltage CT of the neck with 70 kVp: comparison with a standard protocol. *AJNR Am J Neuroradiol.* 2012;33(6):1014–1019.

61. Björkdahl P, Nyman U. Using 100- instead of 120-kVp computed tomography to diagnose pulmonary embolism almost halves the radiation dose with preserved diagnostic quality. *Acta Radiol.* 2010;51(3):260–270.
62. Nyman U, Björkdahl P, Olsson M-L, Gunnarsson M, Goldman B. Low-dose radiation with 80-kVp computed tomography to diagnose pulmonary embolism: a feasibility study. *Acta Radiol.* 2012;53(9):1004–1013.
63. Wichmann JL, Hu X, Kerl JM, et al. 70 kVp computed tomography pulmonary angiography: potential for reduction of iodine load and radiation dose. *J Thorac Imaging.* 2015;30(1):69–76.
64. Li X, Ni QQ, Schoepf UJ, et al. 70-kVp High-pitch Computed Tomography Pulmonary Angiography with 40 mL Contrast Agent: Initial Experience. *Acad Radiol.* 2015;22(12):1562–1570.
65. Shimoyama S, Nishii T, Watanabe Y, et al. Advantages of 70-kV CT Angiography for the Visualization of the Adamkiewicz Artery: Comparison with 120-kV Imaging. *AJNR Am J Neuroradiol.* 2017;38(12):2399–2405.
66. Fukuyama N, Kurata A, Kawaguchi N, et al. Two-Phase Contrast Injection Protocol for Pediatric Cardiac Computed Tomography in Children with Congenital Heart Disease. *Pediatr Cardiol.* 2018;39(3):518–525.
67. Annoni AD, Mancini ME, Andreini D, et al. Overall evaluability of low dose protocol for computed tomography angiography of thoracic aorta using 80 kV and iterative reconstruction algorithm using different concentration contrast media. *J Med Imaging Radiat Oncol.* 2017;61(5):614–621.

68. Park JE, Choi YH, Cheon J-E, et al. Image quality and radiation dose of brain computed tomography in children: effects of decreasing tube voltage from 120 kVp to 80 kVp. *Pediatr Radiol*. 2017;47(6):710–717.
69. Sun J, Zhang Q, Duan X, et al. Application of a full model-based iterative reconstruction (MBIR) in 80 kVp ultra-low-dose paranasal sinus CT imaging of pediatric patients. *Radiol Med*. 2018;123(2):117–124.
70. Zhang LJ, Li X, Schoepf UJ, et al. Non-ECG-Triggered 70-kVp High-Pitch Computed Tomography Angiography of the Whole Aorta With Iterative Reconstruction: Initial Results. *J Comput Assist Tomogr*. 2016;40(1):109–117.
71. Albrecht MH, Bickford MW, Schoepf UJ, et al. Beam-hardening in 70-kV Coronary CT angiography: Artifact reduction using an advanced post-processing algorithm. *European Journal of Radiology*. 2018;101:111–117.
72. Noël PB, Renger B, Fiebich M, et al. Does iterative reconstruction lower CT radiation dose: evaluation of 15,000 examinations. *PLoS ONE*. 2013;8(11):e81141.
73. Noumeir R. Benefits of the DICOM modality performed procedure step. *J Digit Imaging*. 2005;18(4):260–269.
74. Noumeir R. Benefits of the DICOM structured report. *J Digit Imaging*. 2006;19(4):295–306.
75. Jahnen A, Kohler S, Hermen J, Tack D, Back C. Automatic computed tomography patient dose calculation using DICOM header metadata. *Radiat Prot Dosimetry*. 2011;147(1–2):317–320.

76. Boos J, Meineke A, Rubbert C, et al. Cloud-Based CT Dose Monitoring using the DICOM-Structured Report: Fully Automated Analysis in Regard to National Diagnostic Reference Levels. *Rofo*. 2016;188(3):288–294.
77. Guberina N, Suntharalingam S, Naßenstein K, et al. Clinical evaluation of a dose monitoring software tool based on Monte Carlo Simulation in assessment of eye lens doses for cranial CT scans. *Neuroradiology*. 2016;58(10):955–959.
78. Kim YY, Shin HJ, Kim MJ, Lee M-J. Comparison of effective radiation doses from X-ray, CT, and PET/CT in pediatric patients with neuroblastoma using a dose monitoring program. *Diagn Interv Radiol*. 2016;22(4):390–394.
79. Kim J, Yoon Y, Seo D, Kwon S, Shim J, Kim J. Real-Time Patient Radiation Dose Monitoring System Used in a Large University Hospital. *J Digit Imaging*. 2016;29(5):627–634.
80. McCollough CH. CT dose: how to measure, how to reduce. *Health Phys*. 2008;95(5):508–517.
81. Alikhani B, Getzin T, Kaireit TF, et al. Correlation of size-dependent conversion factor and body-mass-index using size-specific dose estimates formalism in CT examinations. *Eur J Radiol*. 2018;100:130–134.
82. Kawashima H, Ichikawa K, Hanaoka S, Matsubara K, Takata T. Relationship between size-specific dose estimates and image quality in computed tomography depending on patient size. *J Appl Clin Med Phys*. 2018;[Epub ahead of print].

83. Boos J, Kröpil P, Bethge OT, et al. Accuracy of size-specific dose estimate calculation from center slice in computed tomography. *Radiat Prot Dosimetry*. 2018;178(1):8–19.
84. Kanal KM, Butler PF, Sengupta D, Bhargavan-Chatfield M, Coombs LP, Morin RL. U.S. Diagnostic Reference Levels and Achievable Doses for 10 Adult CT Examinations. *Radiology*. 2017;284(1):120–133.
85. Butler PF, Kanal KM. Diagnostic Reference Levels for Adult Patients in the United States. *J Am Coll Radiol*. 2018;15(6):932–933.
86. Strauss KJ, Goske MJ, Towbin AJ, et al. Pediatric Chest CT Diagnostic Reference Ranges: Development and Application. *Radiology*. 2017;284(1):219–227.
87. Boos J, Thomas C, Appel E, et al. Institutional computed tomography diagnostic reference levels based on water-equivalent diameter and size-specific dose estimates. *J Radiol Prot*. 2018;38(2):536–548.
88. EuroSafe Imaging Together - for patient safety. <http://www.eurosafeimaging.org/>. Accessed June 12, 2018.
89. EuroSafe Imaging Together - for patient safety. <http://www.eurosafeimaging.org/euclid>. Accessed June 12, 2018.

4. Danksagung

Mein besonderer Dank gilt Herrn Univ.-Prof. Dr. med. Gerald Antoch für die außergewöhnliche Förderung meiner wissenschaftlichen Entwicklung und meiner klinischen Ausbildung.

Herrn Prof. Dr. med. Patric Kröpil danke ich für die fortwährende Förderung, die umfassende Unterstützung und die freundschaftliche Zusammenarbeit bei der Planung, Durchführung und Auswertung von wissenschaftlichen Studien.

Ich danke Herrn Prof. Dr. Christoph Thomas, ohne dessen Unterstützung und umfangreiches Wissen viele der wissenschaftlichen Projekte der letzten Jahre nicht möglich gewesen wären.

Bei Frau Prof. Olga Brook und Herrn Prof. Vassilios Raptopoulos möchte ich mich ganz herzlich für eine aufregende und lehrreiche Zeit am Beth Israel Deaconess Medical Center in Boston bedanken. Beide haben mich außergewöhnlich gefördert und meinen wissenschaftlichen Werdegang maßgeblich geprägt. In diesem Zusammenhang danke ich Herrn Prof. Dr. med. Rotem Shlomo Lanzman für fortwährende Unterstützung danken.

Ich danke Herrn Univ.-Prof. Dr. Cornelius Faber vom Institut für klinische Radiologie der Universitätsklinik Münster, der mir im Rahmen meiner Promotion die Grundlagen des wissenschaftlichen Arbeitens vermittelt hat.

Zudem möchte ich mich bei Herrn Dr. med. Joel Aissa, Herrn Dr. med. Christoph Schleich, Herrn Dr. med. Lino Sawicki und Frau Elisabeth Appel für die freundschaftliche und von Hilfsbereitschaft geprägte Zusammenarbeit in den letzten Jahren bedanken.

Ich danke unseren Kooperationspartnern Dipl.- Ing. Axel Meineke und Marc Piechura. Nur durch die Zusammenarbeit mit unseren Kooperationspartnern waren die durchgeführten Projekte möglich. Gleichzeitig danke ich Herrn Dipl.- Ing. Oliver Th. Bethge, Leiter der Radiologischen Netzwerke des Instituts für Diagnostische und Interventionelle Radiologie der Universitätsklinik Düsseldorf, für die umfassende Unterstützung bei der Umsetzung sämtlicher technischer Fragestellungen.

Darüber hinaus gilt mein Dank allen Mitarbeitern des Instituts für Diagnostische und Interventionelle Radiologie für die stets kollegiale Zusammenarbeit im klinischen Alltag sowie die Unterstützung der wissenschaftlichen Projekte.

Über allem steht aber meine Familie, die mich während dieser gesamten Zeit unterstützt und motiviert hat. Vielen Dank für den Rückhalt und für die Hilfe bei jeglicher Art von Sorgen und Problemen.

Insbesondere danke ich an dieser Stelle meiner Ehefrau Nina. Ohne ihre umfassende, ausdauernde und liebevolle Unterstützung wäre diese Arbeit nicht möglich gewesen.

5. Zugrunde liegende Forschungsarbeiten

Evaluation of the impact of organ-specific dose reduction on image quality in pediatric chest computed tomography

Johannes Boos · Patric Kröpil · Dirk Klee · Philipp Heusch · Lars Schimmöller · Jörg Schaper · Gerald Antoch · Rotem S. Lanzman

Received: 23 October 2013 / Revised: 18 February 2014 / Accepted: 26 February 2014 / Published online: 29 March 2014
© Springer-Verlag Berlin Heidelberg 2014

Abstract

Background Organ-specific dose reduction significantly reduces the radiation exposure of radiosensitive organs.

Objective The purpose of this study was to assess the impact of a novel organ-specific dose reduction algorithm on image quality of pediatric chest CT.

Materials and methods We included 28 children (mean age 10.9 ± 4.8 years, range 3–18 years) who had contrast-enhanced chest CT on a 128-row scanner. CT was performed at 100 kV using automated tube current modulation and a novel organ-specific dose-reduction algorithm (XCare™; Siemens, Forchheim, Germany). Seven children had a previous chest CT performed on a 64-row scanner at 100 kV without organ-specific dose reduction. Subjective image quality was assessed using a five-point scale (1-not diagnostic; 5-excellent). Contrast-to-noise ratio (CNR) and signal-to-noise ratio (SNR) were assessed in the descending aorta.

Results Overall mean subjective image quality was 4.1 ± 0.6 . In the subgroup of the seven children examined both with and without organ-specific dose reduction, subjective image quality was comparable (score 4.4 ± 0.5 with organ-specific dose reduction vs. 4.4 ± 0.7 without it; $P > 0.05$). There was no significant difference in mean signal-to-noise ratio and contrast-to-noise ratio with organ-specific dose reduction (38.3 ± 10.1 and 28.5 ± 8.7 , respectively) and without the reduction (35.5 ± 8.5 and 26.5 ± 7.8 , respectively) ($P > 0.05$). Volume computed tomography dose index (CTDI_{vol}) and size-specific dose estimates did not differ significantly between acquisitions with the organ-specific dose reduction ($1.7 \pm$

0.8 mGy) and without the reduction (1.7 ± 0.8 mGy) ($P > 0.05$).

Conclusion Organ-specific dose reduction does not have an impact on image quality of pediatric chest CT and can therefore be used in clinical practice to reduce radiation dose of radiosensitive organs such as breast and thyroid gland.

Keywords Organ-specific dose reduction · Chest CT · Children · Dose reduction · Image quality

Introduction

Ionizing radiation as used in conventional radiography and CT may increase the risk of malignancies by damaging the DNA [1, 2]. The development of radiation-related risks is time-dependent and accumulates over the years [1, 2]. Because of a longer remaining lifetime and a higher radiosensitivity (e.g., a larger number of faster-dividing cells), the risk for the development of malignancies caused by ionizing radiation is higher in children than in adults [1, 2]. Thus, the indication for pediatric CT examinations must be carefully controlled by the radiologist. Alternative procedures like US imaging and MRI should be performed whenever possible [1, 3–5].

Between 1996 and 2009 the number of CT examinations more than doubled in the Western world [6, 7]. Although only 8% of the diagnostic imaging examinations using ionizing radiation are CT scans, they contribute to 60% of the collective radiation dose [6].

Pediatric chest CT is routinely used for workup of various diseases including staging and follow-up of malignancies as well as acute and chronic inflammatory diseases and anatomical anomalies [8–11]. In chest CT, radiation-sensitive organs like the thyroid gland and the female breast are usually included in the scan volume. Therefore reduction of radiation dose in each CT examination has gained ever more interest in

J. Boos · P. Kröpil (✉) · D. Klee · P. Heusch · L. Schimmöller · J. Schaper · G. Antoch · R. S. Lanzman
Department of Diagnostic and Interventional Radiology,
University Dusseldorf, Medical Faculty,
D-40225 Dusseldorf, Germany
e-mail: Patric.Kroepil@med.uni-duesseldorf.de

modern radiology. For this purpose, organ-specific dose reduction algorithms have been recently introduced [12–14]. This novel algorithm reduces the tube current time product for anterior projections to lower the organ dose of radiosensitive organs near the anterior body surface like breast parenchyma and thyroid gland [13]. Initial phantom studies by Ketelsen et al. [14] have demonstrated a potential organ dose reduction of about 30% in chest CT using organ-specific dose reduction.

Despite efforts to lower radiation exposure, the influence on the image quality has to be kept in mind and non-diagnostic image quality must be avoided.

The purpose of the present study was to investigate the effect of an organ-specific dose-reduction algorithm on objective and subjective image quality in pediatric chest CT.

Materials and methods

This retrospective study was approved by the local ethics committee of the Heinrich-Heine-University, Düsseldorf. We included 28 consecutive children (11 girls and 17 boys, mean age 10.9 ± 4.8 , range 3–18 years) who underwent contrast-enhanced chest CT on a 128-row CT scanner (Somatom Definition AS+; Siemens Healthcare, Forchheim, Germany) with the organ-specific dose reduction algorithm XCare™ (Siemens) installed as an upgrade on the scanner. Seven of the 28 children had undergone a prior contrast-enhanced CT-examination with identical acquisition parameters (tube potential [kV], pitch, rotation time) but without XCare™ on a 64-row CT scanner (Somatom Sensation Cardiac 64, Siemens Healthcare, Forchheim, Germany). The average time interval between CT scans with and without organ-specific dose reduction was 425 days (range 10–929 days) in the seven children.

CT scans were performed following intravenous injection of 1.5 ml/kg body weight of iodinated contrast material (Accupaque 300; GE Healthcare, Munich, Germany). Bolus tracking with a threshold of 100 HU in the descending aorta was used to coincide the beginning of the scan with vascular enhancement.

Automated tube current modulation was activated in all CT scans (CAREDose 4D; Siemens Healthcare, Forchheim, Germany). Scan parameters for CT examinations with and without XCare™ are listed in Table 1.

In the seven children with repeated examinations, CT scans with organ-specific dose reduction were assigned to group A and CT examinations without the algorithm were assigned to group B.

Table 1 CT scan acquisition parameters

Scan parameter	128-row CT scanner	64-row CT scanner
kV	100	100
Reference mAs	87	75
Effective mAs	47 ± 16	44 ± 21
Pitch	0.6	0.6
Rotation time	0.35 s	0.35 s

Effective mAs (mean \pm standard deviation) for 28 and 7 children scanned with the 128- and 64-row scanners, respectively

Radiation dose

CTDI_{vol} was calculated in-line and extracted from the scanning protocol of each examination. Size-specific dose estimates were calculated using the latero-lateral diameter from the scout image according to Brady and Kaufman [15].

Subjective image quality

Two blinded radiologists (one with 7 years and one with 1 year of experience in chest CT) assessed subjective image quality on a PACS workstation (Sectra Medical Systems GmbH, Linköping, Sweden) using transverse 1-mm and 3-mm slices. In addition, sagittal and coronal multiplanar reconstructions were provided. Soft-tissue windows (50/350 [level/width] HU) and lung windows (−500/1,500 HU) were used; the evaluation and modulation of the windows were at the discretion of the reader. Rating was performed using a five-point scale (1-not diagnostic, 2-poor, 3-moderate, 4-good, 5-excellent) in all patients (Table 2).

Objective image quality

Regions of interest (ROIs) were placed on transverse 3-mm slices in the lumen of the descending aorta (ROI 1, 100–

Table 2 Five-point scale for the assessment of subjective image quality

Score	Assessment	
5	Excellent	Excellent resolution and contrast, no artifacts
4	Good	Good resolution and contrast, minimal artifacts
3	Moderate	Satisfying diagnostic value in spite of noise and artifacts
2	Poor	Reduced diagnostic value from artifacts and poor contrast
1	Unacceptable	Non-diagnostic scan

250 mm²), in the erector spinae muscle (ROI 2, 100–250 mm²) and outside the body in the air (ROI 3 100–500 mm²). The standard deviation of ROI 3 (air) was used

as an indicator for image noise. Contrast-to-noise ratio (CNR) and signal-to-noise ratio (SNR) were calculated to assess the objective image quality [16]:

$$\text{SNR Ao} = \text{mean pixel value (ROI 1)}/\text{standard deviation (ROI 3)}$$

$$\text{CNR Ao} = [\text{mean pixel value (ROI 1)} - \text{mean pixel value (ROI 2)}]/\text{standard deviation (ROI 3)}$$

Statistical analysis

Data analysis was performed with IBM SPSS Statistics 21 for Windows (SPSS, Chicago, IL). Data are given as mean \pm standard deviation. A *P* value of <0.05 was considered statistically significant. To test for normal distribution a Kolmogorov–Smirnov test was performed. All continuous variables exhibited normal distribution according to the Kolmogorov–Smirnov test and therefore were tested with the independent student's *t*-test. The Mann–Whitney *U* test was used as a non-parametric test.

Interobserver agreement was assessed with Cohen's kappa statistics: excellent ($\kappa > 0.81$), good ($\kappa = 0.61$ – 0.80), moderate ($\kappa = 0.41$ – 0.60), fair ($\kappa = 0.21$ – 0.40) and poor ($\kappa \leq 0.20$) [17].

Results

Patients

Mean body weight of the 28 children at the time of the CT scan was 39.6 ± 19.9 kg. Mean body mass index (patient weight divided by the square of the patient height) was 18.5 ± 4.4 kg/m² in all patients. Mean age of group A was 11.8 ± 5.5 years compared to 10.4 ± 6.2 in group B ($P = 0.48$). The thyroid gland was included in the scanning volume in 26 of 28 (92.9%) patients.

Radiation dose

Overall mean CTDI_{vol} was 1.5 ± 0.8 mGy. In seven children with repeated CT scans, mean CTDI_{vol} was 1.7 ± 0.8 mGy in group A as compared to 1.7 ± 0.8 mGy in group B ($P = 0.92$). Overall size-specific dose estimates were 1.8 ± 0.9 mGy. In group A the size-specific dose estimates were 2.0 ± 0.7 mGy compared to 2.1 ± 0.8 mGy ($P = 0.8$). Overall difference between size-specific dose estimates and CTDI_{vol} was 18.5% ($P = 0.1$).

Subjective image quality

In 28 children the mean subjective image quality was 4.1 ± 0.6 (reader 1: 4.1 ± 0.6 , reader 2: 4.1 ± 0.7). Eighty-six percent of the CT scans with organ-specific dose reduction had excellent to good image quality. No CT examination was rated as non-diagnostic.

In the seven children with repeated exams, mean subjective image quality was 4.4 ± 0.5 (reader 1: 4.4 ± 0.5 , reader 2: 4.4 ± 0.5) in group A and 4.4 ± 0.7 (reader 1: 4.6 ± 0.8 , reader 2: 4.1 ± 0.7) in group B ($P = 0.96$) (Fig. 1). Inter-observer agreement was good ($\kappa = 0.61$).

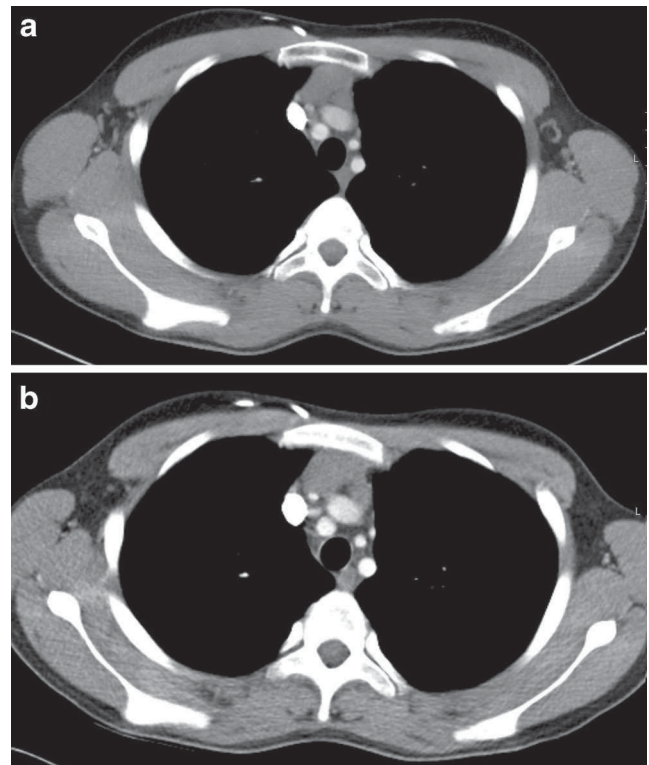


Fig. 1 Axial chest CT scans of the same child acquired with (a) and without (b) organ-specific dose reduction yield comparable image quality

Objective image quality

In the group of 28 children with organ-specific dose reduction the mean signal-to-noise ratio and contrast-to-noise ratio were 30.5 ± 11.4 and 21.8 ± 10.2 . In group A signal-to-noise ratio and contrast-to-noise ratio were 38.3 ± 10.3 and 28.5 ± 8.7 compared to 35.5 ± 8.5 and 26.5 ± 7.8 in group B, respectively (Table 3). Differences in signal-to-noise ratio and contrast-to-noise ratio between groups A and B were not statistically significant ($P=0.58$ and $P=0.65$, respectively).

Discussion

Every medical exposure to ionizing radiation has to be justified and kept as low as reasonably possible according to the ALARA principle (As Low As Reasonably Achievable) [18]. Despite growing concerns regarding exposure from ionizing radiation, the number of CT examinations has consistently increased during the last 30 years [1]. Especially for children, indications for every CT have to be reviewed carefully because children's tissue is more sensitive to radiation and they have a longer life expectancy than adults [1, 19]. In addition, potential radiation-related cancer risks accumulate over time [19]. Therefore it is important to reduce the radiation exposure of every CT scan in children [20]. However the image quality has to meet quality requirements to enable proper diagnosis.

Strategies for the reduction of CT radiation exposure have been introduced into clinical practice, e.g., iterative reconstruction [16], low-dose CT protocols [21], attenuation-based automatic kV selection [22] and bismuth shielding [23, 24]. Bismuth shielding might reduce the radiation exposure to the female breast by up to 37.5%, but it can also lead to an increase in artifacts and image noise [23, 24]. A recent study in children has shown that bismuth breast shields, when combined with angular tube current modulation, lead to increased artifacts and influence the contrast-to-noise ratio [25]. Because patient cooperation is required, bismuth shielding might be difficult to integrate into clinical routine, especially in younger children [26]. Because it is a hardware-based

system, the time per examination and examination costs might be increased [26].

Similar to bismuth shielding, the aim of the organ-specific dose reduction is the protection of radiosensitive organs near the anterior body surface such as the thyroid gland and the female breast from excessive radiation exposure. This is achieved by an angular beam modulation and reduced tube current for the anterior 120° , while tube current is slightly increased for the posterior 240° projections [26, 27].

Studies have demonstrated that radiation exposure to these organs can be significantly reduced by organ-specific dose-reduction techniques in females (breast 25–48%, thyroid gland 20%) [14, 23, 28]. Therefore, it is reasonable to use this dose-reduction technique even in male patients, because in 26 out of 28 CT scans in our study cohort the thyroid gland was included in the image volume.

Any approach to reduce radiation can be integrated into clinical routine only if image quality is not affected significantly. In this study we have shown that organ-specific dose reduction does not compromise the image quality of pediatric chest CT scans—good to excellent image quality was achieved in 86% of all patients and there were no non-diagnostic scans. The 14% with less than good image quality showed discrete blurring and indistinction. Furthermore, in the seven children in whom an intra-individual comparison was available, no significant difference in subjective and objective image quality was observed between scans with and without organ-specific dose reduction.

Because the $CTDI_{vol}$ tends to underestimate the radiation exposure to pediatric patients, the use of size-specific dose estimates is recommended by the American Association of Physicists in Medicine (AAPM) [16]. In this study we calculated size-specific dose estimates by using the anteroposterior scouts because lateral scouts were not available. Overall there was no significant difference in $CTDI_{vol}$ and size-specific dose estimates between groups A and B.

As a software-based technique, organ-specific dose reduction can be integrated into clinical routine relatively effortlessly. Low-dose CT protocols, adaptive statistical iterative reconstruction and attenuation-based automatic kV selection are all software-based techniques that have already been integrated into CT scanners. These techniques can be combined to maintain image quality while reducing radiation dose. Siegel et al. [29] showed a dose reduction of up to 56% for CT angiography when combining automated tube voltage selection and automated tube current modulation on phantoms. In our study XCare™ was combined with automated tube current modulation. Hence, a combination of the organ-specific dose reduction algorithm with other dose-saving algorithms should be feasible, but the potential influence on image quality requires further investigation [30].

Our study has some limitations. In children with an intra-individual comparison, examinations with organ-specific dose

Table 3 Objective image quality

Group	OSDR	SNR	CNR
Overall	+	30.5 ± 11.4	21.8 ± 10.2
A	+	38.3 ± 10.3	28.5 ± 8.7
B	–	35.5 ± 8.5	26.5 ± 7.8

Groups A and B represent the seven children who had scans both with dose reduction (A) and without dose reduction (B)

CNR contrast-to-noise ratio, OSDR used organ-specific dose reduction algorithm, SNR signal-to-noise ratio

Overall means all scans performed with OSDR

reduction were performed on a 128-row scanner whereas examinations without the algorithm were performed on a 64-row scanner. Because basic acquisition parameters were constant, we do not expect a significant influence of the different number of detector rows on our results. We did not perform phantom measurements to quantify dose reduction in breast tissue and the thyroid gland for our imaging parameters. Furthermore, because of the smaller body surface in children, dose reduction to radiosensitive tissues in children might deviate from results in adults. The indication for pediatric chest CT has to be justified, and consequently the number of children included in this analysis is relatively small.

Conclusion

Implementation of a novel organ-specific dose-reduction algorithm into pediatric chest CT protocols is feasible and does not impair image quality. Therefore organ-specific dose reduction can be recommended for clinical routine for pediatric chest CT to reduce radiation to radiosensitive organs such as breast and thyroid gland.

Conflicts of interest None

References

- Brenner DF, Hall EJ (2007) Computed tomography—an increasing source of radiation exposure. *N Engl J Med* 357:2277–2284
- National Research Council (NRC) (2006) Health risks from exposure to low levels of ionizing radiation (BEIR VII)—phase 2. The National Academies Press, Washington DC
- Stephen AE, Segev DL, Ryan DP et al (2003) The diagnosis of acute appendicitis in a pediatric population: to CT or not to CT. *J Pediatr Surg* 38:367–371
- Smyth MD, Narayan P, Tubbs RS et al (2008) Cumulative diagnostic radiation exposure in children with ventriculoperitoneal shunts: a review. *Childs Nerv Syst* 24:493–497
- Mandiwanza T, Saidleir C, Caird J et al (2013) The open fontanelle: a window to less radiation. *Childs Nerv Syst* 29:1177–1181
- Bernhard-Ströl C, Hachenberger C, Trugenberger-Schnabel A et al. (2012) Environmental radioactivity and radiation exposure in 2010. German Federal Ministry for the Environment, Nature Conservation, Building and Nuclear Safety. German government briefing
- Smith-Bindman R, Miglioretti DL, Johnson E et al (2012) Use of diagnostic imaging studies and associated radiation exposure for patients enrolled in large integrated health care systems, 1996–2010. *JAMA* 307:2400–2409
- Bakshi S, Radhakrishnan V, Sharma P et al (2012) Pediatric nonlymphoblastic non-Hodgkin lymphoma: baseline, interim, and posttreatment PET/CT versus contrast-enhanced CT for evaluation – a prospective study. *Radiology* 262:956–968
- Furth C, Denecke T, Steffen I et al (2006) Correlative imaging strategies implementing CT, MRI, and PET for staging of childhood Hodgkin disease. *J Pediatr Hematol Oncol* 28:501–512
- Szolar DH, Zebedin D, Unger B et al (1999) Radiologic staging of renal cell carcinoma. *Radiologe* 39:584–590
- Tiddens HA (2006) Chest computed tomography scans should be considered as a routine investigation in cystic fibrosis. *Paediatr Respir Rev* 7:202–208
- Strauss KJ, Goske MJ, Kaste SC et al (2010) Image Gently: ten steps you can take to optimize image quality and lower CT dose for pediatric patients. *AJR Am J Roentgenol* 194:868–873
- Duan X, Wang J, Christner JA et al. (2011) Dose reduction to anterior surfaces with organ-based tube-current modulation: evaluation of performance in a phantom study. *AJR* 197:689–695
- Ketelsen D, Buchgeister M, Fenchel M et al (2012) Automated computed tomography dose-saving algorithm to protect radiosensitive tissues. *Investig Radiol* 47:148–152
- Brady SL, Kaufman RA (2012) Investigation of American Association of Physicists in Medicine report 204: size-specific dose estimates for pediatric CT implementation. *Radiology* 265:832–840
- Lee SH, Kim MJ, Yoon CS et al (2012) Radiation dose reduction with the adaptive statistical iterative reconstruction (ASIR) technique for chest CT in children: an intra-individual comparison. *Eur J Radiol* 81:938–943
- Landis JR, Koch GG (1977) The measurement of observer agreement for categorical data. *Biometrics* 33(1):159–17
- The Council of the European Union (1997) Council directive 97/43/Euratom of 30 June 1997 on health protection of individuals against the dangers of ionizing radiation in relation to medical exposure, and repealing directive Euratom. Official journal L 180, pp 22–27. <http://eur-lex.europa.eu/LexUriServ/LexUriServ.do?uri=CELEX:31997L0043:EN:HTML>. Accessed 21 Feb 2014
- Pearce MS, Salotti JA, Little MP et al (2012) Radiation exposure from CT scans in childhood and subsequent risk of leukaemia and brain tumours: a retrospective cohort study. *Lancet* 380:499–505
- Lobo L, Antunes D (2013) Chest CT in infants. *Eur J Radiol* 82:1108–1117
- Vazquez JL, Pombar MA, Pumar JM et al (2013) Optimised low-dose multidetector CT protocol for children with cranial deformity. *Eur Radiol* 23:2279–2287
- Eller A, May MS, Scharf M et al (2012) Attenuation-based automatic kilovolt selection in abdominal computed tomography: effects on radiation exposure and image quality. *Investig Radiol* 47:559–565
- Vollmar SV, Kalender WA (2008) Reduction of dose to the female breast in thoracic CT: a comparison of standard-protocol, bismuth-shielded, partial and tube-current-modulated CT examinations. *Eur Radiol* 18:1674–1682
- Kim YK, Sung YM, Choi JH et al (2013) Reduced radiation exposure of the female breast during low-dose chest CT using organ-based tube current modulation and a bismuth shield: comparison of image quality and radiation dose. *AJR Am J Roentgenol* 200:537–544
- Servaes S, Zhu X (2013) The effects of bismuth breast shields in conjunction with automatic tube current modulation in CT imaging. *Pediatr Radiol* 43:1287–1294
- Schimmöller L, Lanzman RS, Heusch P et al (2013) Impact of organ-specific dose reduction on the image quality of head and neck CT angiography. *Eur Radiol* 23:1503–1509
- Strauss KJ, Goske MJ (2011) Estimated pediatric radiation dose during CT. *Pediatr Radiol* 41:S472–S482
- Reimann AJ, Davison C, Bjarnason T et al (2012) Organ-based computed tomographic (CT) radiation dose reduction to the lenses: impact on image quality for CT of the head. *J Comput Assist Tomogr* 36:334–338
- Siegel MJ, Ramirez-Giraldo JC, Holdebolt C et al (2013) Automated low-kilovoltage selection in pediatric computed tomography angiography, phantom study evaluation effects on radiation dose and image quality. *Investig Radiol* 48:584–589
- Schwarz F, Grandl K, Arnoldi A et al (2013) Lowering radiation exposure in CT angiography using automated tube potential selection and optimized iodine delivery rate. *AJR Am J Roentgenol* 200:W628–W634



Dose monitoring using the DICOM structured report: assessment of the relationship between cumulative radiation exposure and BMI in abdominal CT



J. Boos^{a,*}, R.S. Lanzman^a, A. Meineke^b, P. Heusch^a, L.M. Sawicki^a,
G. Antoch^a, P. Kröpil^a

^aDepartment of Diagnostic and Interventional Radiology, Medical Faculty, University of Düsseldorf, Germany

^bSiemens AG, Regional Cluster Deutschland, Sector Healthcare, Germany

ARTICLE INFORMATION

Article history:

Received 24 July 2014

Received in revised form

30 October 2014

Accepted 3 November 2014

AIM: To perform a systematic, large-scale analysis using the Digital Imaging and Communication in Medicine structured report (DICOM-SR) to assess the relationship between body mass index (BMI) and radiation exposure in abdominal CT.

MATERIALS AND METHODS: A retrospective analysis of DICOM-SR of 3121 abdominal CT examinations between April 2013 and March 2014 was performed. All examinations were conducted using a 128 row CT system. Patients (mean age 61 ± 15 years) were divided into five groups according to their BMI: group A $<20 \text{ kg/m}^2$ (underweight), group B $20\text{--}25 \text{ kg/m}^2$ (normal weight), group C $25\text{--}30 \text{ kg/m}^2$ (overweight), group D $30\text{--}35 \text{ kg/m}^2$ (obese), and group E $> 35 \text{ kg/m}^2$ (extremely obese). CT dose index (CTDI_{vol}) and dose-length product (DLP) were compared between all groups and matched to national diagnostic reference values.

RESULTS: The mean CTDI_{vol} and DLP were $5.4 \pm 2.9 \text{ mGy}$ and $243 \pm 153 \text{ mGy}\cdot\text{cm}$ in group A, $6 \pm 3.6 \text{ mGy}$ and $264 \pm 179 \text{ mGy}\cdot\text{cm}$ in group B, $7 \pm 3.6 \text{ mGy}$ and $320 \pm 180 \text{ mGy}\cdot\text{cm}$ in group C, $8.1 \pm 5.2 \text{ mGy}$ and $375 \pm 306 \text{ mGy}\cdot\text{cm}$ in group D, and $10 \pm 8 \text{ mGy}$ and $476 \pm 403 \text{ mGy}\cdot\text{cm}$ in group E, respectively. Except for group A versus group B, CTDI_{vol} and DLP differed significantly between all groups ($p < 0.05$). Significantly more CTDI_{vol} values exceeded national diagnostic reference values in groups D and E (2.1% and 6.3%) compared to group B (0.5%, $p < 0.05$).

CONCLUSION: DICOM-SR is a comprehensive, fast, and reproducible way to analyse dose-related data at CT. It allows for automated evaluation of radiation dose in a large study population. Dose exposition is related to the patient's BMI and is increased by up to 96% for extremely obese patients undergoing abdominal CT.

© 2014 The Royal College of Radiologists. Published by Elsevier Ltd. All rights reserved.

* Guarantor and corresponding author: J. Boos, University Dusseldorf, Medical Faculty, Department of Diagnostic and Interventional Radiology, Moorenstraße 5, 40225 Düsseldorf, Germany. Tel.: +49 (0) 211/8117754.

E-mail address: Johannes.Boos@med.uni-duesseldorf.de (J. Boos).

<http://dx.doi.org/10.1016/j.crad.2014.11.002>

0009-9260/© 2014 The Royal College of Radiologists. Published by Elsevier Ltd. All rights reserved.

Introduction

Dose monitoring of radiological examinations has become ever more important in order to improve radiation protection of patients and to meet legal requirements. In

Germany, CT only accounts for 8% of all diagnostic examinations using ionizing radiation but generates about 60% of the collective medical radiation dose¹ indicating the importance of systematic dose management and analysis of dose-related data in CT.

In recent years, various methods of dose monitoring and analysing have been introduced, for example, Digital Imaging and Communication in Medicine structured report (DICOM-SR), DICOM modality performed procedure step messages (MPPS), and image recognition and usage of the DICOM header.^{2,3} The DICOM standard was introduced in 1993. It was initially established to store and share medical images and image-related data^{4,5} and to provide a structured way to organize radiological reports. Despite ongoing discussions regarding the value and utility of the DICOM-SR,^{6,7} the DICOM standard is today an essential part of almost every medical device using ionizing radiation. The DICOM radiation dose structured report (DICOM-RDSR) provides radiation dose parameters within the DICOM-SR allowing for automated analysis of dose-related data. CT-related dose parameters [volume computed tomography dose index (CTDI_{vol}) and dose-length product (DLP)] for all examinations are stored in the DICOM-RDRS.

Body mass index (BMI) is defined by a person's weight (in kilograms) divided by the square of the height (in metres). BMI is seen as the most useful population-level measurement of weight and obesity.⁸ Obesity is defined as a BMI ≥ 30 kg/m² and a BMI of 25–30 kg/m² is considered overweight.⁸

Worldwide obesity has constantly increased and has nearly doubled since 1980.⁸ The newest data from the World Health Organization (WHO) from 2013 state a total of 1.4 billion adults are overweight and over 500 million men and women are obese. This equals 35% of all adults >20 years being overweight and 11% being obese. In 2011, >40 million children ≤ 5 years were overweight.^{8,9}

There are numerous studies dealing with CT radiation dose reduction, most of them present technical improvements (e.g., iterative reconstruction, automated organ-based tube current modulation, and low dose protocols) and achieved dose reduction in reference to image quality.^{10–13} There have only been a small number of studies performing large-scale analysis of dose-related data in CT.^{13,14} The purpose of the present study was to use DICOM-SR to perform a large-scale, retrospective analysis of radiation exposure in CT. This was done by analysing abdominal CT dose data for patients grouped according to BMI.

Materials and methods

This retrospective study was approved by the local ethics committee of the Medical Faculty of the University of Düsseldorf. All abdominal CT examinations conducted using a 128 section CT machine (SOMATOM Definition AS+, Siemens Healthcare, Forchheim, Germany) between April 2013 and March 2014 were included in this analysis.

All examinations were analysed with regard to CTDI_{vol} and DLP. Data of all study examinations were compared to the reference dose parameters defined by the German Federal Office of Radiation Protection (BfS). Reference levels are set by the BfS according to the third quartiles of the mean patient exposition evaluated in a large collective. The reference parameters for adult patients regarding abdominal CT are a CTDI_{vol} of 20 mGy and a DLP of 900 mGy·cm. As reference parameters are set for every single scan, multiphase examinations were evaluated separately for every scan performed. As the BfS reference parameters are organ based, different imaging protocols are assigned to the same reference parameter.¹⁵ Examinations in this study were performed for abdominal contrast-enhanced CT (1545 scans), low-dose CT for nephrolithiasis (108 scans), abdominal aortography (227 scans), and others (62 scans).

For analysis with respect to the BMI, patients were divided into five groups to account for the clinical classification of underweight, normal weight, overweight, and obesity: group A <20 kg/m², group B 20–25 kg/m², group C 25–30 kg/m², group D 30–35 kg/m², group E > 35 kg/m². To perform a more precise analysis, the obese subgroup (BMI > 30 kg/m²) was subdivided in two groups (30–35 and >35 kg/m²).

A DICOM-SR providing the dose-related CT parameters was automatically generated by the CT system for each examination. Weight and height of the patients were entered into the DICOM-SR during the examination by the technician. Mis-entry was prevented by an inflexible input mask in the database and subsequent manual verification. All indeterminate entries (e.g., >212 kg) were removed from the analysis.

Automated tube current modulation was assessed as a system-indicated measure. It was generally activated in all protocols except for cases in which elevation of the arms was restricted.

Data were extracted from the local picture archiving and communications system (PACS) using the free-of-charge tool CareAnalytics™ (Siemens Healthcare, Forchheim, Germany) and saved in extensible mark-up language (XML); the files were then transferred into Dose-Intelligence (Pulmokard GmbH, Herdecke, Germany). Height and weight of the patients were verified in the database and all unclear or uncertain cases were excluded from the analysis. Dose-Intelligence and Excel 2013 (including Powerview and Powerpivot, Microsoft, Redmond, WA, USA) were used to perform data analysis.

Statistical analysis was conducted using IBM SPSS Statistics 22 for Windows (SPSS, Chicago, IL, USA). A *p*-value of <0.05 was considered to indicate statistical significance.

Data were tested for normal distribution with a Kolmogorov test. Normally distributed data are given as mean \pm standard deviation. A Kruskal–Wallis test was used as a non-parametric test. Analysis of variance (ANOVA) with Tukey's honestly significant difference (Tukey's HSD) and Fisher's exact test were used to test for statistical significance.

Results

Examinations and patients

Three thousand, one hundred and twenty-one CT examinations of the abdomen were performed during the study period. Heights and weights of the patients were available for 1955 examinations. Thirteen CT examinations were excluded from the analysis because the patient's age was <16 years, and therefore, the BMI would have been inaccurate.⁹ Finally, 1942 patients (1139 male, 803 female, mean age 60.9 ± 15 years, mean BMI 25.5 ± 5 kg/m²) were included in the analysis. The distribution of patients to the different BMI groups is shown in Fig. 1. For the different groups, the mean BMI was 18 ± 1.5 kg/m² (group A), 22.7 ± 1.4 kg/m² (group B), 27.3 ± 1.4 kg/m² (group C), 32.1 ± 1.4 kg/m² (group D), and 38.4 ± 3.0 kg/m² (group E; Fig. 1, Table 1). Segmentation according to tube voltage is illustrated in Fig. 1 and Table 2. There were no significant differences in the distribution of different imaging protocols between groups A–E ($p > 0.05$).

The overall mean CTDI_{vol} was 6.7 ± 4.1 mGy and mean DLP was 303 ± 214 mGy·cm, and therefore, were 33% and 34% of the national reference values, respectively (Fig. 2). There were significant differences in the CTDI_{vol} and DLP between all groups ($p < 0.05$) except for group A versus

Table 1

Mean BMI, CTDI_{vol} and DLP for the different groups.

Group	Number	Mean BMI (kg/m ²)	CTDI _{vol} (mGy)	DLP (mGy·cm)
Overall	1942	25.5 ± 5	6.7 ± 4.1	303 ± 214
a	208	18 ± 1.5	5.4 ± 2.9	243 ± 153
b	784	22.7 ± 1.4	6 ± 3.6	264 ± 179
c	628	27.3 ± 1.4	7 ± 3.6	320 ± 180
d	242	32.1 ± 1.4	8.1 ± 5.2	375 ± 306
e	80	38.4 ± 3	10 ± 8	476 ± 403

BMI, body mass index; CTDI_{vol}, CT dose index; DLP, dose–length product.

group B. The CTDI_{vol} and DLP for the different groups are illustrated in Table 1.

National reference values

In reference to the values provided by the BfS, 16 reference values for CTDI_{vol} and 23 reference values for DLP exceeded national reference values. This equals 0.8% for CTDI_{vol} and 1.2% for DLP of all analysed examinations. The distribution of these values according to BMI is illustrated in Fig. 3. The number of CTDI_{vol} and DLP values exceeding the national reference values was significantly higher in groups E and D compared to group B (6.3% and 2.1% versus 0.5% for CTDI, 8.9% and 2.1% versus 0.6% for DLP, $p < 0.05$, respectively; Fig. 3).

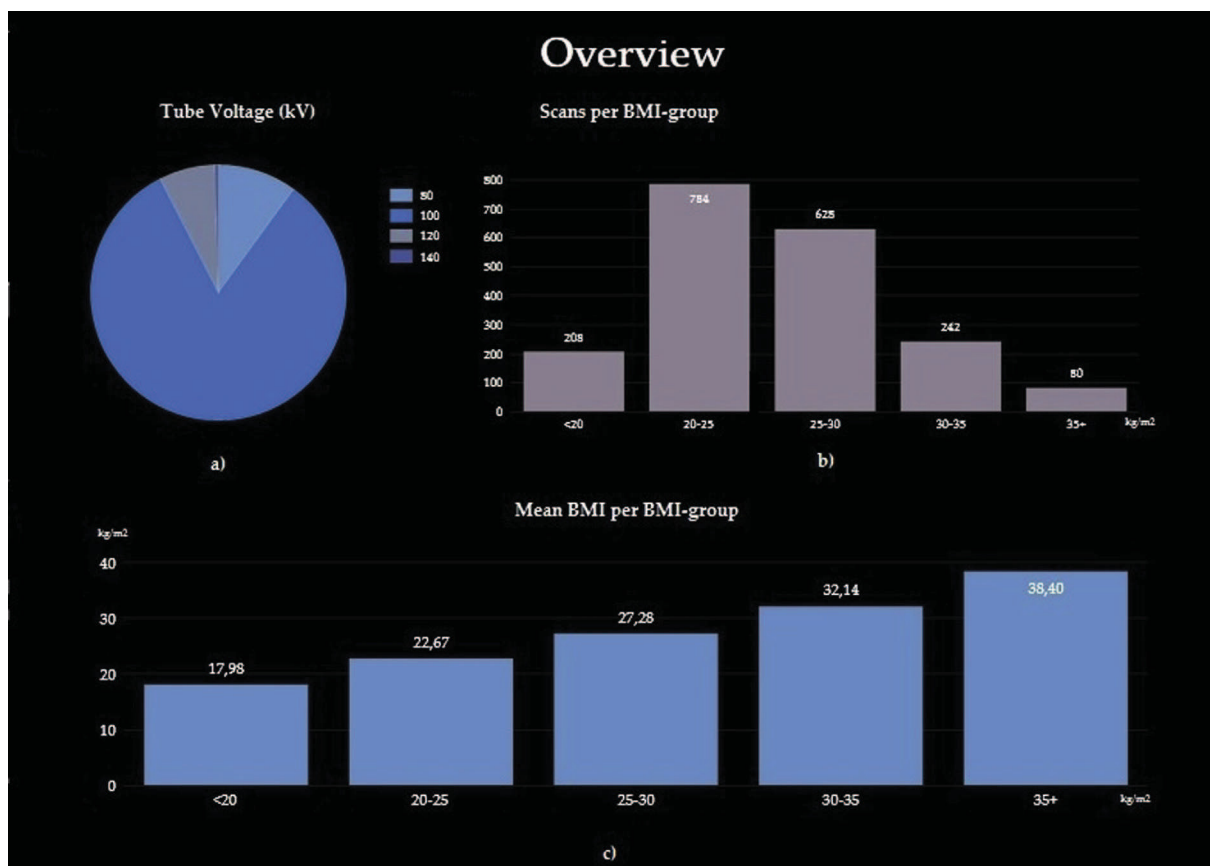


Figure 1 (a) The tube voltage for all CT examinations is illustrated. (b) The overall number of CT examinations per BMI group. (c) The mean BMI for every BMI group.

Table 2

Number of examinations performed with a specific tube voltage overall and within the different BMI groups ($p > 0.05$).

	80 kV	100 kV	120 kV	140 kV
Overall	195	1601	138	8
Group A	15	175	18	0
Group B	80	643	59	2
Group C	73	520	34	1
Group D	22	200	17	3
Group E	5	63	10	2

Automated tube current modulation

Automated tube current modulation (CareDose 4D, Siemens Healthcare, Forchheim Germany) was activated in 1620 examinations. Maximal tube current was reduced by a mean of 48.6% due to the activation of this dose-saving algorithm (Fig. 4). There was a significantly lower tube current reduction for patients in group E compared to all other groups (45.3% compared to 54.4% group A, 53.3% group B, 50.2% group C, and 50.6% group D; $p < 0.05$; Fig. 4).

Discussion

The number and indications for CT examinations have risen constantly over recent decades.^{1,16} In the United

States, for example, the number of CT examinations has increased from 52 to 149 per 1000 inhabitants between 1996 and 2010.¹⁷ Therefore, much effort has been made to reduce the amount of ionizing radiation received during CT. Dose-saving techniques, such as automated tube current modulation, semi-automated tube voltage selection, low-dose protocols, iterative reconstruction techniques, or organ-specific dose reduction, have been introduced into daily practice.^{10–12,18} With respect to the ALARA principle (“as low as reasonably achievable”) radiation dose has been substantially decreased over the past years.^{10,19,20} Whenever dose reduction is performed during CT, image quality remains a crucial factor, as a non-diagnostic examination must be avoided. Subjective image quality is noticed in every examination by the reading physician, and poor subjective image quality often leads directly to a correction of the examination protocol. The applied radiation dose, on the other hand, is often not actively noticed by the radiologist. However, a systematic approach of monitoring and analysis of dose-related data in CT, as presented in the present study, is a key factor for modern quality management and improvement of patient care in radiology.

Manual and semi-automated transfer of dose-related data by the technician or radiologist is a time-consuming procedure and suffers from a considerable error rate of up to 6%.²¹ Automatic approaches (as presented in this study) are preferable as an error of transfer is purged and as it

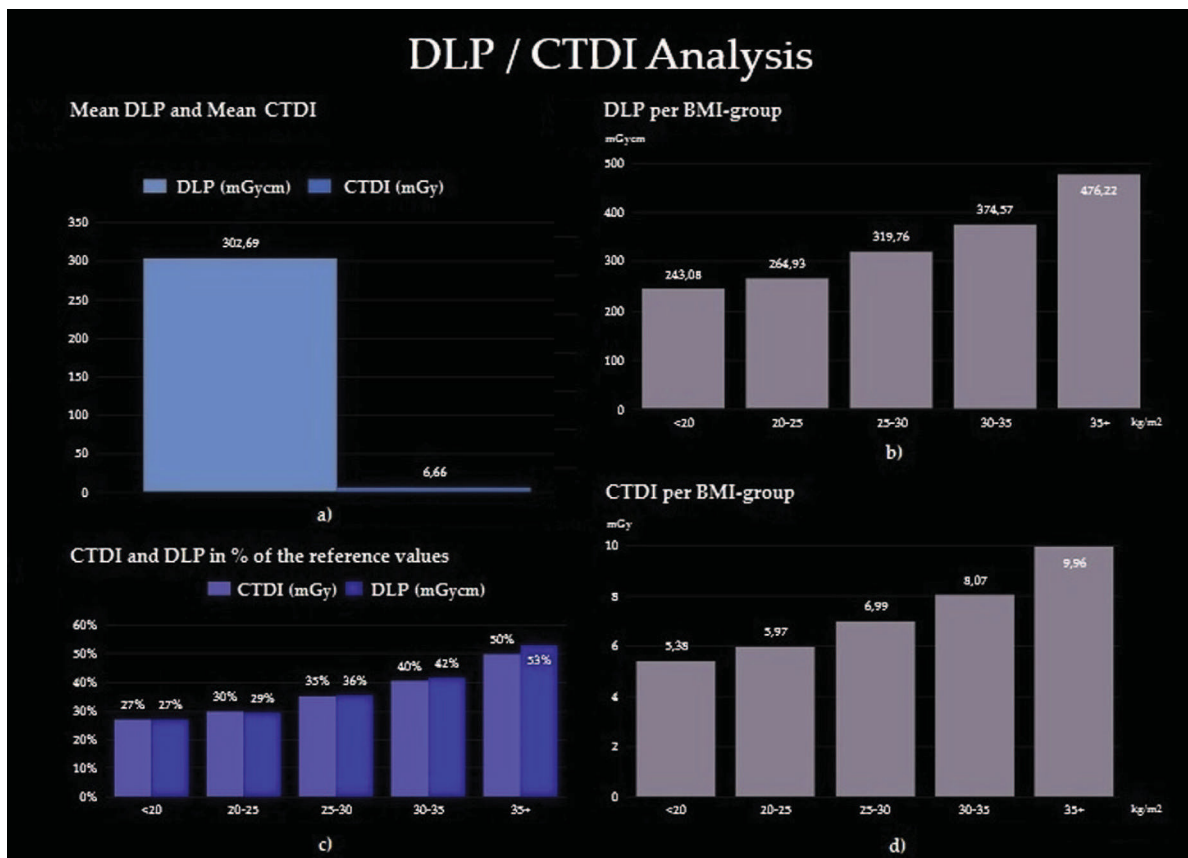


Figure 2 (a) Overall mean CTDI_{vol} and DLP for all examinations. (b) CTDI_{vol} and DLP for the different BMI groups. (c) CTDI_{vol} and DLP for the different BMI groups related to the national reference values.

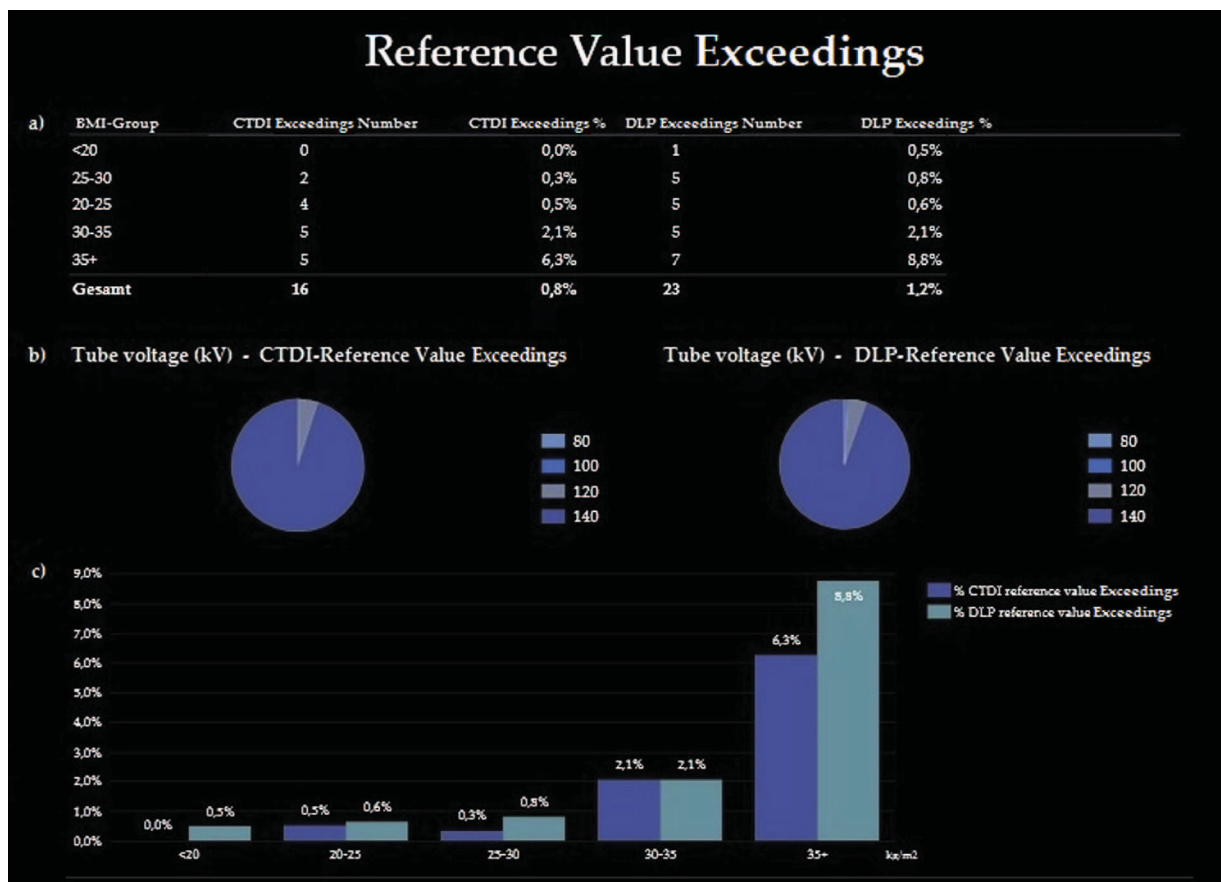


Figure 3 Violations for CTDI_{vol} and DLP according to the reference parameters provided by the BfS. (a) Overall, there were 16 transgressions for CTDI_{vol} and 23 transgressions for DLP. (b) Most examinations exceeding transgressions reference parameters were performed using a tube voltage of 140 kV. (c) The CTDI_{vol}/DLP transgressions according to the BMI group.

saves time. Several automatic methods and software solutions have been introduced lately. In addition to the presented DICOM-SR, MPPS and optical character recognition (OCR) are the most important methods.^{5,6,22} The DICOM-SR structure has several advantages for radiation dose analysis. As part of the DICOM standard, DICOM-SR provides a constant appearance independently of the CT model or the manufacturer. This facilitates modifications and extension of existing analysis. Although MPPS can deliver similar information, they are only temporary files that suffer from a considerable variability, which is a disadvantage in the context of automated analysis.⁷ DICOM-SR is available for CT, angiography, mammography, and fluoroscopy, and differs between the different imaging methods. However, different techniques can be integrated into the analysis by the application of one adaptation.

In the present study, DICOM-SR proved to be a reliable basis for the analysis of the relationship between radiation exposure and BMI in patients undergoing abdominal CT examinations. Obesity is a continuing and growing problem worldwide.^{23,8} Performing CT in overweight and obese patients is still challenging. Elevated radiation doses for overweight and obese patients, when using CT dose-saving devices, have been described.²⁰ Wang et al.²⁴ showed a threefold higher effective dose for obese patients

undergoing abdominal CT for nephrolithiasis with automated tube current modulation.²⁴

A decrease in radiation dose of up to 31% for abdominal CT could be achieved by using iterative reconstruction for patients with a large body habitus.¹⁸ Further research is mandatory to analyse the influence of different dose-reduction methods in relation to patients' habitus. In the future, with the increasing number of CT examinations and the growing numbers of obese patients, radiologists will have to deal with the challenge of choosing the best dose/dose-saving technique according to the patients' habitus more frequently. As illustrated in the present study, continuous monitoring and analysis of radiation dose parameters in reference to BMI can help to find possible deficiencies in existing CT protocols or when modifying CT protocols. In particular, small changes with long-term effects can be detected.

The BfS does not provide separate reference parameters for overweight and obese patients. A significant increase in CTDI_{vol} and DLP was observed when comparing abdominal CT for normal weight and for overweight/obese patients but even for patients of group E, the mean CTDI_{vol} was only approximately 50% of the national reference value. Compared to other studies, the mean DLP, CTDI_{vol}, and effective dose (ED, conversion factor 0.015²⁵) for abdominal

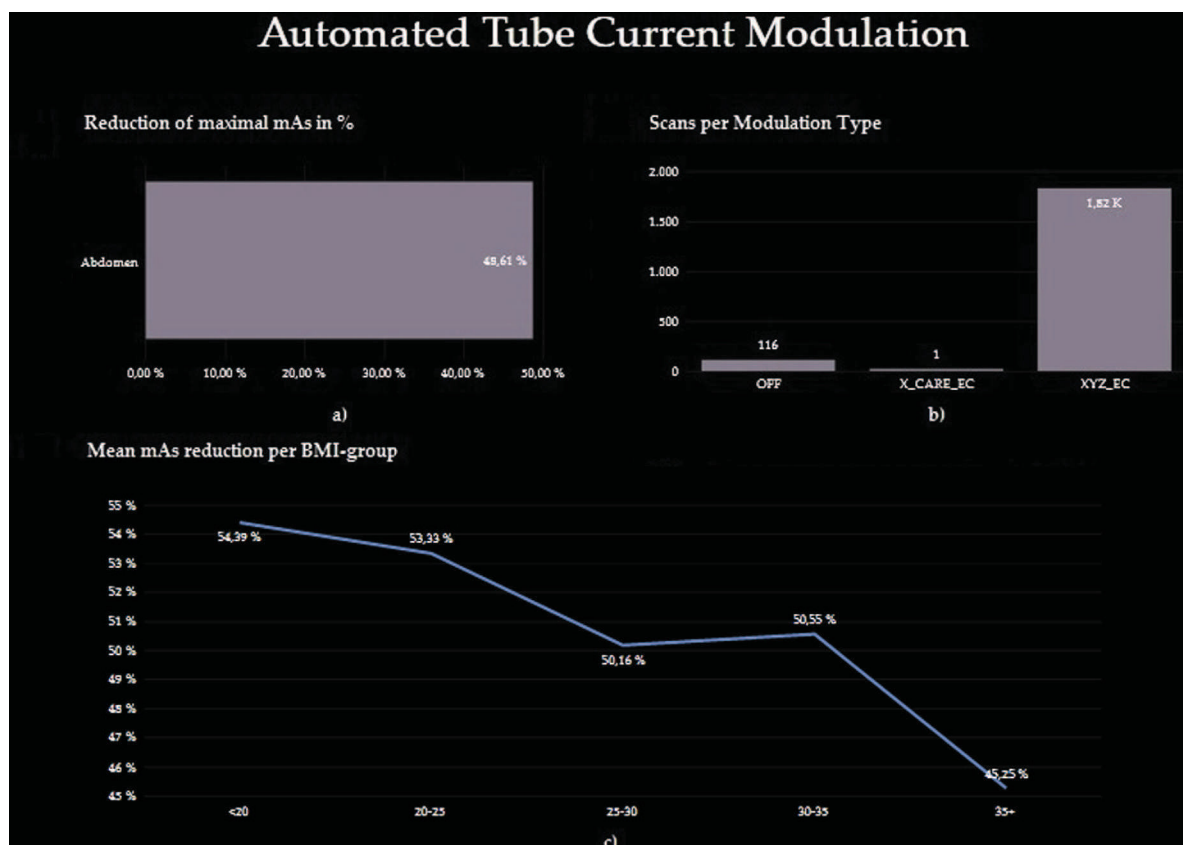


Figure 4 (a) Overall, the maximum tube current was reduced by 48.6%. (b) The different modulation types used. X_CARE_EC is an automatic exposure control program, which is part of the organ-specific dose modulation XCare™ (Siemens Healthcare, Forchheim, Germany). XYZ_EC is part of the ATCM program (CareDose 4D, Siemens Healthcare, Forchheim Germany).

CT was low in the present study (ED for the whole dataset 4.5 mSv compared to 6.5–15 mSv in the literature^{13,14}) while mean height and weight of the present patients was similar. This may be the result of constant monitoring and optimizing applied radiation doses in the Medical Faculty at the University of Düsseldorf, using new dose-reduction tools such as automated tube current modulation, automated tube potential selection, and iterative reconstruction, which were not extensively available at the time when the reference values were published.

Although the radiation dose of CT examinations exceeded the reference values in only 0.8% of CT examinations, an increase of those values exceeding the reference values was seen in overweight and obese patients. This would not have been possible without large-scale systematic analysis. Because of the definition of the reference parameters (third quartile), a certain number of excessive values has to be expected. Nevertheless, significantly more excessive reference values for obese patients were detected when compared with normal-weight patients in the present study. Although higher radiation doses are required when examining overweight and obese patients, further improvement of CT radiation doses and BMI-specific utilization of dose-reduction tools for this collective is mandatory; BMI-specific reference parameters would be preferable.

When performing systematic analysis of CT dose data, participation in cloud systems and dose registers may help to improve applied doses by comparing CT doses to data from other users. For the United States, a dose register has already been introduced [25]. The results presented in the present study illustrate the importance of taking BMI into consideration when performing large-scale analysis of CT dose data, e.g., in cloud systems or dose registers.

The present study has some limitations. The study was performed retrospectively and group sizes for the different BMI groups vary because of an inhomogeneous patient population. Very large patients >212 kg could not be included because the burden of the CT machine was limited. Furthermore, data have only been analysed from one CT system. Further studies should include different machines with different dose-saving algorithms.

As the present analysis was based on one body region, different protocols have been collectively studied, e.g., abdominal contrast-enhanced CT and low-dose CT for nephrolithiasis. Although this may bias the results, the current approach reflects the reference values used in routine clinical practice for abdominal examinations.

In conclusion, DICOM-SR is a comprehensive, fast, and reproducible method to analyse dose-related CT data automatically and systematically. An increase in radiation dose by up to 96% in abdominal CT for extremely obese patients could

be demonstrated in a large study population. The use of DICOM-SR enables the radiologist to have an overall impression of the radiation doses applied in comparison to arbitrary reference values and to monitor radiation application over time. Furthermore, it enables discovery and analysis of deficient radiation applications, as well as single aberrations, and therefore, can be used to improve patient care.

References

1. Federal Ministry for the Environment, Nature Conservation, Building and Nuclear Safety, German Federal Office of Radiation Protection. Umweltradioaktivität und Strahlenbelastung im Jahr 2010: Unterrichtung durch die Bundesregierung, [in German]. <http://nbn-resolving.de/urn:nbn:de:0221-201205118217>. Accessed 25 March 2014.
2. Treichel T, Liebmann P, Burgert O, et al. Applicability of DICOM structured reporting for the standardized exchange of implantation plans. *Int J Comput Assist Radiol Surg* 2010;**5**:1–9.
3. Cook TS, Zimmerman SL, Steingall SR, et al. RADIANCE: an automated, enterprise-wide solution for archiving and reporting CT radiation dose estimates. *RadioGraphics* 2001;**31**:1833–46.
4. National Electrical Manufacturers Association. Digital imaging and communications in medicine, ISO 12052. <http://medical.nema.org/Dicom/about-DICOM.html>. Accessed 16 June 2014.
5. Noumeir R. Benefits of the DICOM structured report. *J Digit Imaging* 2006;**19**:295–306.
6. Talati RK, Dunkin J, Parikh S, et al. Current methods of monitoring radiation exposure from CT. *J AM Coll Radiol* 2013;**10**:202–7.
7. World Health Organization. *Obesity: preventing and managing the global epidemic: report a WHO consultation*. WHO Technical Report Series. Geneva: WHO; 2000.
8. Ogden CL, Carroll MD, Kit BK, et al. Prevalence of obesity and trends in body mass index among US children and adolescents, 1999–2010. *JAMA* 2012;**307**:483–90.
9. Gervaise A, Naulet P, Beuret F, et al. Low-dose CT with automatic tube current modulation, adaptive statistical iterative reconstruction, and low tube voltage for the diagnosis of renal colic: impact of body mass index. *AJR Am J Roentgenol* 2014;**202**:553–60.
10. Duan X, Wang J, Christner JA, et al. Dose reduction to anterior surfaces with organ-based tube-current modulation: evaluation of performance in a phantom study. *AJR Am J Roentgenol* 2010;**197**:689–95.
11. Desai GS, Fuentes Orrego JM, Kambadakone AR, et al. Performance of iterative reconstruction and automated tube voltage selection on the image quality and radiation dose in abdominal CT scans. *J Comput Assist Tomogr* 2013;**37**:897–903.
12. AlSuwaidi JS, AlBalooshi LG, AlAwadhi HM, et al. Continuous monitoring of CT dose indexes at Dubai Hospital. *AJR Am J Roentgenol* 2013;**201**:858–64.
13. Homolka P, Leithner R, Billinger J, et al. Results of the Austrian CT Dose Study 2010: typical effective doses of the most frequent CT examinations [in German]. *Z Med Phys* 2014;**24**:224–30.
14. Federal Office for Radiation Protection. Publication of updated diagnostic reference levels for diagnostic and interventional X-ray examinations, 2010. <http://www.bfs.de/en/ion/medizin/diagnostik/referenzwerte.html>. Accessed 30 October 2014.
15. Brenner DF, Hall EJ. Computed tomography—an increasing source of radiation exposure. *N Engl J Med* 2007;**357**:2277–84.
16. Smith-Bindman R, Miglioretti DL, Johnson E, et al. Use of diagnostic imaging studies and associated radiation exposure for patients enrolled in large integrated health care systems, 1996–2010. *JAMA* 2012;**307**:2400–9.
17. Desai GS, Uppot RN, Yu EW, et al. Impact of iterative reconstruction on image quality and radiation dose in multidetector CT of large body size adults. *Eur Radiol* 2012;**22**:1631–40.
18. The Council of the European Union. *Council Directive 97/43/Euratom of 30 June 1997 on health protection of individuals against the dangers of ionizing radiation in relation to medical exposure, and repealing Directive Euratom. Official Journal NO. L 180*. 1997. p. 0022–7.
19. Hietschold V, Koch A, Laniado M, et al. Computed tomography: influence of varying tube current on patient dose and correctness of effective dose calculations [in German]. *Fortschr Röntgenstr* 2008;**180**:430–9.
20. Pulli B, Fintelmann F, Liu B, et al. Semiautomated fluoroscopy radiation dose capture and reporting. *AJR Am J Roentgenol* 2010;**195**:1180–2.
21. Noumeir R. Benefits of the DICOM modality performed procedure step. *J Digit Imaging* 2005;**18**:260–9.
22. Hossain P, Kavar B, El Nahas M. Obesity and diabetes in the developing world—a growing challenge. *N Engl J Med* 2007;**356**(3):213–5.
23. Wang AJ, Goldsmith ZG, Wang C, et al. Obesity triples the radiation dose of stone protocol computerized tomography. *J Urol* 2013;**189**:2142–6.
24. Bongartz G, Golding S, Jurik A et al. European guidelines for multislice computed tomography. European Commission 2004. http://w3.tue.nl/fileadmin/sbd/Documenten/Leergang/BSM/European_Guidelines_Quality_Criteria_Computed_Tomography_Eur_16252.pdf. Accessed 30 October 2014.
25. American College of Radiology (ACR). About dose Index Registry (DIR). <http://www.acr.org/Quality-Safety/National-Radiology-Data-Registry/Dose-Index-Registry/About-DIR>. Accessed 8 February 2014.

Cloud-Based CT Dose Monitoring using the DICOM-Structured Report: Fully Automated Analysis in Regard to National Diagnostic Reference Levels

Cloud-basiertes Monitoring von CT-Dosisdaten mit Hilfe des DICOM-Structured Report: Analyse im Hinblick auf nationale Referenzwerte

Authors

J. Boos¹, A. Meineke², C. Rubbert¹, P. Heusch¹, R. S. Lanzman¹, J. Aissa¹, G. Antoch¹, P. Kröpil¹

Affiliations

¹ University Dusseldorf, Medical Faculty, Department of Diagnostic and Interventional Radiology, Dusseldorf, Germany
² Cerner Health Services, Idstein, Germany

Key words

- computed tomography
- radiation safety
- dose monitoring
- DICOM
- QA/QC

Zusammenfassung

Ziel: Ziel dieser Studie war die Implementierung eines Cloud-basierten CT-Dosismonitorings basierend auf dem DICOM-Structured Report (DICOM-SR) zur automatischen Überwachung der Dosisexposition im Hinblick auf die nationalen diagnostischen Referenzwerte (DRW).

Material und Methoden: Zur automatischen Erfassung und Überwachung der CT-Dosisdaten wurde eine neuartige, in Kooperation mitentwickelte Software basierend auf dem DICOM-SR eingesetzt. Der DICOM-SR aller CT-Untersuchungen unserer Einrichtung zwischen 09/2011 und 03/2015 wurde automatisch anonymisiert und an einen Cloud-Server verschickt. Die Daten wurden automatisch im Hinblick auf die Körperregion, das Patientenalter und den korrespondierenden DRW für den volumetrischen Computertomografie-Dosis-Index (CTDI_{vol}) sowie für das Dosis-Längen-Produkt (DLP) analysiert.

Ergebnisse: Datensätze von 36 523 CT-Untersuchungen (131 527 Scanserien) von drei verschiedenen CT-Geräten und einem PET-CT wurden analysiert. Insgesamt betrug der mittlere CTDI_{vol} 51,3% und das mittlere DLP 52,8% der nationalen DRW. Bezogen auf die nationalen DRW betragen CTDI_{vol} und DLP für die Abdomen-CT 43,8% und 43,1% (n = 10 590), für die Schädel-CT 66,6% und 69,6% (n = 16 098) und für die Thorax-CT 37,8% und 44,0% (n = 10 387). Insgesamt überschritten 1,9% der CT-Untersuchungen den CTDI_{vol} und 2,9% der Untersuchungen das DLP der nationalen DRW. Zwischen unterschiedlichen CT-Protokollen, die dem gleichen nationalen DRW zugeordnet wurden, variierte die Strahlenexposition um bis zu 50%.

Schlussfolgerung: Das implementierte, Cloud-basierte CT-Dosismonitoring basierend auf dem DICOM-SR ermöglicht eine automatische, umfassende Benchmarkanalyse im Hinblick auf die nationalen DRW. Insgesamt betrug die Dosisexposition

Abstract

Purpose: To implement automated CT dose data monitoring using the DICOM-Structured Report (DICOM-SR) in order to monitor dose-related CT data in regard to national diagnostic reference levels (DRLs).

Materials and Methods: We used a novel in-house co-developed software tool based on the DICOM-SR to automatically monitor dose-related data from CT examinations. The DICOM-SR for each CT examination performed between 09/2011 and 03/2015 was automatically anonymized and sent from the CT scanners to a cloud server. Data was automatically analyzed in accordance with body region, patient age and corresponding DRL for volumetric computed tomography dose index (CTDI_{vol}) and dose length product (DLP).

Results: Data of 36 523 examinations (131 527 scan series) performed on three different CT scanners and one PET/CT were analyzed. The overall mean CTDI_{vol} and DLP were 51.3% and 52.8% of the national DRLs, respectively. CTDI_{vol} and DLP reached 43.8% and 43.1% for abdominal CT (n = 10 590), 66.6% and 69.6% for cranial CT (n = 16 098) and 37.8% and 44.0% for chest CT (n = 10 387) of the compared national DRLs, respectively. Overall, the CTDI_{vol} exceeded national DRLs in 1.9% of the examinations, while the DLP exceeded national DRLs in 2.9% of the examinations. Between different CT protocols of the same body region, radiation exposure varied up to 50% of the DRLs.

Conclusion: The implemented cloud-based CT dose monitoring based on the DICOM-SR enables automated benchmarking in regard to national DRLs. Overall the local dose exposure from CT reached approximately 50% of these DRLs indicating that DRL actualization as well as protocol-specific DRLs are desirable. The cloud-based approach enables multi-center dose monitoring and offers great potential to further optimize radiation exposure in radiological departments.

received 15.7.2015
 accepted 24.9.2015

Bibliography

DOI <http://dx.doi.org/10.1055/s-0041-108059>
 Published online: 3.12.2015
 Fortschr Röntgenstr 2016; 188: 288–294 © Georg Thieme
 Verlag KG Stuttgart · New York ·
 ISSN 1438-9029

Correspondence

Dr. Johannes Boos
 Institut für Diagnostische und
 Interventionelle Radiologie,
 Heinrich-Heine-Universität
 Düsseldorf, Medizinische
 Fakultät
 Moorenstrasse 5
 40225 Düsseldorf
 Germany
 Tel.: ++49/2 11/8 11 61 45
 Fax: ++49/2 11/8 11 77 52
 Johannes.Boos@med.uni-
 duesseldorf.de

tion der CT ungefähr 50% der DRW bei deutlicher Variabilität zwischen den unterschiedlichen CT-Protokollen. Dies deutet darauf hin, dass eine Aktualisierung der DRW sowie die Implementierung von Protokoll-spezifischen DRW wünschenswert ist. Der Cloud-basierte Ansatz ermöglicht ein Multicenter Dosismonitoring und bietet großes Potential, die Strahlenexposition der CT in radiologischen Abteilungen weiter zu optimieren.

Kernaussagen:

- ▶ Die neu entwickelte, cloud-basierte Software nutzt den DICOM-Structured-Report und ermöglicht ein umfassendes CT-Dosismonitoring.
- ▶ Die Software ermöglicht eine automatische Auswertung der Dosisdaten im Hinblick auf nationale Referenzwerte.
- ▶ Die ermittelte Dosisexposition durch CT-Untersuchungen in dieser Studie lag bei ungefähr 50% der nationalen Referenzwerte.
- ▶ Der Cloud-basierte Ansatz bietet großes Potential für ein Multicenter Dosismonitoring.

Introduction

Besides dose optimization for every single CT scan, dose monitoring as part of quality assurance in modern radiology has gained ever more importance [1]. To evaluate CT radiation exposure, diagnostic reference levels (DRLs) for diagnostic and interventional radiology examinations have been published in many countries [1–3]. In CT, these DRLs are usually provided for different body regions such as “head” and “chest” or for specific protocols such as “lung-embolism” or “renal colic” [1, 4].

Systematic analysis of dose-related CT data in regard to the DRLs is an important aspect of quality assurance but requires comprehensive data collection. Different methods to monitor CT dose data have been introduced. Optical character recognition (OCR) can be used to read the dose data from the so-called “patient protocol”, which is stored as an image in the Picture Archiving and Communication System (PACS) [5]. Alternatively, the DICOM header can be used to gain these dose-related data from CT [6]. Modern CT scanners provide the Digital Imaging and Communication in Medicine-Structured Report (DICOM-SR) which supplies important dose parameters and allows for straightforward systematic dose monitoring [7, 8]. Recently, different local dose monitoring software solutions have been made commercially available [1, 5, 9] and initial studies reported great potential for dose optimization [1].

To our knowledge, implementation of a dedicated, cloud-based software device for automated benchmarking of CT dose data with respect to DRLs, which enables dose optimization beyond local analysis, has not been reported so far. Therefore, the aim of this study was to implement automated cloud-based dose monitoring which enables surveillance of CT dose exposure in regard to national DRLs.

Methods

Data acquisition

This retrospective study was approved by the local ethics committee.

The DICOM-SR was automatically created by all institutional CT scanners for every examination. The DICOM-SR was then automatically sent to a local gateway server for anonymization and further

Key Points:

- ▶ The newly developed software based on the DICOM-Structured Report enables large-scale cloud-based CT dose monitoring
- ▶ The implemented software solution enables automated benchmarking in regard to national DRLs
- ▶ The local radiation exposure from CT reached approximately 50% of the national DRLs
- ▶ The cloud-based approach offers great potential for multicenter dose analysis.

Citation Format:

- ▶ Boos J, Meineke A, Rubbert C et al. Cloud-Based CT Dose Monitoring using the DICOM-Structured Report: Fully Automated Analysis in Regard to National Diagnostic Reference Levels. *Fortschr Röntgenstr* 2016; 188: 288–294

processing. Anonymization was performed with a self-developed software device, which is part of the novel in-house co-developed software tool DoseIntelligence™ (DoseIntelligence™, Pulmokard GmbH, Herdecke, Germany). The anonymized DICOM-SR datasets were automatically transferred to a cloud server via an encrypted connection and a database was used to store the data on the server (Fig. 1).

A cloud-based approach was used because it offers great potential for multicenter dose monitoring and potentially enables dose optimization beyond local environments due to comparison of local data with dose data from other cloud participants or cloud-based DRLs.

National diagnostic reference levels (DRLs)

German national DRLs for CT are provided for different body regions for $CTDI_{vol}$ and DLP. Reference levels are defined by the Federal Office of Radiation Protection according to the 3rd quartiles of the mean patient exposition evaluated in a large collective. While a CT examination can consist of several scan series (e.g. non-contrast, arterial, venous phase), the reference parameters are defined for every single scan series. There are different DRLs for children (according to their age group) and for adults. The most important national DRLs are listed in Table 1.

Protocol matching

In order to compare our dose-related CT data to national DRLs, firm protocol matching is necessary. As the large number of different CT scan protocols in our institution surpasses by far the limited amount of different DRLs based on body regions, various scan protocols have to be assigned to the same reference parameter [4]. In our study, this protocol matching to body regions was performed manually by one radiologist (J.B.). Each protocol was assigned to one of the body regions for which national DRLs are provided. If a series could not be matched to a DRL (for example the scout images, any phantom scan or examinations lacking national DRLs like “neck CT”), they were marked as “not to be taken into account”.

Comparison of dose-related data to DRLs

$CTDI_{vol}$ and DLP of every scan series were automatically analyzed and compared to the national DRLs (the ratio being expressed in percent) and values were stored in the database. The correspond-

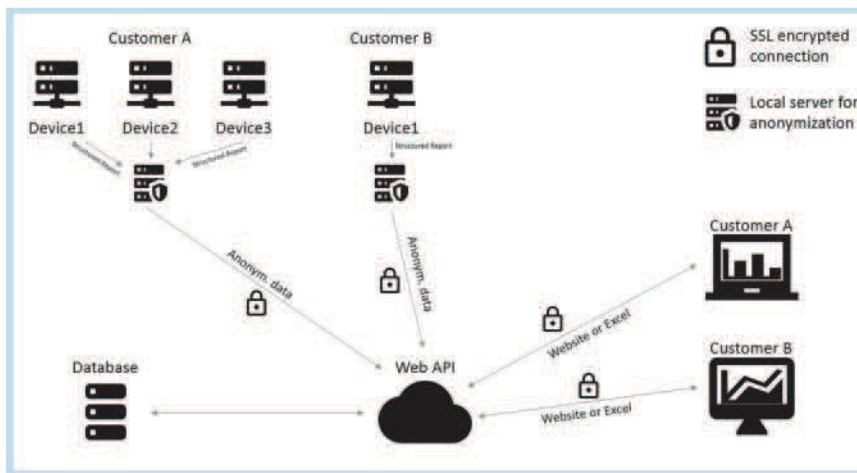


Fig. 1 Structure of automated cloud-based dose monitoring.

Abb. 1 Aufbau des automatischen, Cloud-basierenden Dosismonitorings.

Table 1 National DRLs for the six most common body regions [4].

Tab. 1 Die nationalen DRWs für die sechs wichtigsten Untersuchungsregionen [4].

body region	DRL CTDI _{vol} (mGy)	DRL DLP (mGy*cm)
cranial	65	950
chest	12	400
upper abdomen	20	450
abdomen	20	900
pelvis	20	450
lumbar spine (bone)	16	500

The provided CTDI_{vol} values are supposed to be used for orientation.

ing body region for every protocol as well as patient age was automatically considered to assess the correct DRL.

Analysis in regard to body mass index (BMI)

Patient height and weight were manually recorded by the technician prior to the CT study and added to the DICOM-SR via the CT scanner interface. For further data analysis, BMI was calculated automatically and patients were divided into different groups: Underweight: BMI < 18 kg/m²; normal weight: 18–25 kg/m²; overweight: 25–30 kg/m²; obesity I°: 30–35 kg/m²; obesity II°: 35–40 kg/m²; obesity III°: > 40 kg/m².

Data analysis

Data analysis was performed with a novel in-house co-developed software tool (DoseIntelligence™, Pulmokard GmbH, Herdecke, Germany) and the commercially available Excel 2013™ including Powerpivot and Powerview (Microsoft, Redmond, WA, USA). Only protocols with at least 40 examinations were analyzed in detail.

Results

Examinations and Patients

Overall, the DICOM-SRs of n = 36 523 CT examinations (n = 131 527 scan series) were stored in the database at the time of this retrospective analysis. Examinations were performed on three different CT scanners (CT1: Somatom Definition AS+; CT2: Somatom Definition Flash; CT3: Somatom Definition AS with sliding gantry, Siemens, Healthcare Sector, Forchheim, Germany) and one PET-CT

(Biograph mCT, Siemens, Healthcare Sector, Forchheim, Germany) between 09/2011 and 05/2015.

In total, 90 622 scan series were marked as “not to be taken into account”. These included 18 594 scan series, which could not be matched to a DRL at the time of the analysis, and had to be excluded, e. g. neck CT and CT of extremities. Scout images are accounted for as independent scan series by the dose monitoring software. The remaining 72 073 scan series, which had to be excluded, contained scout images and phantom measurements for research and consistency check. Therefore, overall 41 036 scan series were ultimately analyzed in this study. The most frequent examinations were performed for cranial CT (n = 16 098), abdominal CT (n = 10 590), chest CT (n = 10 387), upper abdomen (n = 2909), mid-face (Sinusitis, n = 505), pelvis (n = 427) and lumbar spine (n = 119).

Comparison of dose-related data to DRLs

The radiation exposure of all included scan series corresponded to 51.3% of the national DRL for CTDI_{vol} and 52.8% of the national DRL for DLP. Specific values for the different body regions are shown in **Table 2**.

Overall, 1.9% (n = 763) of scan series exceeded the national DRLs for CTDI_{vol} and 2.9% (n = 1208) of scan series exceeded the reference DLP.

Dose variation of protocols matched to one body region

There was a high variation in radiation exposure for different scan protocols matched to the same body region. The highest difference in DLP between two protocols with the same DRL was found for two different abdominal CT protocols (CTDI_{vol} / DLP: 2.76 mGy / 126.9 mGycm (13.8% / 14.1% of the DRL) compared to 10.3 mGy / 478.8 mGycm (51.6% / 53.2% of the DRL); **Table 3**). The highest difference between two protocols with the same DRL on the same CT scanner was found for two chest CT protocols (CTDI_{vol} / DLP: 4.48 mGy / 148.4 mGycm (37.4% / 37.1% of the DRL) compared to 7.32 mGy / 270.4 mGycm, (61.0% / 67.6% of the DRL), CT3).

Analysis in regard to body mass index (BMI)

BMI was recorded for 13 321 out of 41 036 patients (32.5%) (**Fig. 2**). There was a continuous increase in the mean CTDI_{vol} and DLP according to the BMI group (underweight: CTDI_{vol}: 34.3% / DLP: 35.8% to obesity III°: CTDI_{vol}: 66.9% / DLP 73.3%). National DRLs were exceeded increasingly more often according to the BMI group (unknown: 3.48%, underweight: 1.11%, normal

Table 2 Overview of dose data for the different body regions compared to the corresponding national DRLs.

Tab. 2 Übersicht über die CT-Dosisdaten der verschiedenen Körperregionen.

region	series	mean age	mean CTDI _{vol}	%CTDI _{vol}	mean DLP	%DLP	%exceeding DLP	%exceeding CTDI _{vol}
abdominal	10 590	60.84	8.74	43.83	386.82	43.14	3.92	3.11
pelvis	427	63.84	9.72	49.07	307.70	69.28	17.80	10.30
mid-face	505	48.60	5.02	55.78	65.90	66.05	7.33	4.55
cranial CT	16 098	63.85	43.01	66.58	656.13	69.64	1.13	0.35
lumbar spine (ax.)	1	53.00	8.80	20.95	35.83	14.33	0.00	0.00
lumbar spine (bone)	119	62.38	11.66	73.46	282.69	57.19	11.76	17.65
upper abdomen	2909	62.66	8.03	40.14	197.67	43.94	0.38	1.48
chest	10 387	59.88	4.49	37.83	173.86	44.03	4.55	2.37
overall	41 036	61.79	21.03	51.25	420.07	52.84	2.94	1.86

Absolute numbers as well as the percentage of national DRLs are shown. Furthermore, the percentage of examinations exceeding the DRLs is shown. Mean age in years; CTDI_{vol}: Volumetric Computed Tomography Dose Index (mGy); DLP: Dose Length Product (mGy*cm); Percentage of examinations exceeding the national DRLs [4]. Series: n; mean age in years; mean CTDI_{vol} in mGy; mean DLP in mGy*cm; lumbar spine (ax): axial CT for the discs.

Die Werte sind sowohl absolut, als auch in Prozent des entsprechenden DRW angegeben. Zusätzlich ist der prozentuale Anteil der Untersuchungen angegeben, welcher die DRW überschreitet.

Table 3 Protocols with the lowest and highest radiation exposure per body region.

Tab. 3 Dargestellt sind die Protokolle mit der jeweils niedrigsten und höchsten Strahlenexposition einer Körperregion.

body region	protocol 1 (low)	mean CTDI _{vol} /DLP	%CTDI _{vol} /%DLP	protocol 2 (high)	mean CTDI _{vol} /DLP	%CTDI _{vol} /%DLP
abdomen	urolithiasis (n = 218)	2.76/126.9	13.8/14.1	abdomen venous (n = 955)	10.3/478.8	51.6/53.2
upper abdomen	upper abdomen non-contrast (n = 67)	2.91/60.2	14.6/13.4	liver late phase (n = 51)	8.9/198.0	44.5/44.0
chest	chest arterial (n = 5137)	3.6/115.5	30.6/29.8	chest incl. liver (n = 397)	7.7/353.2	64.1/88.3
pelvis	pelvis (n = 244)	9.8/269.6	49.0/60.4	pelvis venous (n = 42)	8.9/301.6	43.6/68.6
cranial	head (n = 137)	35.6/614.7	54.7/64.4	3 D dataset for surgical navigation (n = 115)	49.0/1000.4	75.3/105.3

Only protocols with n > 40 examinations were included. Absolute values as well as relative values in comparison to the national DRLs are provided.

Es wurden nur Protokolle mit mehr als 40 Untersuchungen ausgewertet. Angegeben sind sowohl die Absolutwerte für CTDI_{vol} und DLP sowie die prozentualen Werte bezogen auf den entsprechenden DRW.

weight: 0.93%, overweight 1.42%, obesity I°: 2.74%, obesity II°: 3.52%, obesity III°: 16.8%) (Fig. 3).

Comparison of the different CT scanners

CT3 had a considerably higher mean radiation exposure compared to the other two CT scanners (CTDI_{vol}/DLP: 68.5%/69.8% compared to 47.2%/48.9% and 41.6%/42.7%, respectively) (Fig. 4). The difference between the CT scanners varied according to the body region examined. The dose exposure per scanner for the three most frequently examined body regions (cranial CT, chest CT, abdominal CT) is shown in Fig. 5.

Discussion

In the study presented here we used a novel cloud-based software device for monitoring dose-related CT data of a tertiary care radiological department in order to benchmark CT radiation exposure to national DRLs. In this retrospective large-scale analysis of a 3.75-year interval consisting of more than 35 000 CT examinations, national DRLs were not systematically exceeded for any body region. The mean radiation exposure in clinical practice was only approximately 50% of the national DRLs. A marked variation in radiation

exposure between different scan protocols of the same body region (and therefore related to the same DRL) was found.

The radiation exposure between CT3 and the other two CT scanners included in this study differed remarkably. This is most likely the result of CT3 being the only CT scanner without an iterative reconstruction technique. The difference in radiation exposure in this study is in accordance with previous studies, which reported a significant reduction of radiation exposure in CT due to the use of iterative reconstruction instead of filtered back projection [10, 11]. National DRLs for CT examinations have been reported for many countries, e.g. for Ireland [2], Germany [4], the United Kingdom [12], Canada [1], Portugal [13], Switzerland [14] and the US [15]. Mostly these DRLs are defined for examinations of a certain body region, while only very few DRLs are given for specific CT protocols [1]. The national DRLs of different countries vary distinctly from each other, for example there is a DLP range from 787 mGy*cm to 1305 mGy*cm for cranial CT [12, 16], 371 – 1051 mGy*cm for chest CT [3, 16] and 329 – 1306 mGy*cm for abdominal CT [3, 16]. The German DRLs used for analysis in this study do not differ markedly from the center span of other reported DRLs.

Our results demonstrated a remarkable variation in the radiation dose applied by different CT protocols, which are all in clinical use to examine the same body region depending on the clinical issue

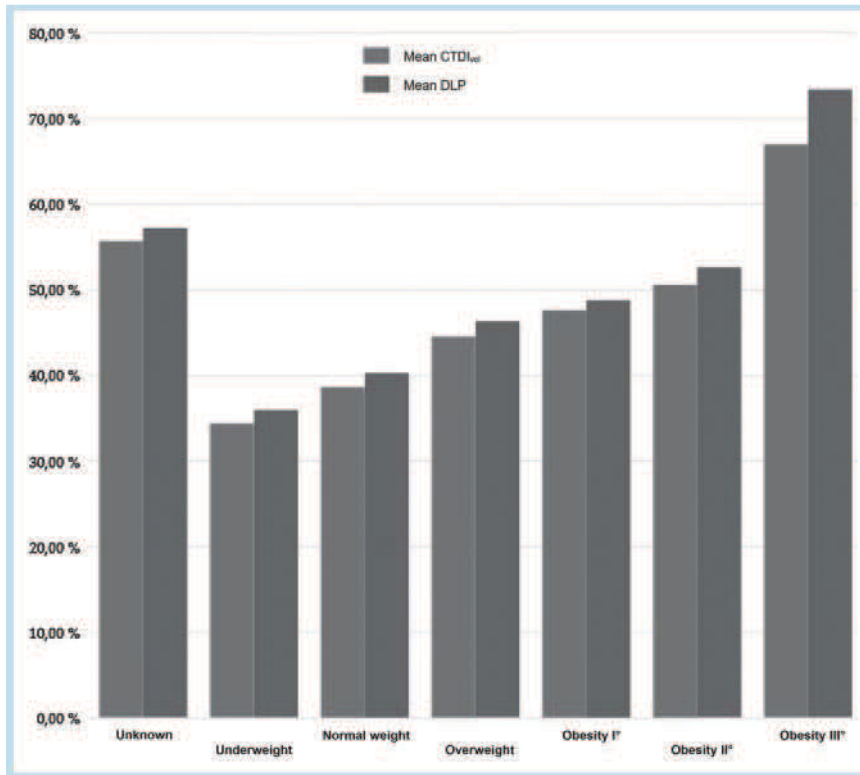


Fig. 2 CTDI_{vol} and DLP as percentage of the national DRL for the different BMI groups.

Abb. 2 Dargestellt sind der CTDI_{vol} und das DLP (in % des jeweiligen DRW) für die verschiedenen BMI-Gruppen.

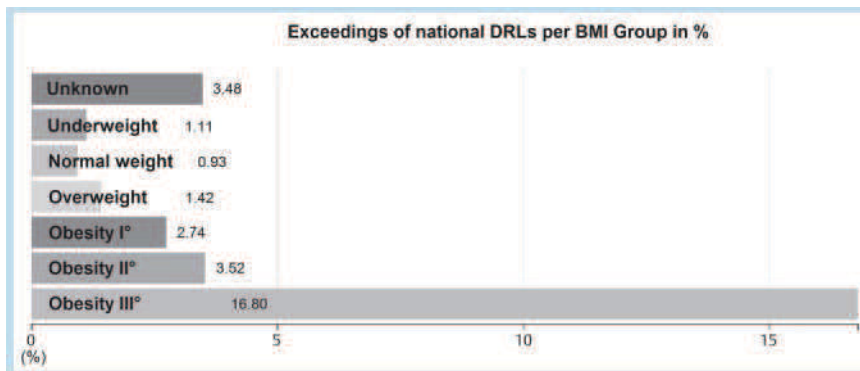


Fig. 3 Exceeding of national DRLs according to patients' BMI group.

Abb. 3 Prozentualer Anteil der Überschreitungen der nationalen DRW für die verschiedenen BMI-Gruppen.

(for abdominal CT, for example, we use a low-dose non-contrast protocol to detect ureteral concretions while our protocol for tumor staging includes a standard dose arterial and venous phase). Of course, these protocols differ essentially regarding radiation dose. Our results are in good accordance with prior studies, which introduced protocol-specific DRLs, for example for "renal colic" or "lung embolism" [1, 2, 17]. Current national DRLs in Germany, however, do not reflect the variety of CT protocols used in the clinical routine today. Therefore, more sophisticated DRLs are desirable and could help to further optimize radiation exposure from CT.

We found an increase in CT radiation exposure according to the BMI. National or international DRLs are traditionally reported for normal-sized patients (e. g. 60 – 80 kg) and do not take patient constitution into account [2, 4, 8]. Initial studies reported local DRLs based on size-specific dose estimates (SSDEs) [18]. To our knowledge, SSDEs have not been implemented in any national DRLs but according to our results, adaption of DRLs to a patient's constitution seems very reasonable.

Today, national DRLs are mostly based on surveys completed by different participating CT sites. Most commonly, the 75th percentile is calculated to account for the national DRL [2, 4]. The accuracy of this method depends on the accuracy of the participants' data and on the number of included examinations. Foley et al. used data that included at least ten average-sized patients for each CT examination [2]. This small group size might not reflect the real dose exposure for the corresponding CT examination. Recently, Taylor et al. reported a high variability for DLP in CT dose surveys depending on the protocol and patient weight [19]. Even when including 50 patients per protocol, a 95% confidence interval lower than 10% of the median (CI95%/med < 10%) was not reached for most protocols. Furthermore, for abdominal CT, n = 420 and for cervical spine n = 900 examinations were needed to reach the CI95%/med < 10% [19]. Only a few studies reported implementation of local DRLs based on systematic dose monitoring [1]. Besides the larger sample size when including all CT examinations in DRL assessment, the lack of manual processing with potential risk for selection bias helps to improve accuracy

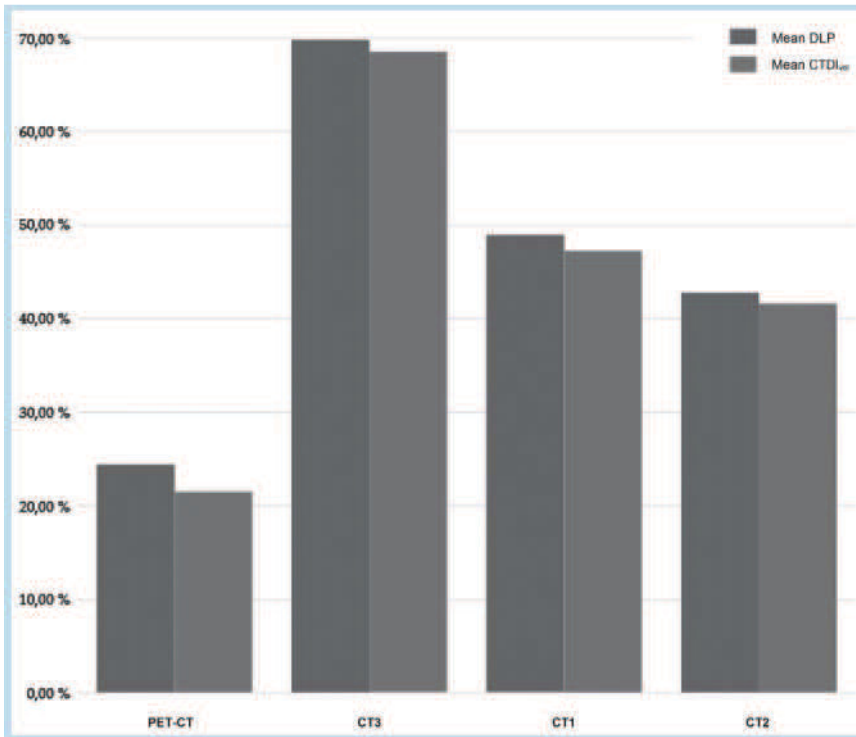


Fig. 4 CTDI_{vol} and DLP in percentage of the national DRLs for the different scanners included in this study.

Abb. 4 Dargestellt sind der CTDI_{vol} und das DLP (in % des jeweiligen DRW) für die unterschiedlichen CT-Geräte.

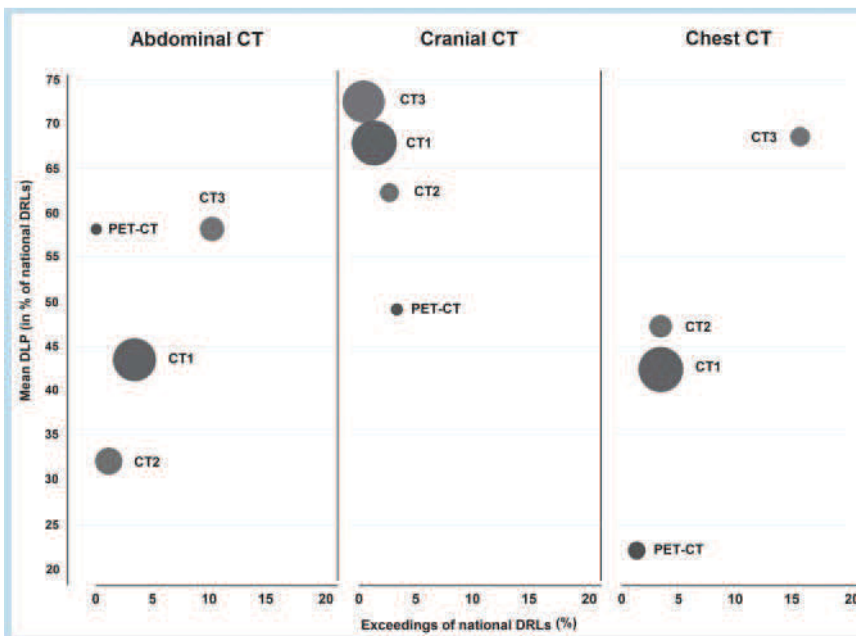


Fig. 5 DLP for the different CT scanners for abdominal CT, cranial CT and chest CT. DLP is shown in percentage of the national DRL (y-axis). The percentage of examinations exceeding DRLs is shown on the x-axis. The size of the dots equals the number of examinations displayed.

Abb. 5 Detaillierte Auswertung der Körperregionen Abdomen, Schädel und Thorax: Dargestellt sind das DLP (in % des DRW, y-Achse) und der Prozentsatz der DRW-Überschreitungen (x-Achse) für die verschiedenen CT-Geräte.

even further. Large-scale analysis of dose-related CT data, as presented here, and particularly cloud-based multicenter dose monitoring, which is possible with the presented software tool, allow for implementation of more accurate and more specific DRLs and therefore help to reduce radiation exposure from CT in the future. Our study has limitations. This study reports initial single-center results. Single-center dose monitoring in regard to national DRLs only allows for limited dose analysis because no improvement may be performed if radiation exposure for a specific protocol is below the corresponding DRL. Nevertheless, the introduced cloud-based approach enables multicenter dose monitoring

which may enable benchmarking with cloud-based reference levels from similar departments, CT scanners and protocols and can help to optimize radiation exposure in CT beyond analysis concerning national or local DRLs.

For some body regions and various CT protocols, no national DRLs have been reported so far, e. g. CT of the neck, cervical CT angiography, whole body CT (PET-CT, skeletal CT for myeloma survey or aortic CT angiography). Therefore, our results cannot be compared to national DRLs for these protocols and we did not include these protocols in our study. Patient weight and height were assessed by statements of the patient or provided patient data, not by our own

measurements. This might have led to an inaccuracy of the data, which cannot be evaluated further. We did not evaluate additional dose reduction techniques like iterative reconstruction or automated tube current modulation. The data provided about these techniques in the DICOM-RDSR are limited and therefore it was not included in our study.

In conclusion, we implemented cloud-based CT dose monitoring to automatically compare CT radiation exposure to national DRLs. Overall, the local dose exposure from CT was approximately 50 % of these DRLs and showed a large variability between different CT protocols matched to the same DRL, indicating that DRL actualization and protocol-specific DRLs are desirable. The cloud-based approach may help to implement more accurate and more specific DRLs in the future by multicenter analysis and thus lead to further optimization of radiation exposure in CT.

References

- 1 MacGregor K, Li I, Dowdell T et al. Identifying Institutional Diagnostic Reference Levels for CT with Radiation Dose Index Monitoring Software. *Radiology* 2015; 20: 141520
- 2 Foley SJ, McEntee MF, Rainford LA. Establishment of CT diagnostic reference levels in Ireland. *Br J Radiol* 2012; 85: 1390–1397. DOI: 10.1259/bjr/15839549 Epub 2012 May 17
- 3 Van der Molen AJ, Schilham A, Stoop P et al. A national survey on radiation dose in CT in The Netherlands. *Insights Imaging* 2013; 4: 383–390
- 4 German Federal Office for Radiation Protection. Publication of updated diagnostic reference levels for diagnostic and interventional x-ray examinations; 2010, <http://www.bfs.de/DE/themen/ion/anwendung-medicin/diagnostik/referenzwerte/referenzwerte.html> German. Accessed on 12.08.2015
- 5 Cook TS, Zimmerman SL, Steingall SR et al. RADIANCE: An automated, enterprise-wide solution for archiving and reporting CT radiation dose estimates. *Radiographics* 2011; 31: 1833–1846
- 6 Vano E, Padovani R, Bernardi G et al. On the use of DICOM cine header information for optimisation: results from the 2002 European DIMOND cardiology survey. *Radiat Prot Dosimetry* 2005; 117: 162–165
- 7 Dave JK, Gingold EL. Extraction of CT dose information from DICOM metadata: automated Matlab-based approach. *Am J Roentgenol* 2013; 200: 142–145
- 8 Boos J, Lanzman RS, Meineke A et al. Dose monitoring using the DICOM structured report: assessment of the relationship between cumulative radiation exposure and BMI in abdominal CT. *Clin Radiol* 2015; 70: 176–182
- 9 General Electrics Healthcare. Dose Watch Data Sheet; 2013, Available at: www3.gehealthcare.com/en/products/dose_management/dosewatch Accessed on 22.06.2015
- 10 Kalmar PI, Quehenberger F, Steiner J. The impact of iterative reconstruction on image quality and radiation dose in thoracic and abdominal CT. *Eur J Radiol* 2014; 83: 1416–1420
- 11 Matsunaga Y, Kawaguchi A, Kobayashi K et al. Survey of volume computed tomography dose index in Japan in 2014. *Br J Radiol* 2015; 4: 20150219
- 12 Shrimpton PC, Hillier MC, Lewis MA et al. National survey of doses from CT in the UK: 2003. *Br J Radiol* 2006; 79: 968–980 [Published correction appears in *Br J Radiol* 2007;80(956):685
- 13 Santos J, Foley S, Paulo G et al. The establishment of computed tomography diagnostic reference levels in Portugal. *Radiat Prot Dosimetry* 2014; 158: 307–317
- 14 Treier R, Aroua A, Verdun FR. Patient doses in CT examinations in Switzerland: implementation of national diagnostic reference levels. *Radiat Prot Dosimetry* 2010; 142: 244–254
- 15 McCollough C, Branham T, Herlihy V et al. Diagnostic reference levels from the ACR CT Accreditation Program. *J Am Coll Radiol* 2011; 8: 795–803
- 16 Elbakri IA, Kirkpatrick ID. Dose-length product to effective dose conversion factors for common computed tomography examinations based on Canadian clinical experience. *Can Assoc Radiol J* 2013; 64: 15–17
- 17 Lukasiewicz A, Bhargavan-Chatfield M, Coombs L et al. Radiation dose index of renal colic protocol CT studies in the United States: a report from the American College of Radiology National Radiology Data Registry. *Radiology* 2014; 271: 445–451
- 18 Imai R, Miyazaki O, Horiuchi T et al. Local diagnostic reference level based on size-specific dose estimates: assessment of pediatric abdominal/pelvic computed tomography at a Japanese national children's hospital. *Pediatr Radiol* 2015; 45: 345–353
- 19 Taylor S, Van Muylem A, Gevenois PA et al. Intra-institution CT dose surveys in adults: what sample size for what precision? ECR 2015, B-0785. DOI: 10.1594/ecr2015/B-0785

Received:
3 September 2015

Revised:
16 December 2015

Accepted:
21 December 2015

doi: 10.1259/bjr.20150734

Cite this article as:

Boos J, Lanzman RS, Heusch P, Aissa J, Schleich C, Thomas C, et al. Does body mass index outperform body weight as a surrogate parameter in the calculation of size-specific dose estimates in adult body CT? *Br J Radiol* 2016; **89**: 20150734.

FULL PAPER

Does body mass index outperform body weight as a surrogate parameter in the calculation of size-specific dose estimates in adult body CT?

JOHANNES BOOS, MD, ROTEM S LANZMAN, MD, PHILIPP HEUSCH, MD, JOEL AISSA, MD, CHRISTOPH SCHLEICH, MD, CHRISTOPH THOMAS, MD, LINO M SAWICKI, MD, GERALD ANTOCH, MD and PATRIC KRÖPIL, MD

University Dusseldorf, Medical Faculty, Department of Diagnostic and Interventional Radiology, Dusseldorf, Germany

Address correspondence to: Dr Johannes Boos
E-mail: Johannes.Boos@med.uni-duesseldorf.de

Objective: To assess the value of body mass index (BMI) in comparison with body weight as a surrogate parameter for the calculation of size-specific dose estimates (SSDEs) in thoracoabdominal CT.

Methods: 401 CT examinations in 235 patients (196 chest, 205 abdomen; 95 females, 140 males; age 62.5 ± 15.0 years) were analysed in regard to weight, height and BMI (kg m^{-2}). Effective diameter (D_{eff} , cm) was assessed on axial CT images. The correlation between BMI, weight and D_{eff} was calculated. SSDEs were calculated based on D_{eff} , weight and BMI and lookup tables were developed.

Results: Overall height, weight, BMI and D_{eff} were 172.5 ± 9.9 cm, 79.5 ± 19.1 kg, 26.6 ± 5.6 kg m^{-2} and 30.1 ± 4.3 cm, respectively. There was a significant correlation between D_{eff} and BMI as well as weight ($r = 0.85$ and $r = 0.84$; $p < 0.05$, respectively). Correlation was significantly

better for BMI in abdominal CT ($r = 0.89$ vs $r = 0.84$; $p < 0.05$), whereas it was better for weight in chest CT ($r = 0.87$ vs $r = 0.81$; $p < 0.05$). Surrogated SSDEs did not differ significantly from the reference standard with a median absolute relative difference of 4.2% per patient (interquartile range 25–75: 3.1–7.89, range 0–25.3%).

Conclusion: BMI and weight exhibit a significant correlation with D_{eff} in adult patients and can be used as surrogates in the calculation of SSDEs. Using the herein-developed lookup charts, SSDEs can be calculated based on patients' weight and BMI.

Advances in knowledge: In abdominal CT, BMI has a superior correlation with effective diameter compared with weight, whereas weight is superior in chest CT. Patients' BMI and weight can be used as surrogates in the calculation of SSDEs.

INTRODUCTION

The volumetric CT dose index (CTDI_{vol} , mGy) and the dose-length product (DLP, mGycm) are the two most common parameters used to describe radiation exposure from CT examinations. The CTDI_{vol} is defined as CTDI_w normalized to the pitch factor. DLP is calculated by multiplying CTDI_{vol} with the length of the scan volume. The value of both, CTDI_{vol} and DLP in regard to the actual radiation exposure is limited, as CTDI_{vol} only accounts for the radiation output within a defined volume based on a phantom. Size-specific dose estimates (SSDEs) have been introduced by the American Association of Physicists in Medicine (AAPM) in 2011.¹ Four independent research groups performed either phantom measurement as well as Monte Carlo simulations and provided size-dependent conversion factors. These factors can be used to correct CTDI_{vol} according to patients' habitus. Different methods to assess SSDEs were provided, whereas diameter measurements on axial CT images and calculation of the

effective diameter (D_{eff}) were considered the most accurate.¹ Automatic measurements and calculation of D_{eff} has not been integrated into modern CT scanners so far. Furthermore, SSDE values are not part of the digital imaging and communications in medicine radiation dose structured report.

Owing to the limitations of CTDI_{vol} as a parameter for patient dose exposure, dose estimates taking into account patients' habitus have gained ever more importance. To manually calculate SSDEs, measurements require the original CT images which may not always be available, e.g. in dose registry analysis or when assessing patients' lifetime radiation dose exposure retrospectively.^{2,3} If images are available, the whole-body circumference has to be in the field of view in order to calculate SSDEs using D_{eff} . This might not always be the case, e.g. in spine-CT studies or CT examinations of obese patients. Nevertheless, dose data taking into account patient's habitus are desirable, and

therefore research has been performed to establish surrogate methods using patients' characteristics. Recently, a method to surrogate SSDEs in paediatric patients was introduced.⁴ A high correlation between D_{eff} and body weight was demonstrated and a lookup table was provided to calculate SSDEs from patients' weight in paediatric patients to simplify the SSDE method.⁴

It has been hypothesized that body mass index (BMI) might be superior to body weight as a surrogate parameter for SSDEs because it also takes the patients' height into account. To our knowledge, the value of BMI as a surrogate parameter for D_{eff} in the calculation of SSDEs has not been investigated so far.

Therefore, the aim of this study was to assess the value of BMI compared with body weight as a surrogate parameter in the calculation of SSDEs in adult clinical abdominal and chest CT.

METHODS AND MATERIALS

Patients

This retrospective study was approved by the local ethics committee. 235 patients (137 males, 98 females; mean patient age 62.5 ± 15.0 years) who underwent 401 clinical CT examinations (196 chest, 205 abdomen) were retrospectively included in this study. CT examinations were performed on three different CT scanners (Definition AS+, Definition Flash and Definition AS with sliding gantry; Siemens AG, Healthcare Sector, Forchheim, Germany). Automated tube current modulation (CareDose 4D; Siemens AG, Healthcare Sector) was activated on all scanners.

Measurements

Diameter measurements were performed on a standard picture archiving and communications system workstation (IDS 7; Sectra Medical Systems GmbH, Linköping, Sweden) by two radiologists (blinded, with 2 and 4 years' of experience with abdominal and chest CT) in consensus mode. Both radiologists were blinded to patients' demographic data. Measurements were performed according to the recommendations of the AAPM report 204 in the axial CT images.¹ Scan volume ranged from the supra-aortic branches to the bottom of the liver for chest CT and from the bottom of the lung to the common femoral arteries for abdominal CT. For method standardization, all measurements were performed on mid slice images of the scan volume according to previous studies.⁵

The largest anterior–posterior diameter (D_{ap}) and lateral diameter (D_{lat}) were measured (Figure 1) and used to calculate D_{eff} :

$$\sqrt{D_{\text{ap}} \times D_{\text{lat}}} \quad (1)$$

Patients' weight and height were routinely assessed by the technician at the time of CT examination and documented in the patient protocol in the picture archiving and communications system. All data were extracted from the patient protocol and verified using the digital patient record. In this study, BMI was calculated using the equation provided by the World Health Organization: $\text{BMI} = \text{weight height}^{-2}$.⁶ CTDI_{vol} was extracted from the patient protocol.

Size-specific dose estimates calculation

As the reference standard, SSDEs were calculated according to the recommendations of the AAPM report 204 based on diameter measurements on axial CT images and calculation of D_{eff} . The conversion factors from the lookup table provided by report 204 and D_{eff} were used to assess SSDEs.¹

Correlation coefficients were calculated for D_{eff} and BMI; D_{eff} and weight; D_{eff} and height; and D_{eff} and age (Figures 2–5) for chest CT and abdominal CT. Regression equations for D_{eff} and BMI as well as D_{eff} and body weight were used to determine D_{eff} values ($D_{\text{eff_bmi}}$; $D_{\text{eff_weight}}$) based on the corresponding BMI and body weight for every patient. Values for either BMI or weight were inserted into the regression equations to calculate the corresponding $D_{\text{eff_bmi}}$ and $D_{\text{eff_weight}}$. The lookup chart from report 204 was used to calculate the corresponding conversion factor using D_{eff} , $D_{\text{eff_weight}}$ and $D_{\text{eff_bmi}}$.¹ Lookup tables were prepared to enable the calculation of SSDEs using weight as a surrogate parameter in chest CT and using BMI as a surrogate parameter in abdominal CT (more information is given in the Results section, the Size-specific dose estimates subsection).

Absolute and relative differences between surrogated SSDEs and the reference standard per patient were assessed. Correlation between relative SSDE difference per patient and patient's weight, height and BMI was determined.

Data analysis

IBM SPSS® Statistics v. 21 for Windows® (IBM Corp., New York, NY; formerly SPSS Inc., Chicago, IL) was used for statistical analysis. Statistical significance is set to $p < 0.05$. Correlation was calculated using Pearson correlation coefficient. A Kolmogorov test was performed to test for normality. A Fisher's Z transformation with the extension published by Steiger⁷ was used to compare correlations. To perform the calculations, we used a software tool provided by Lee and Preacher⁸ (Stanford University). Student's t -test was used to compare normal distributed values. A Mann–Whitney U test was performed as

Figure 1. Measurement of lateral and anteroposterior diameter to calculate effective diameter.

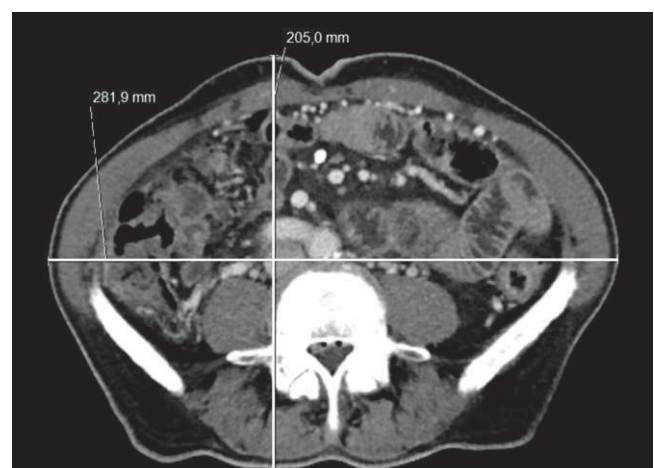
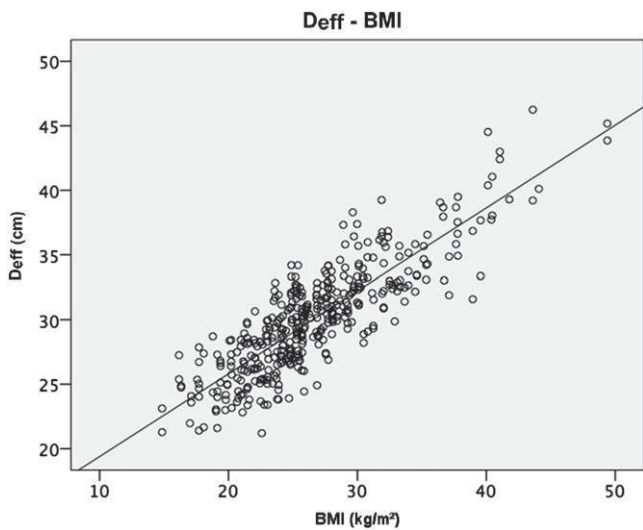


Figure 2. Correlation between effective diameter (D_{eff}) and body mass index (BMI).



a non-parametric test. Data are reported as mean \pm standard deviation with ranges and 95% confidence intervals (95% CIs) or as median with 25–75% interquartile ranges (IQR 25–75). To evaluate the error of the surrogate methods per patient, median absolute relative difference per patient {formula: $[\text{absolute value}(\text{surrogated SSDE} - \text{reference SSDE})]/\text{reference SSDE} \times 100$ } and the respective IQR 25–75 was calculated.

RESULTS

Patients' characteristics and diameter measurements

Patient demographics are listed in Table 1. Mean D_{eff} calculated using the manual measurements was 30.1 ± 4.3 cm (95% CI: 29.7–30.5 cm). Mean D_{eff_weight} was 30.0 ± 3.6 (95% CI: 29.7–30.4 cm) compared with 30.1 ± 3.6 cm for D_{eff_bmi} (95% CI: 29.7–30.4 cm).

Figure 3. Correlation between effective diameter (D_{eff}) and weight.

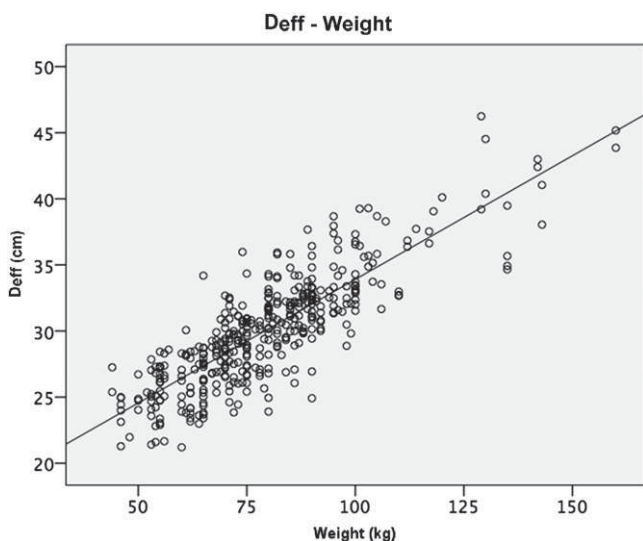
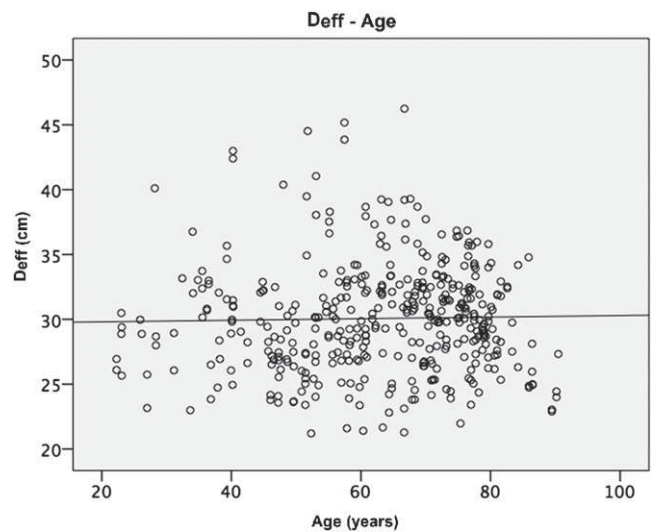


Figure 4. Correlation between effective diameter (D_{eff}) and age.



Absolute difference for D_{eff_weight} and D_{eff_bmi} from D_{eff} was 1.86 ± 1.49 cm (median absolute relative difference: 4.8%; IQR 25–75: 2.5–9.2%) and 1.87 ± 1.36 cm (median absolute relative difference: 5.1%, IQR 25–75: 2.8–8.9%), respectively. This absolute difference could be reduced to 1.64 ± 1.32 cm (median absolute relative difference: 4.5%, IQR 25–75: 2.2–7.6%) when surrogating D_{eff} using weight in chest CT studies and BMI in abdominal CT studies. Detailed results from diameter measurements are shown in Table 1.

Correlations

There was a significant correlation between body weight and BMI ($r = 0.86$, $p < 0.0001$, 95% CI 0.84–0.89) for all CT examinations. Similarly, in all examinations, D_{eff} correlated significantly with BMI ($r = 0.85$, $p < 0.0001$, 95% CI 0.82–0.88) and body weight ($r = 0.84$, $p < 0.0001$, 95% CI 0.81–0.87).

Figure 5. Correlation between effective diameter (D_{eff}) and size.

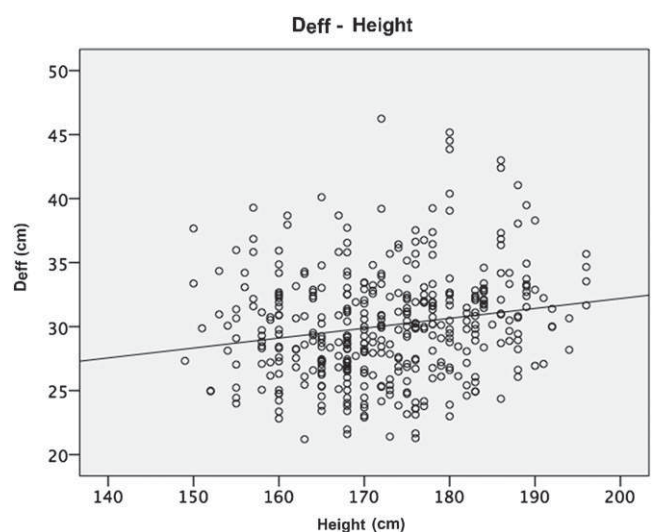


Table 1. Patient characteristics and results from diameter measurements

	Overall	Abdominal CT	Chest CT
Number (<i>n</i>)	401	205	196
Weight (kg)	79.5 ± 19.1 (44–160)	80.0 ± 19.6 (44–160)	78.9 ± 18.5 (44–160)
Height (cm)	172.5 ± 9.9 (149–196)	172.4 ± 10.0 (149–196)	172.6 ± 9.8 (149–196)
Age (years)	62.5 ± 15.0 (22–90)	62.6 ± 14.9 (22–90)	62.5 ± 15.2 (22–90)
BMI (kg m ⁻²)	26.6 ± 5.6 (14.9–49.4)	26.9 ± 5.9 (14.9–49.4)	26.4 ± 5.4 (14.9–49.4)
BMI <20 kg m ⁻² , (<i>n</i>)	31 (14.85–19.91)	17 (14.9–19.9)	14 (14.9–19.9)
BMI 20–25 kg m ⁻² , (<i>n</i>)	145 (20.20–24.97)	72 (20.2–25.0)	74 (20.1–25.0)
BMI 25–30 kg m ⁻² , (<i>n</i>)	137 (25.19–29.98)	68 (25.2–30.0)	69 (25.1–30.0)
BMI 30–35 kg m ⁻² , (<i>n</i>)	53 (30.07–34.60)	27 (30.1–34.6)	26 (30.1–34.6)
BMI >35 kg m ⁻² (<i>n</i>)	35 (35.43–49.38)	21 (35.1–49.4)	14 (35.1–49.4)
Diameter (axial, anteroposterior) (cm)	25.5 ± 4.2	25.3 ± 4.8	25.8 ± 3.3
Diameter (axial, lateral) (cm)	35.2 ± 4.9	35.9 ± 5.5	35.1 ± 4.2
<i>D</i> _{eff} (cm)	30.1 ± 4.3	30.0 ± 4.9	30.1 ± 3.5
<i>D</i> _{eff_weight} (cm)	<i>30.0 ± 3.6^a</i>	<i>30.1 ± 3.7^a</i>	30.1 ± 2.9
<i>D</i> _{eff_bmi} (cm)	<i>30.1 ± 3.6^a</i>	30.1 ± 4.3	29.9 ± 3.4 ^a

BMI, body mass index; *D*_{eff}, effective diameter; *D*_{eff_bmi}, effective diameter calculated from body mass index; *D*_{eff_weight}, effective diameter calculated from weight.

^aValues in italics were calculated with the corresponding correlation equations for the whole data set.

Ranges are shown in parenthesis.

Nevertheless, there was no statistical significant difference between these correlation coefficients (*z*-score: 0.776, *p* = 0.44).

For abdominal CT, *D*_{eff} and BMI (*r* = 0.89; *p* < 0.0001, 95% CI 0.85–0.91) correlated significantly better than *D*_{eff} and body weight (*r* = 0.84; *p* < 0.001, 95% CI 0.79–0.87) (*z*-score: 3.053, *p* = 0.002).

For chest CT, *D*_{eff} and body weight (*r* = 0.87; *p* < 0.0001, 95% CI 0.83–0.90) correlated significantly better than *D*_{eff} and BMI

(*r* = 0.81; *p* < 0.0001, 95% CI 0.76–0.86) (*z*-score: 3.238, *p* < 0.001).

Correlation was comparable for male and female patients in abdominal CT (BMI: *r* = 0.90, respectively; weight: *r* = 0.86 vs *r* = 0.83; *p* = 0.32). Correlation was significantly better for BMI in female patients in chest CT (BMI: *r* = 0.88 vs *r* = 0.82; *p* = 0.03), whereas there was no significant difference for weight (*r* = 0.87 vs *r* = 0.85; *p* = 0.45). There was no significant difference between correlation of BMI and *D*_{eff} and

Figure 6. Bland-Altman plots for effective diameter (*D*_{eff}) calculation based on weight (a, *D*_{eff_weight}) and body mass index (BMI) (b, *D*_{eff_BMI}) compared with *D*_{eff} calculation based on diameter measurements.

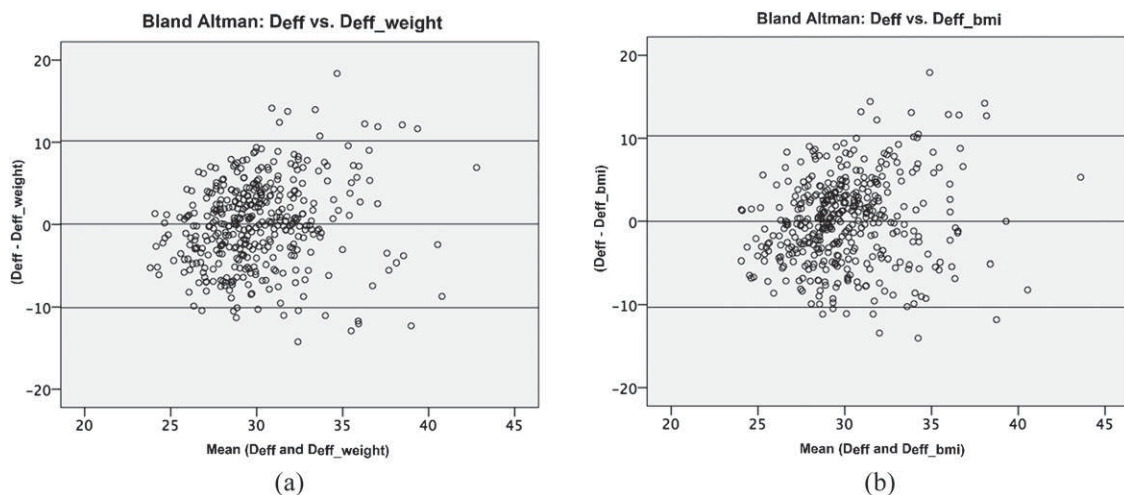
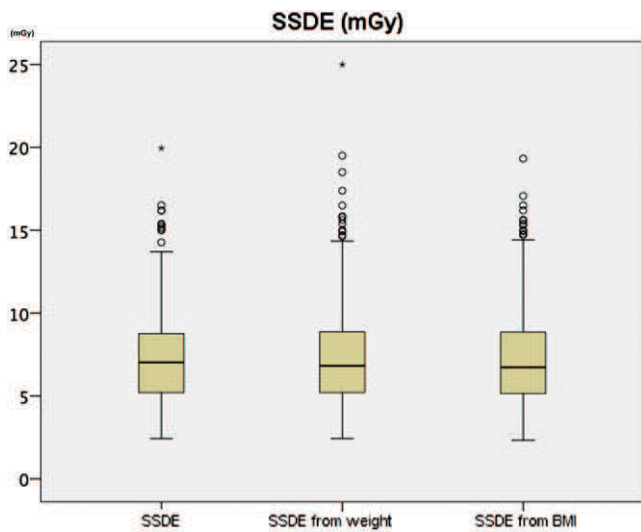


Figure 7. Box plots of calculations of size-specific dose estimate (SSDE) based on manual diameter measurements, body weight and body mass index (BMI).



weight and D_{eff} in chest CT of female patients ($r = 0.88$ vs $r = 0.87$, $p = 0.64$).

Overall there was no statistically significant correlation between D_{eff} and age ($r = 0.02$; $p = 0.6$, 95% CI -0.07 to 0.12). There was a significant correlation for D_{eff} and height for chest CT ($r = 0.33$; $p < 0.0001$, 95% CI $0.2-0.45$), whereas there was no significant correlation for D_{eff} and height in abdominal CT studies ($r = 0.08$; $p = 0.2$, 95% CI -0.06 to 0.22). Correlation between the different surrogate parameters and D_{eff} are illustrated in Figures 2–5. The regression equations for weight in chest CT studies and BMI in abdominal CT studies were:
 Weight in chest CT: $y = 0.1626x + 17.265$.
 BMI in abdominal CT: $y = 0.7374x + 10.225$.

Bland–Altman plots for the calculation of D_{eff_bmi} and D_{eff_weight} compared with manually measured D_{eff} indicate a good agreement between both methods (Figure 6a,b).

Size-specific dose estimates

Mean $CTDI_{vol}$ was 6.1 ± 3.1 mGy. Mean SSDE values were 7.28 ± 2.76 mGy for the reference standard (diameter

measurements; 95% CI $7.0-7.6$ mGy), 7.35 ± 3.05 mGy (95% CI $7.1-7.6$ mGy) for body weight as a surrogate parameter and 7.33 ± 2.90 mGy (95% CI $7.1-7.6$ mGy) for BMI as a surrogate parameter. There was no significant difference between surrogated SSDEs and the reference standard (weight: $p = 0.76$; BMI: $p = 0.81$) (Figure 7).

Using the dedicated chest and abdominal CT correlation equations for the calculation of SSDEs separately, the value for D_{eff_weight} in chest CT was 5.61 ± 2.07 mGy (95% CI $5.3-5.9$ mGy) and for D_{eff_bmi} abdominal CT was 8.97 ± 2.58 mGy (95% CI $8.6-9.3$ mGy).

SSDEs per patient using the overall correlation differed from the reference standard by a median of 4.4% for weight (mean of 6.73%, range abdominal $0-25.5\%$, range chest $0-23.9\%$) and 6.5% for BMI (mean 6.85%, range abdominal $0-29.4\%$, range chest: $0-20.2\%$). The median absolute relative difference was improved to 4.2% (mean 5.97%, range abdominal: $0-25.3\%$, range chest: $0-23.9\%$) when using the dedicated regression equations for weight in chest CT studies and for BMI in abdominal CT studies (Table 2). There was no significant correlation between body weight, BMI or height and the variation of surrogated SSDEs per patient (weight: $r = 0.1$; BMI: $r = 0.1$ and height $r = 0.02$; $p > 0.05$, respectively).

The provided lookup charts (Tables 3 and 4) can be used to calculate SSDEs based on patients' weight in chest CT and BMI in abdominal CT.

DISCUSSION

This study documented a significant correlation between body weight and D_{eff} as well as BMI and D_{eff} in adult CT examinations of the abdomen and chest. Overall, correlation was slightly, but not significantly, increased for BMI compared with body weight. Detailed analysis revealed a significantly improved correlation for weight compared with D_{eff} in chest CT studies and for BMI to D_{eff} in abdominal CT studies. Although overall the calculation of SSDEs using either method as a surrogate parameter did not differ significantly from calculations of SSDEs based on axial diameter measurements, mean difference per patient was improved when using weight for chest and BMI for abdominal CT studies. Therefore, we created lookup charts, which can be used to

Table 2. Median absolute relative difference (%) and interquartile range (25–75%) of size-specific dose estimates per patient for the different regression equations

Regression equation used	Overall	Abdominal CT	Chest CT
BMI (chest + abdominal) ^a	6.5 (3.4–10.5)	6.6 (3.4–10.5)	5.5 (3.5–10.4)
Weight (chest + abdominal) ^b	4.4 (3.4–10.0)	7.3 (3.5–11.8)	4.1 (3.1–7.7)
BMI (abdominal) ^c	4.2 (3.1–7.9)	7.0 (3.4–10.3)	–
Weight (chest) ^d	–	–	3.9 (3.0–7.5)

BMI, body mass index.

All values are given in percent of SSDE calculated with the reference standard.

^aRegression equation for BMI (chest + abdominal): $y = 12.976 + 0.6414x$.

^bRegression equation for weight (chest + abdominal): $y = 15.204 + 0.187x$.

^cRegression equation for BMI (abdominal): $y = 10.225 + 0.7374x$.

^dRegression equation for weight (chest): $y = 17.265 + 0.1626x$.

Table 3. Conversion factors to calculate size-specific dose estimates in abdominal CT using body mass index (BMI) as a surrogate parameter

BMI (kg m^{-2})	Conversion factors
10	1.93
11	1.88
12	1.83
13	1.78
14	1.73
15	1.68
16	1.64
17	1.59
18	1.55
19	1.51
20	1.47
21	1.43
22	1.39
23	1.35
24	1.32
25	1.28
26	1.25
27	1.21
28	1.18
29	1.15
30	1.12
31	1.09
32	1.06
33	1.03
34	1.00
35	0.97
36	0.95
37	0.92
38	0.90
39	0.87
40	0.85
41	0.83
42	0.81
43	0.78
44	0.76
45	0.74
46	0.72
47	0.70

calculate SSDE values using weight and BMI as surrogate parameters in case diameter measurements cannot be performed.

Initially, the SSDE concept was introduced to correct the scanner indicated CTDI_{vol} value according to the patients' constitution.^{1,9} This has to be performed because radiation exposure of patients depends on both the radiation output of the scanner and the patient habitus.⁸ Different studies have been performed for SSDE validation, optimization and simplification of the SSDE concept.^{1,4,10–13} Commercial and non-commercial software tools have been introduced to automatically perform diameter measurements and assess SSDEs.^{4,12,14} These software tools as well as manual diameter measurements require axial CT images or the scout images, which may not be always available, e.g. in the setting of cloud-based dose monitoring or retrospective data analysis.^{2,3} The AAPM recommended integration of automatic SSDEs reporting into the CT scanner software and into the digital imaging and communications in medicine radiation dose structured report, but this has not yet been executed by the manufacturers. To simplify the SSDE method and to calculate SSDEs without patients' images, different studies evaluated body weight as a surrogate parameter for SSDEs.^{4,15,16}

The initial AAPM report 204 introduced patient age (and not weight or BMI) as a surrogate parameter in paediatric patients.¹ Correlation between age and D_{eff} in this study was not significant in our adult collective. This has to be expected, as age in childhood may correlate with growth (and therefore D_{eff}) but it does not do so in adulthood.

Pourjabbar et al¹⁶ reported a correlation of $r = 0.89/r = 0.92$ between weight and anteroposterior/lateral transverse diameter. A significant correlation between patient's weight and SSDEs calculated from the diameter measurements on scout image was shown. Those results, however, cannot be compared with the results presented here, as only the lateral/anteroposterior diameter was measured and D_{eff} was not calculated. Furthermore, BMI was not part of the study and SSDEs were not calculated using surrogate parameters.¹⁶

Cook et al¹⁵ investigated the correlation between patient weight and D_{eff} in CT examinations of the chest and abdomen. They determined D_{eff} automatically on central CT images using a commercially available software tool (Radimetrics eXposure®; Bayer Healthcare, Toronto, ON, Canada). A linear relationship between patient weight and D_{eff} was reported, which is in accordance to our results. Detailed comparison of our results to those reported by Cook et al cannot be performed because BMI was not investigated in their study.

Khawaja et al⁴ reported a correlation between body weight and D_{eff} of $r = 0.87$ and did not find a statistical difference between SSDEs based on measurements and SSDEs based on weight in the paediatric population. This is similar to our results found in an adult population. Although Khawaja et al⁴ provided a comprehensive subgroup analysis in regard to body weight and age groups in their paediatric population, BMI as a surrogate parameter was not assessed. Our results indicate that different surrogate parameters are favourable for abdominal and chest CT studies, respectively. Because chest CT studies and abdominal

Table 4. Conversion factors to calculate size-specific dose estimates in chest CT using patient's weight as a surrogate parameter

Weight (kg)	Conversion factors
<44	1.50
45–47	1.48
48–51	1.45
52–54	1.42
55–58	1.39
59–61	1.36
62–65	1.33
66–68	1.30
69–72	1.28
73–77	1.24
78–81	1.21
82–85	1.18
86–90	1.15
91–94	1.12
95–99	1.09
100–104	1.06
105–109	1.03
110–114	1.00
115–120	0.96
121–130	0.92
131–140	0.86
141–150	0.81
151–160	0.77
161–170	0.72
>170	0.70

CT studies were not investigated separately by Khawaja et al,⁴ comparability with our study is limited.

Our study has certain limitations. Although median absolute relative difference of SSDE values in our population was only 4% per patient when using weight for chest CT and BMI

for abdominal CT, respectively, the difference between the reference standard and surrogated values was up to 25% in two cases. We used median and IQR and provided Bland–Altman plots to describe our method as exact as possible. We did not find a significant correlation between patient's weight, height or BMI and the variation of SSDEs. Owing to the restricted sample size of this study with a very limited number of outliers, we could not perform a more detailed analysis to further assess the reason for the deviation in single cases. Larger studies have to be conducted to verify our results and to determine in which patients BMI and weight might not be suitable as surrogate parameters for SSDEs.

All diameter measurements were performed manually as automatic measurement software was not available. This may lead to variability but reflects clinical routine. In a recent report, the AAPM proposed an alternative method of calculation of SSDEs based on the water equivalent diameter (D_w) which comprises patients' attenuation to correct $CTDI_{vol}$.¹⁰ We did not calculate D_w and therefore cannot give a statement about correlation of either weight or BMI and D_w . Further studies to assess the correlation between the parameters evaluated here and D_w are desirable. Nevertheless, according to the AAPM report 220, it is reasonable to use geometric data to calculate SSDEs when D_w is not available, and therefore D_{eff} is frequently used for the calculation of SSDEs in clinical routine as well as in various recent studies investigating radiation dose exposure from CT.^{10,17–19} The number of wide-detector CT scanners is increasing. $CTDI_{vol}$ is calculated based on a 10-cm pencil chamber and therefore SSDEs might not be applicable on these scanners.²⁰

In conclusion, a good correlation between body weight and effective diameter as well as BMI and effective diameter in adult chest and abdominal CT examinations was shown in the presented study. BMI demonstrated a significantly better correlation with D_{eff} for abdominal CT, whereas weight showed a significantly better correlation in chest CT. On average, SSDE value per patient calculated with one of the two surrogate parameters for abdominal and chest CT, respectively, differed <6% from those calculated with the reference standard. The lookup charts provided here can be used to assess SSDEs in adult CT of the torso in cases where patient images are not available.

REFERENCES

- American Association of Physicists in Medicine. *Size-specific dose estimates (SSDE) in pediatric and adult body CT. Examinations (Report 204)*. 2011. [Accessed 20 April 2015.] Available from: http://www.aapm.org/pubs/reports/rpt_204.pdf
- General Electrics Healthcare, Dose Watch Explore Product Data Sheet. [Accessed 2 May 2015.] Available from: www.gehealthcare.com/dwexplore
- Boos J, Lanzman RS, Meineke A, et al. Dose monitoring using the DICOM structured report: assessment of the relationship between cumulative radiation exposure and BMI in abdominal CT. *Clin Radiol* 2015; **70**: 176–82. doi: [10.1016/j.crad.2014.11.002](https://doi.org/10.1016/j.crad.2014.11.002)
- Khawaja RD, Singh S, Vettiyl B, et al. Simplifying size-specific radiation dose estimates in pediatric CT. *AJR Am J Roentgenol* 2015; **204**: 167–76. doi: [10.2214/AJR.13.12191](https://doi.org/10.2214/AJR.13.12191)
- Cheng PM. Automated estimation of abdominal effective diameter for body size normalization of CT dose. *J Digit Imaging* 2013; **26**: 406–11. doi: [10.1007/s10278-012-9525-z](https://doi.org/10.1007/s10278-012-9525-z)
- World Health Organisation. *Obesity: preventing and managing the global epidemic*:

- report a WHO consultation. *WHO Technical Report Series* 894. 2000.
7. Steiger JH. Test for comparing elements of a correlation matrix. *Psychol Bull* 1980; **87**: 245–51. doi: [10.1037/0033-2909.87.2.245](https://doi.org/10.1037/0033-2909.87.2.245)
 8. Lee IA, Preacher KJ. Calculation for the test of the difference between two dependent correlations with one variable in common [computer software]. 2013. [Accessed 25 August 2015.] Available from: <http://quantpsy.org>
 9. Brink JA, Morin RL. Size-specific dose estimation for CT: how should it be used and what does it mean? *Radiology* 2012; **265**: 666–8. doi: [10.1148/radiol.12121919](https://doi.org/10.1148/radiol.12121919)
 10. American Association of Physicists in Medicine. *Use of water equivalent diameter for calculating patient size and size-specific dose estimates (SSDE) in CT (Report 222)*. 2014. [Accessed 2 May 2015.] Available from: http://www.aapm.org/pubs/reports/RPT_220.pdf
 11. Brady SL, Kaufman RA. Investigation of American Association of Physicists in Medicine Report 204 size-specific dose estimates for pediatric CT implementation. *Radiology* 2012; **265**: 832–40. doi: [10.1148/radiol.12120131](https://doi.org/10.1148/radiol.12120131)
 12. Leng S, Shiung M, Duan X, Yu L, Zhang Y, McCollough CH. Size-specific dose estimates for chest, abdominal, and pelvic CT: effect of inpatient variability in water-equivalent diameter. *Radiology* 2015; **277**: 308–9. doi: [10.1148/radiol.2015151209](https://doi.org/10.1148/radiol.2015151209)
 13. Phillips GS, Stanescu AL, Alessio AM. Relationships of pediatric anthropometrics for CT protocol selection. *AJR Am J Roentgenol* 2014; **203**: W85–91. doi: [10.2214/AJR.13.10794](https://doi.org/10.2214/AJR.13.10794)
 14. General Electric Healthcare, Dose Watch Data Sheet. 2013. [Accessed 20 April 2015.] Available from: www3.gehealthcare.com/en/products/dose_management/dosewatch
 15. Cook TS, Chadalavada SC, Boonn WW. How inaccurate is weight as a metric for patient size? Comparing patient weight to effective diameter for size-specific dose estimation. 2013; *Proc SPIE* **8674**. 867408. doi: [10.1117/12.2006132](https://doi.org/10.1117/12.2006132)
 16. Pourjabbar S, Singh S, Padole A, Saini A, Blake MA, Kalra MK. Size-specific dose estimates: localizer or transverse abdominal computed tomography images? *World J Radiol* 2014; **6**: 210–17. doi: [10.4329/wjr.v6.i5.210](https://doi.org/10.4329/wjr.v6.i5.210)
 17. Waszczuk ŁA, Guziński M, Czarnecka A, Szaśiadek MJ. Size-specific dose estimates for evaluation of individual patient dose in CT protocol for renal colic. *AJR Am J Roentgenol* 2015; **205**: 100–5. doi: [10.2214/AJR.14.13573](https://doi.org/10.2214/AJR.14.13573)
 18. Andrabi Y, Pinykh O, Agrawal M. Radiation dose consideration in kidney stone CT examinations: integration of iterative reconstruction algorithms with routine clinical practice. *AJR Am J Roentgenol* 2015; **204**: 1055–63. doi: [10.2214/AJR.14.13038](https://doi.org/10.2214/AJR.14.13038)
 19. Berlin SC, Weinert DM, Vasavada PS, et al. Successful dose reduction using reduced tube voltage with hybrid iterative reconstruction in pediatric abdominal CT. *AJR Am J Roentgenol* 2015; **205**: 392–9. doi: [10.2214/AJR.14.12698](https://doi.org/10.2214/AJR.14.12698)
 20. de Denaro M, Bregant P. Dosimetric evaluation of a 320 detector row CT scanner unit. *Radiol Oncol* 2011; **45**: 64–7. doi: [10.2478/v10019-010-0049-1](https://doi.org/10.2478/v10019-010-0049-1)



CT angiography of the aorta using 80 kVp in combination with sinogram-affirmed iterative reconstruction and automated tube current modulation: Effects on image quality and radiation dose

Johannes Boos,* Joel Aissa, Rotem S Lanzman, Philipp Heusch, Lars Schimmöller, Christoph Schleich, Christoph Thomas, Gerald Antoch and Patric Kröpil

Department of Diagnostic and Interventional Radiology, Medical Faculty, University Dusseldorf, Dusseldorf, Germany

J Boos Dr. Med.; **J Aissa** Dr. Med.; **RS Lanzman** Prof. Dr. med.; **P Heusch** Dr. med.; **L Schimmöller** Dr. med.; **C Schleich** Dr. med.; **C Thomas** PD Dr. med.; **G Antoch** Univ-Prof. Dr. med.; **P Kröpil** PD Dr. med.

Correspondence

Dr Johannes Boos, Department of Diagnostic and Interventional Radiology, Medical Faculty, University Dusseldorf, D-40225 Dusseldorf, Germany.

Email: Johannes.Boos@med.uni-duesseldorf.de

*Present address: Department of Radiology, Beth Israel Deaconess Medical Center, Harvard Medical School, 330 Brookline Avenue, Boston, MA 02215, USA.

Conflict of interest: The authors declare that there is no conflict of interest.

Submitted 16 August 2015; accepted 4 November 2015.

doi:10.1111/1754-9485.12425

Abstract

Introduction: The objective of this study was to evaluate image quality and radiation dose of a CT angiography (CTA) protocol using 80 kVp in combination with iterative reconstruction and automated tube current modulation.

Methods: Ninety-five aortic CTA examinations were included in this study. A novel 80 kVp aortic CTA-protocol with iterative reconstruction was introduced in our department in March 2012 for patients with a body mass index (BMI) below 32 kg/m². The first 72 consecutive examinations were retrospectively assigned to group A (56 patients, 42 men, 14 women, mean age 69.6 ± 10.7 years, BMI range 19.7–31.1 kg/m²). For comparison, the last 23 consecutive examinations performed with the old protocol (100 kVp) were assigned to group B (21 patients, 13 men, 8 women, mean age 67.4 ± 11.1 years, BMI range 19.7–31.9 kg/m²). Thoracic and abdominal contrast-to-noise ratio (CNR), signal-to-noise ratio (SNR) and aortic attenuation were assessed. Subjective image quality was rated on a 5-point scale (1 = *non diagnostic*; 5 = *excellent*). Furthermore, dose length product (DLP) and volumetric computed tomography dose index (CTDI_{vol}) were analysed.

Results: All examinations achieved diagnostic image quality. Attenuation of the aorta was significantly higher in group A compared with B (thoracic: 443.5 ± 90.5 Hounsfield units (HU) vs. 296.0 ± 61.0 HU; abdominal: 426.3 ± 94.2 HU vs. 283.6 ± 60.5 HU; *P* < 0.05, respectively). CNR, SNR and subjective image quality were comparable between both groups (CNR: 12.8 ± 3.7 vs. 13.0 ± 7.4; SNR 14.4 ± 3.9 vs. 14.9 ± 8.2; subjective image quality: 4.3 ± 0.6 vs. 4.5 ± 0.6; *P* > 0.05, respectively). CTDI_{vol} and DLP were significantly lower in group A (1.9 ± 0.5 mGy; 139.2 ± 41.1 mGy × cm) as compared with group B (4.2 ± 1.4 mGy; 292.1 ± 91.5 mGy × cm; *P* < 0.001, respectively).

Conclusion: Low-dose CTA of the aorta using 80 kVp with iterative reconstruction enables a significant dose reduction of up to 50% compared with a 100 kVp protocol in patients with a BMI below 32 kg/m² while diagnostic image quality is maintained.

Key words: aorta; computed tomography; diagnostic imaging; radiation dose; vascular.

Introduction

Optimizing radiation exposure from medical examinations is of constant interest because of the potential risk of inducing carcinogenic effects.¹ The number of CT examinations has constantly increased within the last decades accounting for approximately 60% of the cumulative medical radiation exposure.² Therefore, further efforts are required to minimize the radiation dose of each single CT scan.

CT angiography (CTA) of the aorta is routinely used in clinical practice for the evaluation of a variety of diseases, such as aortic dissection or aortic aneurysms.^{3–6} The number of aortic CTA might further increase in the future because of improvements in minimal invasive therapeutic modalities requiring pre-interventional imaging as well as post-interventional follow up.⁷ Particularly because of the need for repeated examinations and the large scan volume, special efforts should be undertaken to minimize radiation exposure of aortic CTA. Various approaches have been introduced during the last years, whereby decreasing the tube current time product (mAs) and the tube potential (kVp) are the most common ways to reduce radiation dose.

Decreasing the tube potential while mAs is maintained generally leads to an increase in image noise, and therefore to a reduced image quality (IQ), possibly worsening diagnostic accuracy. However, as the tube voltage converges to the k-edge of iodine, the contrast material attenuation increases in this scenario. While the soft tissue contrast might be reduced because of noise, vascular structures can still be evaluated in good and diagnostic IQ particularly in an arterial phase of contrast enhancement.^{8,9} Additional dose-saving techniques as iterative image reconstruction (IR) can further support an increase of IQ and therefore enable a reduction of radiation exposure while maintaining IQ.¹⁰

The aim of this study was to evaluate the impact of a reduced tube potential (80 kVp) in combination with automatic tube current modulation and IR for CTA of the aorta on IQ and radiation dose.

Methods

Patients

This retrospective study was approved by the local ethics committee of the Heinrich Heine University Dusseldorf, Germany. A new 80 kVp aortic CTA protocol was introduced in our department for all patients with a body mass index (BMI) below 32 kg/m² in March 2012. We included the first 72 examinations using this low-dose protocol and assigned them to group A (56 patients, 42 men, 14 women, mean age 69.6 ± 10.7 years, mean BMI: 25.5 ± 3.0 kg/m², range 19–32 kg/m²). The last 28 examinations using the standard protocol with 100 kVp were included for comparison (26 patients, 17 men, 9

women, mean age 66.3 ± 12.0 years, mean BMI 29.0 ± 5.2 years). Five of these patients were excluded from the analysis as BMI was above 32 kg/m². The remaining 23 examinations were assigned to group B (21 patients, 13 male, 8 female, mean age 67.4 ± 11.1 years, mean BMI 27.1 ± 3.7 kg/m²). Both, 100 and 80 kVp examinations within the same patients were available for analysis in eight subjects (4 men, 4 women, mean age 67.2 ± 9.7 years, mean BMI 24.9 ± 3.1 kg/m²). These examinations were assigned to subgroups (group A_{intra} and group B_{intra}) for further analysis.

CT protocols

All examinations were performed on a 128-row CT scanner (Siemens Definition AS +, Siemens Healthcare GmbH, Erlangen, Germany). Scanning parameter for both protocols were as follows: pitch: 1.2, detector collimation: 64 × 0.6 (with z-flying focal spot) and rotation time: 0.5 s. One hundred millilitres of contrast medium (Accupaque® 300, GE Healthcare, Munich, Germany; 300 mg iodine/mL) was intravenously applied using a power injector (MedTron Injektron CT2, MEDTRON AG, Saarbrücken, Germany) at 4 mL/s. Contrast medium injection was followed by a 30-mL saline flush. A bolus trigger technique was used with a threshold of 100 Hounsfield units (HU) in the descending thoracic aorta. The scan volume included the cervical aortic branches, the entire aorta and the pelvic arteries terminating at the level of common femoral arteries.

A medium level (level 3) of advanced raw data-based IR technique (Sinogram Affirmed Iterative Reconstruction, SAFIRE, Siemens Healthcare GmbH) was used in all examinations (groups A and B, respectively) and automated tube current modulation (ATCM, CareDose 4D, Siemens Healthcare GmbH) was activated in both protocols.

Objective image analysis

Contrast-to-noise ratio (CNR) and signal-to-noise ratio (SNR) were assessed as parameters for objective IQ. Circular region of interest (ROI) measurements were performed in axial 5-mm images. ROIs (10–25 mm) were placed in the thoracic aorta (ROI1), abdominal aorta (ROI2), paravertebral spinal muscle at the level of the aortic arc (ROI3) and in the paravertebral spinal muscle at the level of the celiac trunk (ROI4). ROI1 and ROI2 were placed exactly in the centre of the aorta to omit calcifications. Standard deviation of ROI1 and ROI2 was used as an indicator of image noise.^{7,9} SNR and CNR for the thoracic (SNR1 and CNR1) and abdominal aorta (SNR2 and CNR2) were calculated:

$$SNR1 = ROI1 / \text{standard deviation} (ROI1)$$

$$CNR1 = (ROI1 - ROI3) / \text{standard deviation} (ROI1)$$

$$SNR2 = ROI2/\text{standard deviation } (ROI2)$$

$$CNR2 = (ROI2 - ROI4)/\text{standard deviation } (ROI2)$$

Subjective image analysis

Subjective IQ was assessed separately by two independent readers (J.A. with 4 and J.B. with 2 years of experience in reading CTA) on a 5-point scale (1 = *non-diagnostic*; 2 = *poor*; 3 = *moderate*; 4 = *good*; 5 = *excellent*). Both readers were blinded to image assessment parameters. Excellent IQ was defined as no artefacts, excellent vessel wall definition and excellent attenuation of the vessel lumen. IQ was rated 'good' for good vessel wall delineation and attenuation and minimal image noise. Moderate IQ was defined as adequate attenuation and vessel wall delineation and only slight minimal impact of image noise. IQ was rated 'poor' for poor vessel wall mark-off and increase image noise leading to a decreased diagnostic accuracy.^{5,9,11} For subjective analysis, all images were provided on a Picture Archiving and Communication System (PACS) workstation (Sectra Medical Systems GmbH, Linköping, Sweden). Five-millimetre axial images as well as sagittal and coronal multi-planar reformations were evaluated. Images were reconstructed using a soft tissue kernel (I30f). Modulation of the CT window was to the discretion of the readers.

Radiation dose and statistical analysis

CTDI_{vol} and DLP were extracted from the scanning protocol automatically sent to the PACS. Data analysis was performed using IBM SPSS Statistics 22™ for Windows (SPSS Inc., Chicago, IL, USA). Statistical significance was set to $P < 0.05$. All data are given in mean \pm standard deviation. A Kolmogorov test was used to test for normal distribution. Student's *t*-test was performed for all normally distributed parameters. A Mann-Whitney *U*-test was performed as a non-parametric test. Kappa value was calculated to evaluate the inter-observer agreement: excellent ($\kappa > 0.81$), good ($\kappa = 0.61$ – 0.80), moderate ($\kappa = 0.41$ – 0.60), fair ($\kappa = 0.21$ – 0.40) and poor ($\kappa \leq 0.20$).¹²

Results

Patients

Indications for CTA examinations and patient characteristics can be seen in Tables 1 and 2, respectively. There was no significant difference between both groups regarding age, height, weight and BMI (all $P > 0.05$, Table 2).

In groups A_{intra} and B_{intra}, mean time between both examinations was 291 ± 165 days (range 147–618 days).

Table 1. Indications for CT angiography examinations separated by group A (low dose with 80 kVp) and group B (standard protocol with 100 kVp)

Underlying pathology	Overall	Group A	Group B
Aneurysm	35	28	7
Dissection	29	24	5
After endovascular aneurysm repair	25	15	10
Others	6	5	1

Image quality

All examinations were of diagnostic IQ. Overall subjective IQ was rated good to excellent in 92.4% in group A (133/144 ratings) and 95.7% (44/46 ratings) in group B. Subjective IQ for groups A and B is listed in Table 2.

Subjective IQ of group A_{intra} (4.4 ± 0.5) was not significantly different compared with group B_{intra} (4.8 ± 0.5). Inter-observer agreement was good ($k = 0.70$). An example for comparable IQ between 100 and 80 kVp examinations in a 78-year-old patient is shown in Figure 1a,b. Figure 2a,b demonstrate diagnostic IQ in maximum intensity projections of a 77-year-old woman undergoing endovascular aortic repair (EVAR) intervention.

Objective IQ was comparable between groups A and B (all $P > 0.05$, Table 3). For group A_{intra}, SNR2 was significantly lower compared with group B_{intra} ($P = 0.046$) while there was no significant difference for SNR1. There was no statistically significant difference for CNR between both groups. Attenuation of the aorta was significantly higher in group A compared with group B (thoracic and abdominal $P < 0.001$, respectively) and in group A_{intra} compared with group B_{intra} (thoracic: $P = 0.02$; abdominal: $P = 0.01$). Analysis of objective IQ is illustrated in Table 3.

Radiation dose

There was a significant difference in radiation dose between group A (CTDI_{vol} 1.9 ± 0.5 mGy, DLP 139.2 ± 41.1 mGy \times cm) and group B (CTDI_{vol} 4.2 ± 1.4 mGy, DLP 292.1 ± 91.5 mGy \times cm) ($P < 0.001$, respectively, Table 2). CTDI_{vol} and DLP were significantly lower for group A_{intra} compared with group B_{intra} (2.1 ± 0.8 vs. 4.9 ± 1.3 mGy and 153.1 ± 56.0 vs. 305.1 ± 99.1 mGy \times cm, $P < 0.001$, respectively).

Discussion

This study documented a significant reduction in radiation exposure in aortic CTA in patients with a BMI below 32 kg/m^2 while diagnostic IQ was maintained by reducing the tube potential to 80 kVp in combination with ATCM and medium levels of IR.

Various dose-reduction strategies have been introduced for CT examinations, such as low-dose protocols,⁷

Table 2. Patient characteristics, subjective IQ and radiation parameters

	Overall	Group A	Group B	P value
Age (years)	69.0 ± 10.8	69.6 ± 10.7	67.4 ± 11.1	0.42
Height (cm)	172.8 ± 9.3	172.4 ± 9.2	174.0 ± 9.6	0.48
Weight (kg)	77.6 ± 12.9	76.1 ± 11.6	82.8 ± 15.8	0.09
Body mass index (kg/m ²)	25.9 ± 3.2	25.5 ± 3.0	27.1 ± 3.7	0.09
Subjective IQ	4.4 ± 0.6	4.3 ± 0.6	4.5 ± 0.6	0.31
Mean mAs	103.2 ± 27.4	103.0 ± 25.9	103.8 ± 32.4	0.92
CTDI _{vol} (mGy)	2.5 ± 1.2	1.9 ± 0.5	4.2 ± 1.4	<0.001
DLP (mGy × cm)	176.2 ± 87.0	139.2 ± 41.1	292.1 ± 91.5	<0.001

CTDI_{vol}, volumetric computed tomography dose index; DLP, dose length product; IQ, image quality.

ATCM,¹³ automated tube potential selection (ATPS),¹⁴ organ-specific dose reduction¹⁵ and IR.¹⁶ ATCM and ATPS enable an adjustment of radiation dose to the patients' anatomy in CTA examinations without significant deterioration of IQ.^{7,9} Nowadays, ATCM is provided by all major CT vendors. The reduction of tube current correlates linearly with the achieved dose reduction.¹⁷ In contrast, the reduction in tube potential correlates rather exponentially than linearly with the overall dose reduction.¹⁷ However, reduction of tube potential is limited, as

it requires a highly effective X-ray tube providing a high peak tube current to compensate for the resulting higher image noise.^{1,11} The recently introduced ATPS algorithm adapts the tube potential automatically according to the patients' anatomy using scout images and corresponding attenuation information. Schwarz *et al.*⁷ demonstrated a dose reduction of 30% combining ATPS with a reduced tube current time product and a high iodide delivery rate (IDR). However, no attenuation values of 80 kVp measurements comparable with this study were performed.

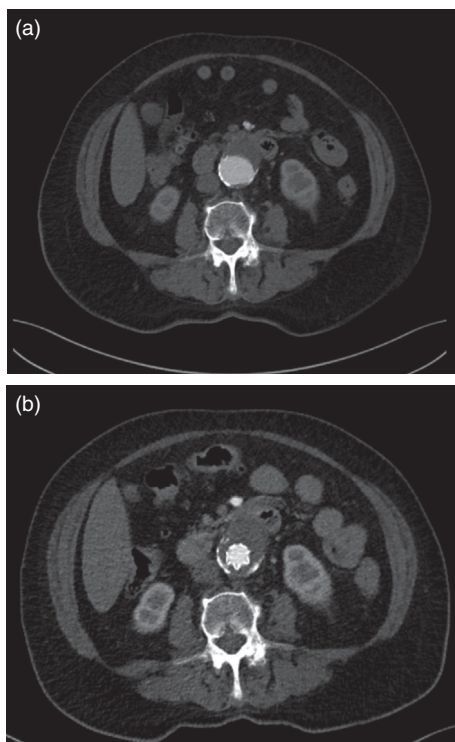


Fig. 1. (a, b) 100 kVp (a; volumetric computed tomography dose index, (CTDI_{vol}): 5.7 mGy, dose length product (DLP): 414 mGy × cm) and 80 kVp (b; CTDI_{vol}: 2.1 mGy, DLP: 142 mGy × cm) axial CT images of a 78-year-old female patient (169 cm, 75 kg, body mass index (BMI): 26 kg/m²) show comparable image quality.

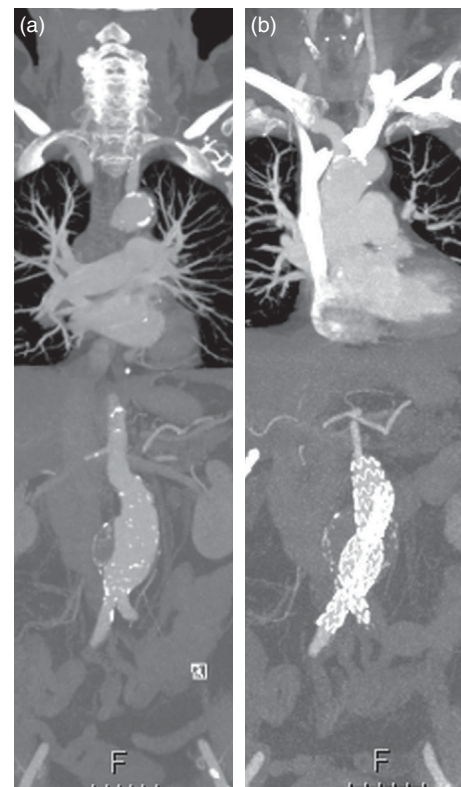


Fig. 2. (a, b) Maximum intensity projections of a 77-year-old female patient before (a), 100 kVp) and after (b), 80 kVp) endovascular aortic repair. Both examinations provide diagnostic image quality (IQ).

Table 3. Objective image quality: SNR, CNR and attenuation of the thoracic and abdominal aorta of group A (100 kVp), group B (80 kVp), group A_{intra} and group B_{intra}

	Overall	Group A	Group B	Group A _{intra}	Group B _{intra}
Attenuation of the thoracic aorta (HU)	407.6 ± 105.3	443.3 ± 90.5	296.0 ± 61.0	430.8 ± 86.1	329.9 ± 58.2
Attenuation of the abdominal aorta (HU)	397.7 ± 106.4	426.3 ± 94.2	283.6 ± 60.5	413.6 ± 72.4	312.4 ± 71.4
SNR1	14.5 ± 5.2	14.4 ± 3.9	14.9 ± 8.2	14.4 ± 3.7	19.4 ± 6.6
SNR2	12.2 ± 4.8	11.9 ± 3.3	13.0 ± 7.9	12.3 ± 2.9	18.7 ± 7.3
CNR1	12.8 ± 4.8	12.8 ± 3.7	13.0 ± 7.4	12.9 ± 3.5	17.0 ± 6.0
CNR2	10.7 ± 4.3	10.6 ± 3.2	11.2 ± 6.9	10.9 ± 2.9	16.2 ± 6.4

CNR1, thoracic contrast to noise ratio; CNR2, abdominal contrast to noise ratio; HU, Hounsfield units; SNR1, thoracic signal to noise ratio; SNR2, abdominal signal to noise ratio.

Low kVp protocols are of increasing interest in CTA and several previous studies have demonstrated a significant dose reduction.^{11,17–19} Initially, CTA examinations were often performed at 120 kVp. In 2005, Wintersperger *et al.*⁹ reported a dose reduction of 37% using 100 kVp compared with 120 kVp with constant mAs for aortic CTA. A dose reduction for CTA examinations with 80 kVp was reported by previous studies.^{11,17–19} Schindera *et al.*¹¹ showed a reduction of radiation exposure while maintaining IQ when comparing an 80 kVp with a 100-kVp CTA protocol using ATCM. The presented attenuation of the aorta was higher (621 ± 91 HU) compared with the results presented in this study; however, this can be explained by the increased IDR (1480 mg I/s) used in their study. Furthermore, there is a notable difference in CTDI_{vol} which is most likely based on a higher reference tube current time product (ref. mAs) of 260 mAs compared with 120 mAs in our study. A comparison of the CNR values is limited between the two studies as measurements of the image noise were performed in a different manner.¹¹ Iezzi *et al.*¹⁷ reported higher mean aortic attenuation values of 566 ± 100 HU for the aorta for low-dose 80 kVp/100 mAs CTA examinations. This might be explained by the use of 400 mg/mL iodine contrast medium with an IDR of 1200 mg I/s. Reported dose values are not comparable with our study because of a limited scan range solely of the abdominal aorta. In contrast to the previous studies, Chen *et al.*¹⁸ performed measurements with a reduced iodine delivery rate of 538 mg I/s. They demonstrated a reduction of radiation dose using an 80 kVp protocol in 48 patients undergoing follow-up CT aortography after endovascular aortic repair. Their reported tube current time product was markedly higher than in the here presented study (range: 320–550 mAs vs. 98–428 mAs). Consecutively, mean CTDI_{vol} and DLP (10.1 ± 1.5 mGy; 651 ± 105 mGy × cm) were essentially higher compared with this study at similar scan volumes. Overall attenuation of the aorta was lower (373 ± 38 HU),¹⁸ most likely as a result of the reduced iodine delivery rate. The CNR values cannot be compared between the two studies as measurement of the image noise was performed in a different manner.¹⁸ The results published by Chen *et al.*¹⁸ demonstrate the

potential of a combined reduction of the tube potential and the iodine delivery rate in order to save contrast material in CTA. This can be of importance particularly in patients with acute or chronic renal failure.

A significant dose reduction because of IR has been reported for various CT examinations.^{16,20} For CTA, several studies demonstrated a significant dose reduction when comparing IR with filtered back projection.^{19,21} However, only very few studies have investigated the combination of CTA protocols using a low tube potential and IR. Pontana *et al.*¹⁹ reported CTDI_{vol} values of approximately 80 mGy × cm for thoracic CTA with 80 kVp and sinogram-affirmed IR. As in this study, sinogram-affirmed IR was applied at medium strength (level 3). While SNR and CNR were slightly lower (Pontana: 12.3 ± 2.6 and 11.2 ± 2.6), dose parameters cannot be compared because of a scan volume limited to the thoracic aorta. However, the reported DLP and CTDI_{vol} values for thoracic CTA were very low in that study (77.3 mGy × cm and 1.2 mGy, respectively), which is in good accordance to the here presented results for the entire aorta. Although low-kVp CT scan techniques are particularly well suited for thoracic CTA examinations because of the air in the lungs, diagnostic subjective IQ was achieved in all scans in this study. Nevertheless, the advantage in thoracic CTA examinations can be seen in the higher SNR and CNR in the chest compared with the abdomen.

Even though IR techniques have been known for decades, implementation into clinical routine suffered from the requirement for distinct computational power and initial IR techniques used to be very time consuming. Recent developments in processing power have enabled implementation of IR algorithms into modern CT scanner software. The investigated IR algorithm was fully integrated into the CT scanner software and IR of the whole scan volume required significantly less than 1 min (medium level of IR, 5-mm axial slices). All reconstructions were performed by the technician in clinical routine and no impact on clinical workflow was observed.

For future investigations a combination of a high IDR (highly concentrated contrast medium and high injection

rate), a reduced tube potential of 70–80 kVp and advanced IR technique seems to be promising to further optimize radiation and contrast medium dose in CTA. New technical developments can help to improve patient care, such as dual-energy CT (DECT) providing virtual non-contrast images or novel X-ray tubes providing higher tube current time products and enable even further tube potential reduction.^{22,23} Initial studies regarding DECT were recently published with non-linear blending technique leading to a significant reduction of applied contrast material in aortic CTA.²³ However, as these techniques are not extensively available, low-kVp examinations will remain a helpful tool to reduce either radiation dose or the amount of contrast material in order to improve patient safety.

Our study has certain limitations. Although diagnostic IQ was achieved in all scans, apparent differences for SNR and CNR in the intra-individual comparison were detected. This might be the result of the small group size. Nevertheless, there was no significant difference between both groups in the subjective evaluation. A certain but non-significant difference for body weight and BMI was noted between groups A and B, although patients with a BMI above 32 kg/m² were excluded from the analysis. However, the 80 kVp protocol was used in patients up to 96 kg still leading to diagnostic IQ. CTA examinations of the aorta can always reveal incidental findings, which have been reported to appear in up to 68% during CTA prior to transcatheter aortic valve implantation.²⁴ We only assessed the subjective overall diagnostic IQ, incidental and secondary findings were not evaluated in the present study. Therefore, our results can only be adducted in reference to IQ of the thoracic and abdominal aorta. As we wanted to compare low-tube-potential protocols when using IR, we did not compare our results to filtered back projection.

In conclusion, our results demonstrate a dose reduction of up to 50% for low-dose CTA of the aorta with 80 kVp, medium levels of IR and ATCM in patients with a BMI of up to 32 kg/m² compared with a 100 kVp protocol. Therefore, a low-dose 80 kVp CTA protocol of the entire aorta can be suggested for these patients in clinical routine. Furthermore, our results indicate that diagnostic IQ can be achieved with radiation dose levels below values reported in literature today.

References

1. Siegel MJ, Ramirez-Giraldo JC, Hildebolt C, Bradley D, Schmidt B. Automated low-kilovoltage selection in pediatric computed tomography angiography. *Invest Radiol* 2013; **48**: 584–9.
2. Bundesamt für Strahlenschutz (BfS) (2011) Jahresbericht 2010, urn:nbn:de:0221-201205118217. Article in German [Cited 26 Nov 2015.] Available from URL: <http://nbn-resolving.de/urn:nbn:de:0221-201109056248>.
3. Yoshida S, Akiba H, Tamakawa M *et al.* Thoracic involvement of type A aortic dissection and intramural hematoma: diagnostic accuracy – comparison of emergency helical CT and surgical findings. *Radiology* 2003; **228**: 430–5.
4. Alerci M, Oberson M, Fogliata A, Gallino A, Vock P, Wyttenbach R. Prospective, intraindividual comparison of MRI versus MDCT for endoleak detection after endovascular repair of abdominal aortic aneurysms. *Eur Radiol* 2009; **19**: 1223–31.
5. Leipsic J, Labounty TM, Heilbron B *et al.* Adaptive statistical iterative reconstruction: assessment of image noise and image quality in coronary CT angiography. *AJR* 2010; **195**: 649–54.
6. Wuest W, Anders K, Schuhbaeck A *et al.* Dual source multidetector CT-angiography before trans-catheter aortic valve implantation (TAVI) using a high-pitch spiral acquisition mode. *Eur Radiol* 2012; **22**: 51–8.
7. Schwarz F, Grandl K, Arnoldi A *et al.* Lowering radiation exposure in CT angiography using automated tube potential selection and optimized iodine delivery rate. *AJR* 2013; **200**: 628–34.
8. Alkadhi H, Schindera ST. State of the art low-dose CT angiography of the body. *Eur J Radiol* 2011; **80**: 36–40.
9. Winklehner A, Goetti R, Baumüller S *et al.* Automated attenuation-based tube potential selection for thoracoabdominal computed tomography angiography: improved dose effectiveness. *Invest Radiol* 2011; **46**: 767–73.
10. Deák Z, Grimm JM, Mueck F *et al.* Endoleak and in-stent thrombus detection with CT angiography in a thoracic aortic aneurysm phantom at different tube energies using filtered back projection and iterative algorithms. *Radiology* 2014; **271**: 574–84.
11. Schindera ST, Graca P, Patak MA *et al.* Thoracoabdominal-aortoiliac multidetector-row CT angiography at 80 and 100 kVp: assessment of image quality and radiation dose. *Invest Radiol* 2009; **44**: 650–5.
12. Landis JR, Koch GG. The measurement of observer agreement for categorical data. *Biometrics* 1977; **33**: 159–74.
13. Mayer C, Meyer M, Fink C *et al.* Potential for radiation dose savings in abdominal and chest CT using automatic tube voltage selection in combination with automatic tube current modulation. *AJR* 2014; **203**: 292–9.
14. Schimmöller L, Lanzman RS, Dietrich S *et al.* Evaluation of automated attenuation-based tube potential selection in combination with organ-specific dose reduction for contrast-enhanced chest CT examinations. *Clin Radiol* 2014; **69**: 721–6.
15. Boos J, Kröpil P, Klee D *et al.* Evaluation of the impact of organ-specific dose reduction on image quality in pediatric chest computed tomography. *Pediatr Radiol* 2014; **44**: 1065–9.
16. Kröpil P, Bigdeli AH, Nagel HD, Antoch G, Cohnen M. Impact of increasing levels of advanced iterative

- reconstruction on image quality in low-dose cardiac CT angiography. *Rofo* 2014; **186**: 567–75.
17. Iezzi R, Cotroneo AR, Giammarino A, Spigonardo F, Storto ML. Low-dose multidetector-row CT-angiography of abdominal aortic aneurysm after endovascular repair. *Eur J Radiol* 2011; **79**: 21–8.
 18. Chen CM, Chu SY, Hsu MY, Liao YL, Tsai HY. Low-tube-voltage (80 kVp) C aortography using 320-row volume CT with adaptive iterative reconstruction: lower contrast medium and radiation dose. *Eur Radiol* 2014; **24**: 460–8.
 19. Pontana F, Pagniez J, Duhamel A *et al*. Reduced-dose low-voltage chest CT angiography with Sinogram-affirmed iterative reconstruction versus standard-dose filtered back projection. *Radiology* 2013; **267**: 609–18.
 20. Padole A, Singh S, Ackman JB *et al*. Submillisievert chest CT with filtered back projection and iterative reconstruction techniques. *AJR* 2014; **203**: 772–81.
 21. Cornfeld D, Israel G, Detroy E, Bokhari J, Mojibian H. Impact of adaptive statistical iterative reconstruction (ASIR) on radiation dose and image quality in aortic dissection studies: a qualitative and quantitative analysis. *AJR* 2011; **196**: W336–40.
 22. Carrascosa P, Capunay C, Rodriguez-Granillo GA, Deviggiano A, Vallejos J, Leipsic JA. Substantial iodine volume load reduction in CT angiography with dual-energy imaging: insights from a pilot randomized study. *Int J Cardiovasc Imaging* 2014; **30**: 1613–20.
 23. Liu J, Lv PJ, Wu R *et al*. Aortic dual-energy CT angiography with low contrast medium injection rate. *J Xray Sci Technol* 2014; **22**: 689–96.
 24. Showkathali R, Sen A, Brickham B, Dworakowski R, Wendler O, MacCarthy P. 'Incidental findings' during TAVI work-up: more than just an inconvenience. *EuroIntervention* 2014; **28**: 20130626-03.

Received:
17 December 2015

Revised:
21 February 2016

Accepted:
22 March 2016

<http://dx.doi.org/10.1259/bjr.20151059>

Cite this article as:

Boos J, Kröpil P, Lanzman RS, Aissa J, Schleich C, Heusch P, et al. CT pulmonary angiography: simultaneous low-pitch dual-source acquisition mode with 70 kVp and 40 ml of contrast medium and comparison with high-pitch spiral dual-source acquisition with automated tube potential selection. *Br J Radiol* 2016; **89**: 20151059.

FULL PAPER

CT pulmonary angiography: simultaneous low-pitch dual-source acquisition mode with 70 kVp and 40 ml of contrast medium and comparison with high-pitch spiral dual-source acquisition with automated tube potential selection

JOHANNES BOOS, MD, PATRIC KRÖPIL, MD, ROTEM S LANZMAN, MD, JOEL AISSA, MD, CHRISTOPH SCHLEICH, MD, PHILIPP HEUSCH, MD, LINO M SAWICKI, MD, GERALD ANTOCH, MD and CHRISTOPH THOMAS, MD

Medical Faculty, Department of Diagnostic and Interventional Radiology, University Dusseldorf, Dusseldorf, Germany

Address correspondence to: Dr Johannes Boos
E-mail: johannes.boos@med.uni-duesseldorf.de

Objective: To assess the feasibility of a 70-kVp CT pulmonary angiography (CTPA) protocol using simultaneous dual-source (SimDS) acquisition mode with 40 ml of contrast medium (CM) and comparison with a high-pitch spiral dual-source (SpiralDS) acquisition protocol with automated tube potential selection (ATPS).

Methods: Following the introduction of a new 70-kVp/40-ml SimDS-CTPA protocol in December 2014 for all patients with a body mass index (BMI) below 35 kg m^{-2} , the first 35 patients were retrospectively included in this study and assigned to Group A (BMI: $27 \pm 4 \text{ kg m}^{-2}$, age: 66 ± 15 years). The last 35 patients with a BMI below 35 kg m^{-2} who had received SpiralDS-CTPA with ATPS were included for comparison (Group B) (70 ml CM; BMI: $27 \pm 4 \text{ kg m}^{-2}$, age: 68 ± 16 years). Subjective image quality (image quality) was assessed by two radiologists (from 1, non-diagnostic, to 4, excellent). Signal-to-noise ratio (SNR), contrast-to-noise ratio (CNR), volumetric CT

dose index (CTDI_{vol}), dose-length product (DLP) and effective dose were assessed.

Results: All examinations were of diagnostic image quality. Subjective image quality, SNR and CNR were comparable between Groups A and B (3.7 ± 0.6 vs 3.7 ± 0.5 , 14.6 ± 6.0 vs 13.9 ± 3.7 and 12.4 ± 5.7 vs 11.6 ± 3.3 , respectively; $p > 0.05$). CTDI_{vol} , DLP and effective dose were significantly lower in Group A than in Group B (4.5 ± 1.6 vs $7.5 \pm 2.1 \text{ mGy}$, 143.3 ± 44.8 vs $278.3 \pm 79.44 \text{ mGy cm}$ and 2.0 ± 0.6 vs $3.9 \pm 1.1 \text{ mSv}$, respectively; $p < 0.05$).

Conclusion: 70-kVp SimDS-CTPA with 40 ml of CM is feasible and provides diagnostic image quality, while radiation dose and CM can be reduced by almost 50% and 40%, respectively, compared with a SpiralDS-CTPA protocol with ATPS.

Advances in knowledge: 70-kVp SimDS-CTPA with 40 ml of CM is feasible in patients with a BMI up to 35 kg m^{-2} and can help reduce radiation exposure and CM in these patients.

INTRODUCTION

Dual-source CT scanners feature two independent X-ray tube/detector combinations, allowing for three different dual-source scan modes. The first mode, dual-energy scanning, uses different tube voltages on both tubes, allowing assessment of material compositions.¹ The second mode, dual-source high-pitch spiral acquisition mode, allows for very fast scanning with pitch settings of up to 3.4. Both X-ray tubes operate at the same tube potential. Sampling gaps appearing in single-source CT at pitch factors > 2 are filled using the second X-ray tube and detector array arranged in the gantry with a 95° shift from the first detector. As the sampling gaps are scanned with only the second tube/detector array, this technique is limited by the X-ray tube output in patients who are obese. The third

mode, dual-source simultaneous acquisition, also utilizes both X-ray tubes at the same tube potential. Scanning is performed with standard pitch factors. No sampling gaps appear for either detector, and the whole field of view is covered by both tube/detector arrays. This corresponds to a doubling of the X-ray tube output of the CT system.²

Previous studies have shown that a reduction of the tube potential in CT angiography (CTA) can result in higher intravascular iodine enhancement with reduced radiation dose in comparison with standard protocols with a higher tube voltage.^{3–11} Low tube potential CT protocols in clinical routine are, however, limited by the maximum available tube current time product, since high tube currents are necessary to counterbalance the reduced photon generation

efficiency of the tube and the lower X-ray energy, especially in patients who are overweight and obese. Since low tube potential scanning is generally limited by the maximum achievable tube current, time product the simultaneous acquisition dual-source scanning mode appears promising for use in low-peak kilovoltage (kVp) scanning, especially in patients who are bigger.

The purpose of this study was to evaluate the feasibility, image quality (image quality) and radiation dose of a 70-kVp simultaneous acquisition dual-source CT pulmonary angiography (CTPA) protocol with 40 ml of contrast medium (CM) and to compare the image quality and radiation dose to a high-pitch spiral acquisition CTPA protocol with automated tube potential selection (ATPS).

METHODS AND MATERIALS

Study setup

This retrospective study was approved by the local ethics committee. The novel scanning protocol was integrated into clinical routine in December 2014 following phantom measurements. All non-paediatric patients referred for CTPA owing to suspected pulmonary embolism with a body mass index (BMI) less than 35 kg m^{-2} are currently scanned with this protocol.

The first 35 consecutive patients who underwent CTPA using the novel protocol were analyzed in this study (Group A). For comparison, 35 consecutive patients with a BMI $<35 \text{ kg m}^{-2}$ who had received a CTPA examination using the previous high-pitch protocol (Protocol B) were included in this study (Group B). There were no further inclusion or exclusion criteria.

Scanning protocols

All scans were performed on a second-generation 128-slice (64 detector rows with double z-sampling) dual-source CT scanner (Siemens Definition Flash; Siemens Healthcare GmbH, Erlangen, Germany) equipped with a fully integrated circuit detector (Stellar®; Siemens Healthcare GmbH, Erlangen, Germany). Patients were placed in supine position with arms extended above the head. Image acquisition direction was caudocranial. The CM (Accupaque™ 300, iohexol, 300 mg iodine/ml; GE Healthcare, Munich, Germany) was injected using a power

injector (Medrad® Stellant® Injector; Bayer Vital GmbH, Leverkusen, Germany) with a flow rate of 3 ml s^{-1} in all patients. CM injection was followed by a saline flush (40 ml, 3 ml s^{-1}). The classical bolus trigger technique (CareBolus; Siemens Healthcare GmbH) (80 kVp) in the pulmonary trunk (PT) with a threshold of 130 HU was used to trigger the examinations. Breath-hold command (no deep inspiration) was given after bolus triggering. A minimal 3-s delay was applied after bolus triggering before the start of the scan.

Patients in Group A underwent CTPA with the novel protocol [simultaneous dual-source (SimDS) scanning]: both X-ray tubes were operated at 70 kVp with a low-pitch setting (labelled “dual-source obese mode” by the manufacturer). Automated tube current modulation (ATCM) (CareDose 4D; Siemens Healthcare GmbH) was activated; 40 ml of CM was injected.

Patients in Group B underwent examinations with a dual-source high-pitch spiral acquisition mode (labelled “Flash” by the manufacturer). ATPS (CareKV, Siemens Healthcare GmbH) with ATCM was activated in Protocol B to adopt tube voltage and current automatically to patient body habitus (120 kVp, $n = 29$; 100 kVp, $n = 6$, 80 and 140 kVp were not selected). 70 ml of CM was injected. Detailed scanning parameters of both protocols are listed in Table 1.

Image reconstruction

Images were reconstructed with a soft-tissue kernel in 1-mm axial slices using a medium level of iterative reconstruction (Level 3, sinogram-affirmed iterative reconstruction) (SAFIRE; Siemens Healthcare GmbH). Furthermore, coronal and sagittal multiplanar reformations and maximum intensity projections were reconstructed.

Objective image analysis

All measurements were performed on a standard picture archiving and communication system workstation (Sectra Medical Systems GmbH, Linköping, Sweden). Objective image analysis was performed in accordance with prior studies using regions of interest (ROI) to assess the signal

Table 1. Scanning protocols and radiation dose evaluation

Parameter	Protocol A	Protocol B
Acquisition mode	Dual source, simultaneous	Dual source, high pitch
Detector collimation (mm)	64×0.6	128×0.6
Pitch	0.9	2.2
Tube voltage (kVp)	70	ATPS (120 kVp: $n = 29$, 100 kVp: $n = 6$)
Reference tube current time product (mAs_{eff})	110	118
Contrast medium volume (ml)	40	70
Mean CTDI_{vol} (mGy)	4.5 ± 1.6	7.5 ± 2.2
Mean DLP (mGy cm)	143.3 ± 44.8	278.3 ± 79.4
Estimated effective radiation dose (mSv)	2.0 ± 0.6	3.9 ± 1.1

ATPS, automated tube potential selection; CTDI_{vol} , volumetric CT dose index; DLP, dose-length product. All values are given as mean \pm standard deviation.

Table 2. Patient data

Characteristics	Group A	Group B	<i>p</i> -value
<i>n</i>	35	35	–
Age (years)	65.7 ± 15.3	68.2 ± 16.0	0.46 (95% CI: –4.7 to 10.2)
Sex (M/F)	13/22	15/20	0.32
Body height (cm)	168.2 ± 8.0 (145–185)	172.3 ± 10.1 (150–192)	0.07 (95% CI: –8.4 to 0.27)
Body weight (kg)	75.7 ± 11.7 (45–96)	79.3 ± 12.8 (55–105)	0.22 (95% CI: –2.22 to 9.53)
BMI (kg m ⁻²)	26.8 ± 3.9 (21–34)	26.8 ± 4.2 (20–35)	0.98 (95% CI: –1.89 to 1.94)
Incidence of pulmonary embolism	10	12	0.06

BMI, body mass index; F, female; M, male.

Ranges are provided in parenthesis for both groups for height, weight and BMI; 95% CI: 95% confidence intervals for *p*-values.

All values are given as mean ± standard deviation.

intensity (SI) in Hounsfield units and noise index (NI standard deviation of SI in Hounsfield units).^{8,9} ROIs were placed in the PT in a lower lobe segmental artery (LLSA) and in the paravertebral muscle (BACKGROUND). The size of the ROIs was adapted to the size of the corresponding structures to avoid partial volume effects.

Signal-to-noise ratio (SNR) and contrast-to-noise ratio (CNR) were calculated for the PT and the LLSA:

$$\text{SNR} = \text{SI}/\text{NI}$$

$$\text{CNR} = (\text{SI} - \text{BACKGROUND})/\text{NI}$$

Subjective image analysis

Subjective image quality was assessed separately by two independent readers (CT and JB; with 8 and 2 years' experience in reading CTPA) on a four-point scale: (1) non-diagnostic, (2) suboptimal, (3) adequate and (4) excellent. Image evaluation was based on vascular attenuation, image noise, artefacts and diagnostic confidence. Non-diagnostic was defined as a lack of interpretability of the segmental arteries. Examinations were rated suboptimal, when the sub-segmental arteries could not be evaluated properly. Adequate was defined as minor artefacts or image noise, while all pulmonary arteries showed an optimal contrast. Excellent was defined as excellent vascular enhancement in all pulmonary arteries (PT to subsegmental arteries) and the absence of artefacts and image noise.

Both readers were blinded to image assessment parameters and clinical information.

For subjective analysis, all images were provided on a picture archiving and communication system workstation. Axial images (slice thickness of 1 mm) as well as sagittal and coronal multi-planar reformations and maximum intensity projections were evaluated. Modulation of the CT window was at the discretion of the individual readers.

Both readers independently assessed the frequency of pulmonary embolism. Interreader agreement for the diagnosis of pulmonary embolism was assessed.

Radiation dose

Volumetric CT dose index and dose-length product (DLP) were extracted from the patient protocol. Effective dose was calculated using a conversion factor of 0.014.¹²

Statistical analysis

Data analysis was performed using MedCalc (MedCalc Software, Ostend, Belgium). Data are given as mean ± standard deviation, together with range. Statistical significance was set to $p < 0.05$. 95% confidence intervals (95% CI) and interquartile ranges are provided. Normal distribution was tested with Kolmogorov test. Student's *t*-test was performed for all normally distributed parameters. Mann-Whitney *U* test and χ^2 test were performed as non-parametric tests. A κ value was calculated to evaluate interobserver agreement and interpreted as follows: excellent ($\kappa > 0.81$), good ($\kappa = 0.61$ – 0.80), moderate ($\kappa = 0.41$ – 0.60), fair ($\kappa = 0.21$ – 0.40) and poor ($\kappa \leq 0.20$).¹³

RESULTS

Patient demographics

There were no statistical differences in sex, patient age, body weight, BMI and frequency of pulmonary embolism between both protocols (all $p > 0.05$) (Table 2). Pulmonary embolism was diagnosed in 31% of all patients (Group A: 10 (29%) cases and Group B: 12 (34%) cases; $p = 0.06$). Interobserver agreement for the diagnosis of pulmonary embolism was 100%.

Radiation dose

Mean tube current time product was significantly higher in Group A than in Group B (268 ± 91 mA s, range 100–397 mA s, vs

Table 3. Subjective ratings for both readers and both groups

Rating	Reader 1		Reader 2	
	Group A	Group B	Group A	Group B
Excellent	24	26	28	25
Adequate	8	8	5	9
Suboptimal	3	1	2	1
Non-diagnostic	0	0	0	0

Table 4. Attenuation, signal-to-noise ratio (SNR), contrast-to-noise ratio (CNR) and subjective image quality

Imaging characteristics	All patients	Group A	Group B	<i>p</i> -value
Attenuation trunk (HU)	338.1 ± 138.8	414.3 ± 149.4	259.6 ± 69.7	<0.0001 (99–211)
Attenuation LLSA (HU)	337.3 ± 136.4	416.4 ± 139.3	256.0 ± 75.0	<0.0001 (107–214)
SNR _{Trunk}	14.2 ± 5.0	14.6 ± 6.0	13.9 ± 3.7	0.56 (–3.1 to 1.7)
SNR _{LLSA}	13.5 ± 7.2	15.1 ± 8.9	12.0 ± 4.5	0.08 (–0.36 to 6.4)
CNR _{Trunk}	12.0 ± 4.7	12.4 ± 5.7	11.6 ± 3.3	0.48 (–3.0 to 1.4)
CNR _{LLSA}	11.4 ± 6.7	12.9 ± 8.5	10.0 ± 4.1	0.08 (–6.0 to 0.4)
Subjective image quality	3.7 ± 0.6	3.7 ± 0.6	3.7 ± 0.6	0.98

LLSA, left lower segmental pulmonary artery; Trunk, pulmonary trunk. 95% confidence intervals for *p*-values are provided in parenthesis. All values are given as mean ± standard deviation.

144 ± 35 mAs, range 82–211 mAs; *p* < 0.0001, 95% CI: 91–158 HU). Volumetric CT dose index and DLP were significantly lower in Group A than in Group B (4.5 ± 1.6 mGy vs 7.4 ± 2.2 mGy and 143.3 ± 44.8 mGy cm vs 272.3 ± 80.4 mGy cm; *p* < 0.0001, 95% CI: 2.18–3.97 HU and 104–166 HU, respectively) (Table 1). On an average, radiation dose was lowered by 48% in Group A compared with Group B.

Image quality

None of the CT studies were rated as non-diagnostic by any of the two readers (Table 3). There was no significant difference in the subjective image quality between Groups A and B (3.7 ± 0.6 vs 3.7 ± 0.6; median 4, interquartile range 3–4, respectively; *p* = 0.98) (Table 4).

The CT numbers showed a statistically significant difference between Group A and Group B for the PT (range 202–1018 HU vs 149–456 HU, *p* < 0.0001, 95% CI: 99–211 HU) and the LLSA (range: 211–948 HU vs 130–454 HU, *p* < 0.0001, 95% CI: 107–214 HU). There was no significant difference between Group A and Group B for SNR (SNR in the pulmonary trunk: 14.6 ± 6.0 vs 13.9 ± 3.7 and SNR in the LLSA: 15.1 ± 8.9 vs 12.0 ± 4.5) and CNR (CNR in the pulmonary trunk 12.4 ± 5.7 vs 11.6 ± 3.3 and CNR in the LLSA 12.9 ± 8.5 vs 10.0 ± 4.1) (all *p* > 0.05) (Table 4).

Examples of image quality for Group A are shown in Figures 1 and 2 (Figure 1: overweight patient, BMI of 30 kg m⁻² and effective dose of 2.3 mSv; Figure 2: normal weight patient, BMI of

24 kg m⁻² and effective dose of 0.7 mSv). An example for diagnostic image quality in a patient who is obese with a BMI of 34 kg m⁻² in Group A is shown in Figure 3. Comparison between both protocols is demonstrated in Figure 4.

DISCUSSION

This study demonstrated the feasibility of 70-kVp CTPA using a dual-source CT protocol with low-pitch dual-source simultaneous acquisition mode and 40 ml of CM. Furthermore, the new protocol provided subjective image quality, SNR and CNR comparable with a high-pitch spiral acquisition dual-source CT protocol with ATPS, while the radiation dose was reduced by almost 50%.

A variety of previous studies investigated CTPA protocols with different dose reduction techniques. Dose reduction has been reported through reduction of milliamperes seconds,^{4,14,15} reduction of kVp^{16–18} or application of iterative reconstruction.^{19,20} Furthermore, high-pitch protocols in combination with automated tube potential selection have been shown to enable a significant dose reduction compared with standard protocols.⁷ Out of these options, reduction of kVp is especially valuable in CTA because the evaluability of the vessels is mainly driven by iodine enhancement. We found comparable SNR and CNR in both CTPA protocols, while radiation dose and CM dose were reduced in Group A. This reduction of radiation dose when lowering kVp can be achieved only if the tube current time product does not completely counterbalance the dose reduction gained by the reduced kVp. The decrease in

Figure 1. A 71-year-old female patient who is obese (height 162 cm, 78 kg and body mass index 29.7 kg m⁻²) with suspected pulmonary embolism. Examination was performed with 70 kVp and 40 ml of contrast medium. Effective radiation dose was 2.3 mSv. Axial image (a) and coronal maximum intensity projection (b) demonstrating excellent image quality. A, anterior view.

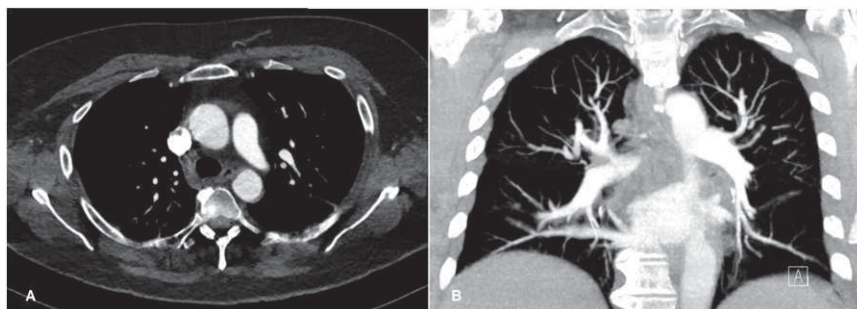


Figure 2. A 92-year-old patient who is slim (height 162 cm, 63 kg and body mass index 24 kg m^{-2}) with suspected pulmonary embolism. Examination was performed with the 70-kVp protocol with 40 ml of contrast medium. Effective radiation dose was 0.7 mSv.



overall radiation inevitably leads to an increase in image noise. However, lowering the kVp also leads to an increase in vascular attenuation, which arises from higher relative iodine attenuation with its k -edge of 33.2 keV.³ The higher attenuation enables either radiation dose reduction, CM dose reduction or, as investigated in this study, a combination of both. The overall increase in vascular attenuation helps overcome the increased image noise and leads to a comparable SNR and CNR in CTA. In addition, ATCM is an effective dose reduction technique in low-pitch CT studies, whereas its performance is limited in high-pitch CT. This can increase the radiation dose reduction of low-pitch SimDS mode compared with high-pitch spiral acquisition. Initial studies evaluating kVp reduction in CTPA compared 120-kVp with 100-kVp studies and demonstrated a dose reduction of up to 50%.⁸ Mean vessel attenuation as well as a SNR were comparable with our results (463 HU and 12, respectively), but the overall iodine load and the iodine delivery rate were markedly higher than in our 70-kVp protocol (21 g at 1833 mgL^{-1} compared with 12 g at 900 mgL^{-1} in our

study). More recent studies investigated 80-kVp CTPA in combination with iterative reconstructions and reported a significant dose reduction.¹⁷ A DLP of 73 mGy cm for the 80-kVp CTPA protocol was reported,¹⁷ which is lower than that in our 70-kVp protocol. However, patients weighting only up to 80 kg were included in their 80-kVp CTPA protocol and the amount of CM was twice as high compared with our study.

Initial results were reported for 70-kVp CT examinations of different body regions; e.g. for CTA,^{6,11,18,21} chest CT,²² paediatric CT²³ and cranial CT.²⁴ These studies also showed feasibility, diagnostic image quality and a potential for reduction of radiation dose and CM. Up to date, only two studies have reported the results for dual-source 70-kVp CTPA.^{18,20}

Li et al²¹ investigated the feasibility of a 70-kVp high-pitch CTPA protocol with 40 ml of CM and reported sufficient image quality at a mean DLP of 28 mGy cm. Because they were not able to report the height, weight and BMI of the patients, Li et al²¹ used diameter measurements to compare groups. Nevertheless, no ranges for diameter measurements were reported and therefore, limitations of their protocol in regard to X-ray tube output in patients who are larger cannot be appraised. Although a 70-kVp CTPA protocol was investigated, the protocol used by Li et al²¹ cannot be compared with our 70-kVp protocol. The feasibility of using a reduced amount of CM in high-pitch CTPA is mainly limited by image quality (and therefore maximal tube current time product) and not by the amount of CM. Because of the fast table movement, high-pitch protocols do not require a large CM bolus, but depend on a perfect timing to start the examination. The major limitation of these protocols, when performed with low kVp, is image quality in patients who are overweight and obese because of the limitations in X-ray tube output. In contrast, our protocol enables a higher X-ray tube output because both X-ray tubes are used simultaneously for image acquisition.

To our knowledge, only one other study reported the utilization of simultaneous acquisition dual-source CT for the detection of pulmonary embolism.¹⁸ Wichmann et al¹⁸ compared a standard 100-kVp protocol with a single-source 70-kVp protocol and

Figure 3. A 63-year-old patient (height 168 cm, 96 kg and body mass index 34.0 kg m^{-2}); axial image (a) and coronal maximum intensity projection (b) were examined with the 70-kVp protocol with 40 ml of contrast medium. Effective dose was 2.2 mSv (mean tube current time product: 366 mAs and volumetric CT dose index: 6.1 mGy). Bilateral pulmonary embolism was diagnosed (white arrows).

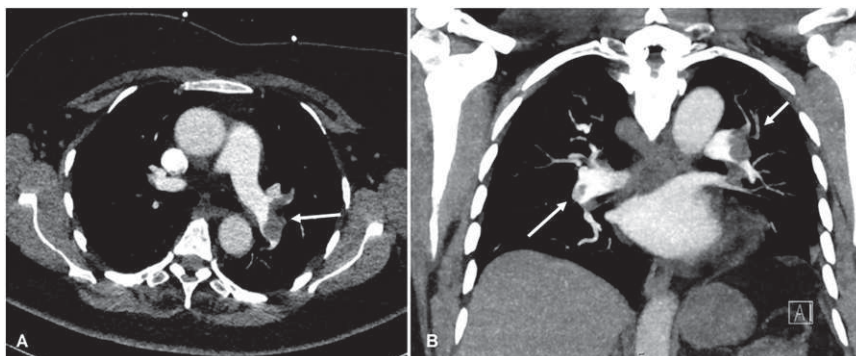
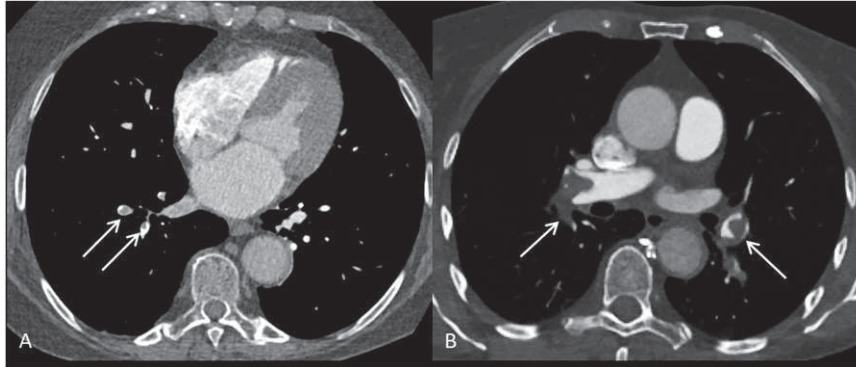


Figure 4. (a) A 76-year-old female patient [height 173 cm, 80 kg and body mass index (BMI) 26.7 kg m^{-2}] with suspected pulmonary embolism. The patient was examined with the high-pitch protocol (Group B) with 100 kVp. Pulmonary embolism was detected in the right lower lobe segmental arteries (white arrows). (b) A 74-year-old female patient (158 cm, 56 kg and BMI 22.4 kg m^{-2}) with D-dimers above 30 and suspected pulmonary embolism. The patient was examined with the 70-kVp dual-source CT pulmonary angiography protocol (Group A). Bilateral central pulmonary embolism was detected (white arrows).



a dual-source 70-kVp protocol with simultaneous acquisition mode. Although a dual-source simultaneous acquisition CTPA protocol was performed just as in our study, 70 ml of 300 mg I ml^{-1} CM was used. Mean attenuation values of the PT were slightly higher than that in this study ($490 \pm 148 \text{ HU}$), which is most likely the result of the larger amount of CM (1.75 times the amount used in this study), resulting in a higher iodine delivery rate (1200 mg I s^{-1} , overall iodine load 21 g).¹⁶ Although it has been reported that the image quality for 70 kVp was comparable with that for 100 kVp, a limitation of their study was the missing data on height, weight and BMI, which restrict comparison with our results. Furthermore, no statement can be made from their study about the feasibility of further CM reduction in 70-kVp CTPA using the SimDS mode, which is demonstrated in our study.

The downside of the CT dual-source simultaneous acquisition mode arises from its major strength: the simultaneous acquisition enables high X-ray tube outputs but also limits the pitch factor. While the high-pitch factor provided by modern CT scanners has led to feasibility of CTPA with 20 ml of CM when using a test bolus scan, the reduction of CM may be limited in SimDS acquisition mode, owing to the short bolus transit time.²² Even with perfect timing using bolus triggering or a test bolus, the CM bolus may not be too small to enable scanning at a low pitch. Nevertheless, using 40 ml of CM was feasible in our study and led to diagnostic image quality in patients with a BMI of up to 35 kg m^{-2} .

It would be possible to decrease the injection rate or dilute the CM to increase the length of the CM bolus transit time; however, both methods are limited by the resulting reduction of image quality. For further studies, reduction of injection rate in combination with a higher iodine concentration CM could be used to extend the CM bolus transit time without reducing vascular attenuation and therefore maintaining image quality, when using the simultaneous acquisition dual-source mode in patients who are overweight and obese.

This study has certain limitations. Since initial results are reported, the number of patients is limited. Further prospective

studies with larger cohorts have to be performed to confirm the results presented here, including larger subgroups with patients who are extremely obese. Subjective image quality was rated by two independent readers, but we did not assess intrareader variability. As this was a retrospective study, no interindividual comparison was available. Because we wanted to use a high-pitch protocol with ATPS for comparison in this study, acquisition parameters between both protocols are diverse. Therefore, our results in regard to dose reduction may not be generalizable to other CTPA protocols. Nevertheless, high-pitch protocols have been described for CTPA,^{19,21} and our main goal was to show the feasibility of 70-kVp CTPA using the low-pitch dual-source simultaneous acquisition mode in patients with a BMI up to 35 kg m^{-2} . We did not evaluate the extent of chest coverage of both protocols and the impact on secondary findings. The second detector of the herein used dual-source CT scanner has an x - y width of 33.2 cm. Thus, using the high-pitch dual-source protocol, reconstruction is limited to a circular field of view of about 33 cm in the centre of the gantry. In the low-pitch simultaneous acquisition mode, the whole field of view is covered by the first (larger) detector. Full dose and full image quality are available only at the central 33-cm field of view. This limitation is partly compensated by the fact that image noise in CT examinations is generally lower in the periphery than at the centre. Although we did not include a detailed evaluation of volume coverage and its impact on secondary findings, all subsegmental pulmonary vessels were visible in all patients. Correct placement of the patient at the centre of the gantry can minimize the risk of incomplete coverage of parts of the chest. This has to be kept in mind when using the dual-source acquisition technique in chest CT.

CONCLUSION

In conclusion, the 70-kVp dual-source CTPA protocol using simultaneous acquisition of both X-ray tubes with 40 ml of CM is feasible in patients with a BMI up to 35 kg m^{-2} and allows for a reduction of radiation dose by almost 50% and a reduction of CM dose by 40% compared with a spiral acquisition high-pitch CTPA protocol with ATPS, while maintaining diagnostic image quality.

REFERENCES

- Johnson TR, Krauss B, Sedlmair M, Grasruck M, Bruder H, Morhard D, et al. Material differentiation by dual energy CT: initial experience. *Eur Radiol* 2007; **17**: 1510–7. doi: <http://dx.doi.org/10.1007/s00330-006-0517-6>
- Petersilka M, Bruder H, Krauss B, Stierstorfer K, Flohr TG. Technical principles of dual source CT. *Eur J Radiol* 2008; **68**: 362–8. doi: <http://dx.doi.org/10.1016/j.ejrad.2008.08.013>
- Megyeri B, Christe A, Schindera ST, Horkay E, Sikula J, Cullmann JL, et al. Diagnostic confidence and image quality of CT pulmonary angiography at 100 kVp in overweight and obese patients. *Clin Radiol* 2015; **70**: 54–61. doi: <http://dx.doi.org/10.1016/j.crad.2014.09.014>
- Heusch P, Lanzman RS, Aissa J, Schimmöller L, Antoch G, Krix M, et al. Evaluation of a high iodine delivery rate in combination with low tube current for dose reduction in pulmonary computed tomography angiography. *J Thorac Imaging* 2014; **29**: 293–7. doi: <http://dx.doi.org/10.1097/RTI.0000000000000099>
- Chen CM, Chu SY, Hsu MY, Liao YL, Tsai HY. Low-tube-voltage (80 kVp) CT aortography using 320-row volume CT with adaptive iterative reconstruction: lower contrast medium and radiation dose. *Eur Radiol* 2014; **24**: 460–8. doi: <http://dx.doi.org/10.1007/s00330-013-3027-3>
- Meyer M, Haubenreisser H, Schoepf UJ, Vliegenthart R, Leidecker C, Allmendinger T, et al. Closing in on the K edge: coronary CT angiography at 100, 80, and 70 kV-initial comparison of a second- versus a third-generation dual-source CT system. *Radiology* 2014; **273**: 373–82. doi: <http://dx.doi.org/10.1148/radiol.14140244>
- Lurz M, Lell MM, Wuest W, Eller A, Scharf M, Uder M, et al. Automated tube voltage selection in thoracoabdominal computed tomography at high pitch using a third-generation dual-source scanner: image quality and radiation dose performance. *Invest Radiol* 2015; **50**: 352–60. doi: <http://dx.doi.org/10.1097/RLI.0000000000000133>
- Szucs-Farkas Z, Strautz T, Patak MA, Kurmann L, Vock P, Schindera ST. Is body weight the most appropriate criterion to select patients eligible for low-dose pulmonary CT angiography? Analysis of objective and subjective image quality at 80 kVp in 100 patients. *Eur Radiol* 2009; **19**: 1914–22. doi: <http://dx.doi.org/10.1007/s00330-009-1385-7>
- Nyman U, Björkdahl P, Olsson ML, Gunnarsson M, Goldman B. Low-dose radiation with 80-kVp computed tomography to diagnose pulmonary embolism: a feasibility study. *Acta Radiol* 2012; **53**: 1004–13. doi: <http://dx.doi.org/10.1258/ar.2012.120327>
- Björkdahl P, Nyman U. Using 100- instead of 120-kVp computed tomography to diagnose pulmonary embolism almost halves the radiation dose with preserved diagnostic quality. *Acta Radiol* 2010; **51**: 260–70. doi: <http://dx.doi.org/10.3109/02841850903505222>
- Zhang LJ, Zhao YE, Schoepf UJ, Mangold S, Felmly LM, Li X, et al. Seventy-peak kilovoltage high-pitch thoracic aortic CT angiography without ECG gating: evaluation of image quality and radiation dose. *Acad Radiol* 2015; **22**: 890–7. doi: <http://dx.doi.org/10.1016/j.acra.2015.03.007>
- McCullough CH, Primak AN, Braun N, Kofler J, Yu L, Christner J. Strategies for reducing radiation dose in CT. *Radiol Clin North Am* 2009; **47**: 27–40. doi: <http://dx.doi.org/10.1016/j.rcl.2008.10.006>
- Landis JR, Koch GG. The measurement of observer agreement for categorical data. *Biometrics* 1977; **33**: 159–74. doi: <http://dx.doi.org/10.2307/2529310>
- Tack D, De Maertelaer V, Petit W, Scillia P, Muller P, Suess C, et al. Multi-detector row CT pulmonary angiography: comparison of standard-dose and simulated low-dose techniques. *Radiology* 2005; **236**: 318–25. doi: <http://dx.doi.org/10.1148/radiol.2361040190>
- Montet X, Hachulla AL, Neroladaki A, Lador F, Rochat T, Botsikas D, et al. Image quality of low mA CT pulmonary angiography reconstructed with model based iterative reconstruction versus standard CT pulmonary angiography reconstructed with filtered back projection: an equivalency trial. *Eur Radiol* 2015; **25**: 1665–71. doi: <http://dx.doi.org/10.1007/s00330-014-3563-5>
- Apfalter P, Sudarski S, Schneider D, Nance JW Jr, Haubenreisser H, Fink C, et al. Value of monoenergetic low-kV dual energy CT datasets for improved image quality of CT pulmonary angiography. *Eur J Radiol* 2014; **83**: 322–8. doi: <http://dx.doi.org/10.1016/j.ejrad.2013.11.005>
- Laqmani A, Regier M, Veldhoen S, Backhaus A, Wassenberg F, Sehner S, et al. Improved image quality and low radiation dose with hybrid iterative reconstruction with 80 kV CT pulmonary angiography. *Eur J Radiol* 2014; **83**: 1962–9. doi: <http://dx.doi.org/10.1016/j.ejrad.2014.06.016>
- Wichmann JL, Hu X, Kerl JM, Schulz B, Frellesen C, Bodelle B, et al. 70 kVp computed tomography pulmonary angiography: potential for reduction of iodine load and radiation dose. *J Thorac Imaging* 2015; **30**: 69–76. doi: <http://dx.doi.org/10.1097/RTI.0000000000000124>
- Pontana F, Henry S, Duhamel A, Faivre JB, Tacelli N, Pagniez J, et al. Impact of iterative reconstruction on the diagnosis of acute pulmonary embolism (PE) on reduced-dose chest CT angiograms. *Eur Radiol* 2015; **25**: 1182–9. doi: <http://dx.doi.org/10.1007/s00330-014-3393-5>
- Kaul D, Grupp U, Kahn J, Ghadjar P, Wiener E, Hamm B, et al. Reducing radiation dose in the diagnosis of pulmonary embolism using adaptive statistical iterative reconstruction and lower tube potential in computed tomography. *Eur Radiol* 2014; **24**: 2685–91. doi: <http://dx.doi.org/10.1007/s00330-014-3290-y>
- Li X, Ni QQ, Schoepf UJ, Wichmann JL, Felmly LM, Qi L, et al. 70-kVp high-pitch computed tomography pulmonary angiography with 40 ml contrast agent: initial experience. *Acad Radiol* 2015; **22**: 1562–70. doi: <http://dx.doi.org/10.1016/j.acra.2015.08.026>
- Bodelle B, Klement D, Kerl JM, Lehnert T, Frellesen C, Bauer R, et al. 70 kV computed tomography of the thorax: valence for computer-assisted nodule evaluation and radiation dose—first clinical results. *Acta Radiol* 2014; **55**: 1056–62. doi: <http://dx.doi.org/10.1177/0284185113513258>
- Niemann T, Henry S, Duhamel A, Faivre JB, Deschildre A, Colas L, et al. Pediatric chest CT at 70 kVp: a feasibility study in 129 children. *Pediatr Radiol* 2014; **44**: 1347–57. doi: <http://dx.doi.org/10.1007/s00247-014-3027-8>
- Cho ES, Chung TS, Ahn SJ, Chong K, Baek JH, Suh SH. Cerebral computed tomography angiography using a 70 kVp protocol: improved vascular enhancement with a reduced volume of contrast medium and radiation dose. *Eur Radiol* 2015; **25**: 1421–30. doi: <http://dx.doi.org/10.1007/s00330-014-3540-z>

ACCURACY OF SIZE-SPECIFIC DOSE ESTIMATE CALCULATION FROM CENTER SLICE IN COMPUTED TOMOGRAPHY

Johannes Boos, Patric Kröpil, Oliver Th. Bethge, Joel Aissa, Christoph Schleich*, Lino Morris Sawicki, Niklas Heinzler, Gerald Antoch and Christoph Thomas
Department of Diagnostic and Interventional Radiology, Medical Faculty, University Dusseldorf, Moorenstraße 5, 40 225 Düsseldorf, Germany

*Corresponding author: Christoph.Schleich@med.uni-duesseldorf.de

Received 14 February 2017; revised 10 May 2017; editorial decision 11 May 2017; accepted 15 May 2017

To evaluate the accuracy of size-specific dose estimate (SSDE) calculation from center slice with water-equivalent diameter (Dw) and effective diameter (Deff). A total of 1812 CT exams (1583 adult and 229 pediatric) were included in this retrospective study. Dw and Deff were automatically calculated for all slices of each scan. SSDEs were calculated with two methods: (1) from the center slice; and (2) from all slices of the volume, which was regarded as the reference standard. Impact of patient weight, height and body mass index (BMI) on SSDE accuracy was assessed. The mean difference between overall SSDE and the center slice approach ranged from $2.0 \pm 1.7\%$ (range: 0–15.5%) for pediatric chest to $5.0 \pm 3.2\%$ (0–17.2%) for adult chest CT. Accuracy of the center slice SSDE approach correlated with patient size (BMI: $r = 0.15$ – 0.43 ; weight $r = 0.26$ – 0.49) which led to SSDE overestimation in small and underestimation in large patients. SSDE calculation using the center slice leads to an error of 2–5%; however, SSDE is underestimated in large patients and overestimation in small patients.

INTRODUCTION

Volumetric computed tomography dose index (CTDIvol) and the dose length product (DLP) are common metrics of computed tomography (CT) scanner radiation dose output and are widely used for radiation dose reporting^(1, 2). However, CTDIvol is calculated based on phantom measurements using a 16 or 32 cm cylindrical phantom and DLP is calculated by multiplying CTDIvol by the scan length. Thus, both values only account for the scanner output while the patient radiation exposure also depends on the patient size and attenuation^(3–5).

The American Association of Physicists in Medicine (AAPM) has introduced the size-specific dose estimates (SSDE) method to correct CT scanner output values for patient size. This can be achieved by measuring the effective diameter (Deff)⁽⁴⁾ or the water-equivalent diameter (Dw)⁽⁵⁾. SSDE are commonly used as a dose metric in recent studies^(6–12) and local dose reference values based on SSDE have been developed⁽¹³⁾.

Acquiring patient diameters and SSDE on a slice-by-slice basis manually is time intensive, and automatic methods are currently not widely available⁽¹⁴⁾. Additionally, the entire axial CT scan volume is required. To simplify the diameter measurements and thus SSDE calculation, diameter measurements in the center slice of the scan volume were proposed to be used for SSDE calculation⁽¹⁵⁾.

Body shape and distribution of different body tissues (and thus attenuation) vary between patients of

different ages and sizes and may lead to a large difference of SSDE values when calculated with the center slice only. Initial studies reported an excellent interpatient SSDE variability of 2–9% when performed with the center slice diameters of the scan compared to the slice-by-slice approach in adult patients⁽³⁾. Although the authors of⁽³⁾ included a wide range of adult patient sizes, the number of patients was limited and the value of the center slice approach for pediatric patients remains unknown.

Therefore, the goal of our study was to evaluate accuracy of the center slice approach and to quantify the impact of patient size on accuracy of SSDE values based on center slice Dw and Deff in a large collective.

METHODS

Patients

This retrospective study was approved by the local ethics committee. In our institution, patient height and weight are routinely documented by the technologist in the Digital Imaging and Communication (DICOM) header at the time of the scan. Axial volumes of consecutive abdominal and chest CT scans in adult patients with documented patient height and weight from the time of the CT study in the DICOM header performed between 06/2015 and 03/2016 were extracted from the PACS. Pediatric abdominal and chest CTs performed between 10/2011 and 05/2016 with available height and weight

ACCURACY OF CENTER-SLICE SSDE-CALCULATION

were exported. Patients were screened for inconclusive entries of height or weight, which was considered an exclusion criterion of the study. CT studies performed under the abdominal or chest protocol name but consisting of different scan areas were also excluded (Figure 1). Body mass index (BMI) was calculated using the formula $BMI = \text{weight}/\text{height}^2$. CTDIvol of the scan series and CTDIvol of every slice were obtained from the DICOM headers and the radiation dose structured reports.

Technical parameters

Scan series were performed on three different multislice CT scanners with 64–128 slices (Definition AS+; Definition Flash; Definition AS with sliding gantry, Siemens Healthineers, Erlangen, Germany). Scan region of the abdomen included the diaphragm to the mid femoral neck. Scan region of the chest CT included the thoracic apex to the base of the liver. Contrast- and non-contrast scans were included in this study. Automated tube current modulation (CareDose 4D, Siemens Healthineers) was activated in all scans.

Automatic method to obtain patient dimensions

An automatic approach using the MATLAB environment (version R2014a, The Mathworks, Natick, MA) was used to calculate lateral diameter (Dlat), anterior–posterior diameter (Dap), Dw and Deff. Axial DICOM images were exported to an offline workstation. In each image, the patient was segmented using automatic thresholding and filling of air-containing areas. The largest connected area in each image was used for further evaluation, thus eliminating the

examination Table from the images. Deff was calculated using the automatically obtained Dlat and Dap⁽⁴⁾:

$$Deff = \sqrt{(Dlat * Dap)} \quad (1)$$

For the calculation of Dw, the following properties of the segmented body area were used: Mean Hounsfield number (meanHU) and area (calculated using the number of pixels and the pixel-spacing attribute from the DICOM header) according to AAPM recommendations⁽⁵⁾. The pixel-spacing attribute represents the physical distance between the center of adjacent pixels. The area represents the physical area of the body in the slice and is calculated by multiplying the number of pixels of the ROI by pixel spacing.

$$Dw = 2 * \sqrt{((1/1000 * \text{meanHU} + 1) * \text{area}/\pi)} \quad (2)$$

Validation of the image segmentation algorithm

To validate the institutional image segmentation algorithm, two radiologists (J.B. and N.H.) with 5 and 3 years of experience in radiology independently reviewed 100 randomly chosen segmentation slices from 100 consecutive CT examinations. Image segmentation accuracy was rated on a 5-point scale: 5—perfect segmentation, no false segmentation; 4—very good segmentation, no relevant false segmentation; 3—good segmentation, only minimal false segmentation; 2—imperfect segmentation with distinct parts of false segmentation; 1—complete failure of segmentation.

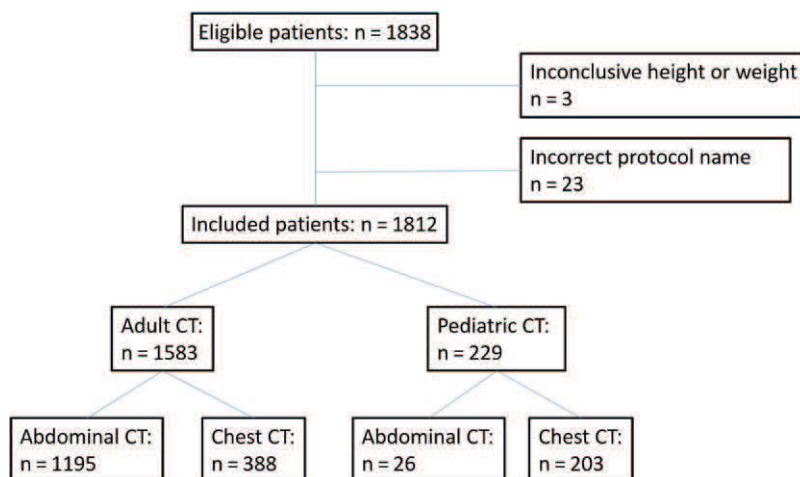


Figure 1. Standards for reporting of diagnostic accuracy (STARD) graph of the patient collective in this study.

Calculation of SSDE

SSDE calculation was performed with Octave (version 4.0.1, John W Eaton and others, www.octave.org). The number of slices of the scan volume and the number of the center slice of the scan volume were calculated in all patients. SSDE values were calculated with two methods in this study:

(1) SSDE values were calculated for the overall scan volume with a slice-by-slice approach, which was regarded as the reference standard. SSDE values were determined automatically according to AAPM recommendations⁽⁴⁾ and previous studies⁽³⁾ by using the Dw and Deff of every slice to obtain a respective conversion factor with the formula:

$$\begin{aligned} \text{conversion factor} \\ = 3.704369 * e^{-0.03671937 * x} \end{aligned} \quad (3)$$

with x being the mean Deff or Dw of the scan volume, respectively⁽⁵⁾. The conversion factor was multiplied with CTDIvol of the respective slice to obtain the SSDE value of the slice. SSDE values from all slices were averaged to calculate the overall SSDE value of the scan series.

(2) SSDE values were calculated using the center slice approach^(3, 15). Center slice diameters were used to obtain the conversion factors, which was then multiplied with mean CTDIvol of the whole exam to obtain SSDE values.

All calculations were performed with Dw and Deff separately, thus we obtained four SSDE values per patient: (1) SSDE from Deff and SSDE from Dw calculated with diameters and CTDI values from all slices and (2) SSDE from Deff and SSDE from Dw calculated with the diameters from center slice. The absolute difference between the slice-by-slice SSDE values and the center slice SSDE values was calculated for every CT scan. The mean absolute difference between the overall and the center slice approach and the mean absolute relative difference (in percent) across all patients were calculated.

Analysis of accuracy

The accuracy of the center slice approach compared to the slice-by-slice approach was compared in adult and pediatric chest and abdominal CT for Dw and Deff. The influence of patient characteristics such as height, weight and BMI on the accuracy of the center slice SSDE approach were assessed. Patients with a difference of more than 10% between the center slice approach and the slice-by-slice approach were analysed in detail. Adult abdominal CT examinations in which the entire body circumference was in the field of view were analysed separately.

Data analysis

All data is given as mean \pm standard deviation. 95% Confidence intervals (95% CI) are provided wherever appropriate. Pearson correlation was performed to compare the different SSDE approaches. Normally distributed variables were compared using Student's t -test. Mann–Whitney U test was used as a non-parametric test. Fleiss kappa was calculated for inter-observer agreement. The level of significance was set to $p < 0.05$.

RESULTS

Patient characteristics

A total of 1812 CT scan series including 1583/1812 (87.4%) CT scans of adult patients (age = 61.5 ± 15.7 , range: 18–94 years) and 229/1812 (12.6%) CT scans of pediatric patients (age = 9.3 ± 5.0 , range: 0.01–17 years) were included in this study (Figure 1). Patient's size included a wide spectrum of BMIs (range: $10.3\text{--}74.1 \text{ kg/m}^2$). Patient characteristics are shown in Table 1. The entire body circumference was in the field of view in all slices of the scan volume in 249/1195 (20.8%) adult abdominal CT scans, 22/388 (5.7%) adult chest CT scans, 2/26 (7.7%) pediatric abdominal and 1/203 (0.5%) pediatric chest CT scans.

Validation of the image segmentation algorithm

Segmentation was excellent (median: 5, IQR = 4–5). There was no false segmentation in any of the reviewed CT exams. 95% of all segmentations were rated perfect or very good. Agreement for the ratings was good ($k = 0.71$).

Diameter measurements

Mean Dw was 29.6 ± 3.7 cm (range: 19.8–45.1 cm) in adult patients and 19.2 ± 3.8 cm (range: 8.6–31.4 cm) in pediatric patients (Table 1). Correlation between overall Dw and overall Deff was strong ($r = 0.99$ for pediatric and adult abdominal CT, $r = 0.98$ for pediatric and adult chest CT). On average, the difference in center slice Dw and Deff was $3.2 \pm 1.1\%$ (0–10.2%) for adult abdominal CT, $4.6 \pm 2.4\%$ (0–8.6%) in adult chest CT, $2.0 \pm 1.6\%$ (0–4.6%) in pediatric abdominal CT and $4.9 \pm 5.4\%$ (0–24.6%) in pediatric chest CT.

Accuracy of the center slice approach

There was a strong correlation between SSDE values calculated with center slice diameters and the reference standard for both, Dw and Deff (Table 2, Figure 2). Using Dw, the mean relative absolute difference between the center slice approach and the slice-by-slice approach was smallest for pediatric chest CT ($2.0 \pm$

Table 2. Correlation coefficients between size-specific dose estimate (SSDE) values calculated with the center slice diameters and SSDE calculated with the overall mean diameter obtained by the slice-by-slice SSDE approach.

	Effective diameter	Water-equivalent diameter
Adult		
Abdominal	0.995	0.995
Chest	0.995	0.985
Pediatric		
Abdominal	0.998	0.997
Chest	0.999	0.999

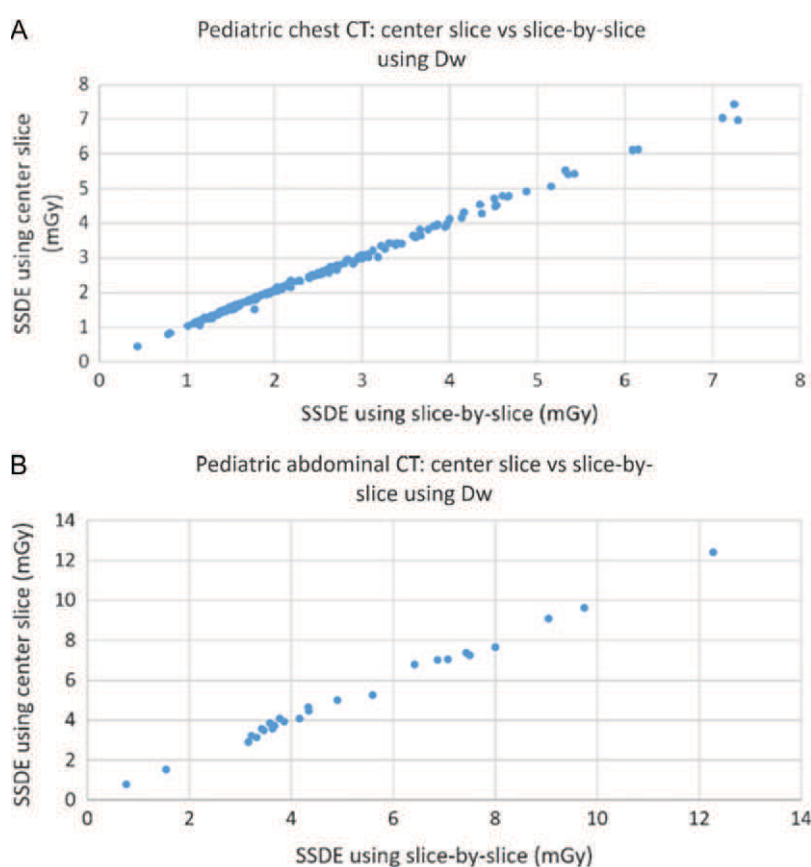


Figure 2. Correlation between the center-slice and the slice-by-slice SSDE approach in pediatric CT using water-equivalent diameter. **(A)** Correlation in chest CT. **(B)** Correlation in abdominal CT.

Adult patients that underwent abdominal CT and had a SSDE deviation of more than 10% had a higher weight and BMI than patients with a difference of less than 10% (weight = 86.2 ± 21.7 kg, range: 54–180 kg vs 78.3 ± 19.3 kg, range: 36–183 kg; $p = 0.03$; BMI = 29.0 ± 6.2 kg/m², range: 19.6–52.6 kg/m² vs 26.1 ± 5.8 kg/m², range: 14.2–74.1 kg/m²; $p = 0.007$). There

was no difference for height (172.3 ± 9.5 vs 172.7 ± 9.6 cm, $p = 0.76$). In adult chest CT, weight, height and BMI were similar in patients with difference of more than 10% between both methods. The only children with a difference above 10% underwent abdominal CT, were 2 and 4 years old, 102 and 125 cm tall, and both weight 25 kg.

Table 3. Patient dose data.

	All adult		Adult abdominal		Adult chest		All pediatric		Pediatric abdominal		Pediatric chest	
	Mean ± SD	Range	Mean ± SD	Range	Mean ± SD	Range	Mean ± SD	Range	Mean ± SD	Range	Mean ± SD	Range
Overall CTDIvol (mGy)	8.3 ± 5.7	2.5-57.9	9.2 ± 6.2	5.6 ± 2.5	5.6 ± 2.5	1.5-16.6	1.5 ± 1.2	3.2 ± 2.0	3.2 ± 2.0	0.3-8.5	1.3 ± 0.8	0.2-5.4
Overall SSDE Deff (mGy)	9.7 ± 5.3	3.7-53.0	10.7 ± 5.6	6.6 ± 2.2	6.6 ± 2.2	2.2-15.6	2.6 ± 1.7	5.2 ± 2.7	5.2 ± 2.7	0.8-12.7	2.3 ± 1.2	0.4-7.1
Overall SSDE Dw (mGy)	9.9 ± 5.4	3.9-54.6	10.8 ± 5.8	7.0 ± 2.3	7.0 ± 2.3	2.3-16.8	2.7 ± 1.7	5.2 ± 2.7	5.2 ± 2.7	0.8-12.3	2.4 ± 1.2	0.4-7.3
Center Slice SSDE Deff (mGy)	9.4 ± 5.0	3.8-47.5	10.4 ± 5.2	6.5 ± 2.2	6.5 ± 2.2	2.2-15.3	2.5 ± 1.7	5.2 ± 2.7	5.2 ± 2.7	0.8-12.7	2.2 ± 1.1	0.4-7.0
Center Slice SSDE Dw (mGy)	9.7 ± 5.0	3.9-50.3	10.5 ± 5.4	7.1 ± 2.2	7.1 ± 2.2	2.4-16.7	2.7 ± 1.7	5.2 ± 2.6	5.2 ± 2.6	0.8-12.4	2.4 ± 1.2	0.4-7.4
SSDE Deff overall vs center slice mGy	0.4 ± 0.5	0-7.9	0.5 ± 0.7	0.2 ± 0.2	0.2 ± 0.2	0-1.3	0.09 ± 0.08	0.1 ± 0-1	0.1 ± 0-1	0-0.3	0.08 ± 0.07	0.0-0.4
%	3.8 ± 3.0	0-31.0	4.1 ± 3.5	3.0 ± 2.4	3.0 ± 2.4	0-17.6	3.2 ± 2.0	2.8 ± 2.0	2.8 ± 2.0	0.0-7.4	3.3 ± 2.0	0.0-14.5
SSDE Dw overall vs center slice mGy	0.4 ± 0.5	0-7.7	0.5 ± 0.7	0.3 ± 0.2	0.3 ± 0.2	0-1.5	0.06 ± 0.07	0.2 ± 0.1	0.2 ± 0.1	0.0-0.4	0.5 ± 0.05	0.0-0.3
%	4.1 ± 3.1	0-30.5	3.9 ± 3.4	5.0 ± 3.2	5.0 ± 3.2	0-17.2	2.1 ± 1.8	3.1 ± 2.6	3.1 ± 2.6	0.0-9.2	2.0 ± 1.7	0.0-15.5

SD, standard deviation; SSDE_v, size-specific dose estimates; CTDIvol, volumetric computed tomography dose index; Deff, effective diameter; Dw, water-equivalent diameter.

DISCUSSION

In this study, we demonstrated a high accuracy of the center slice SSDE approach for adult and pediatric abdominal and chest CT with a mean relative absolute difference of 2–5%. The accuracy of the center slice approach was correlated with patient size, especially in adult abdominal CT. Our results indicate that a higher error has to be expected in larger patients and that radiation dose is overestimated in small patients and underestimated in large patients when using the center slice approach. Depending on patient age and body region, the difference between center slice SSDE approach and the reference standard exceeded 10% in 0–6% of patients.

The center slice SSDE approach with Dw led to a relative mean absolute difference of 2–5% compared to the reference standard. This is comparable to previously reported values for adult patients in chest (6%) and abdominal (3%) CT⁽³⁾ and to systems based on the scout images⁽¹⁶⁾. Additionally, we found that using the center slice SSDE method was slightly more accurate in pediatric patients, which was not evaluated in previous studies. However, the difference between the center slice approach and the reference standard was up to 8 mGy/31% of the SSDE value in single cases.

We found a moderate correlation between the absolute difference between center slice and slice-by-slice method per patient and patient BMI and body weight. Thus, in larger patients a lower accuracy of the center slice SSDE method has to be expected. Previous studies demonstrated a good correlation of SSDE with patient size metrics^(17–19). However, the impact of patient size on the accuracy of the reported SSDE values when obtained by center slice approach was not part of prior studies. Of note, we found a tendency for underestimation of SSDE in patients with a high BMI whereas SSDE were overestimated in patients with a low BMI in abdominal CT. This indicates that in very slim or very large patients, the center slice SSDE approach may lead to a systematic error in SSDE calculations. Although our and previous⁽³⁾ results demonstrate the high accuracy of the center slice SSDE approach, assessing Dw from more than one (e.g. center) slice is preferable for SSDE calculation, at least in very small and large patients. This may become especially important when cumulative doses over time are monitored, as the error will constantly distort patients SSDE.

The center-slice SSDE method led to a mean relative absolute difference of 2.1% in pediatric abdominal and chest CT. The center slice approach has been used with Deff^(17, 18), however, the accuracy of the center slice Dw for SSDE calculation in pediatric patients has not been reported. Our results indicate

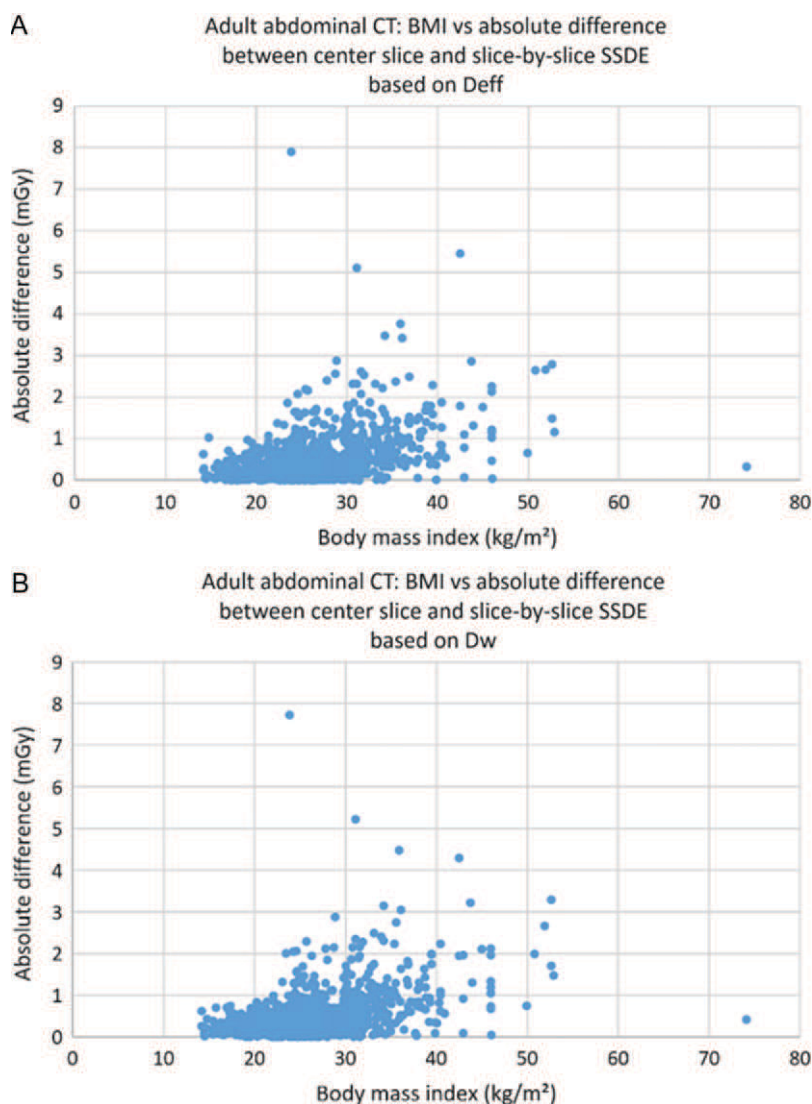


Figure 3. Adult abdominal CT: correlation between body mass index (BMI, x-axis) and the absolute difference between center slice SSDE values and slice-by-slice SSDE values (in mGy, y-axis) for effective diameter (A) and water-equivalent diameter (B).

that Dw can be used in pediatric abdominal and chest CT which may improve accuracy of radiation dose calculations in pediatric patients.

Automated calculation of Dw has been reported before^(3, 7) and reliably worked in all patients in our study. Of note, only in a small percentage of patients, the entire outer body circumference was in the field of view on all CT-slices. Previous studies⁽³⁾ only included patients in which the entire anatomy was not truncated. However, our results demonstrate that this is not typically the case in clinical routine. In chest CT,

the shoulders typically exceed beyond the field of view⁽²⁰⁾ and particularly in very large patients, a smaller field of view may be chosen to improve the spatial resolution. The small field of view may lead to underestimation of Dw and Deff and thus an overestimation of SSDE. Therefore, having at least one reconstruction with the entire body circumference in the field of view is desirable. However, we found accuracy of the center slice approach to be comparable in patients with and without the entire body circumference in the field of view. In clinical routine

ACCURACY OF CENTER-SLICE SSDE-CALCULATION

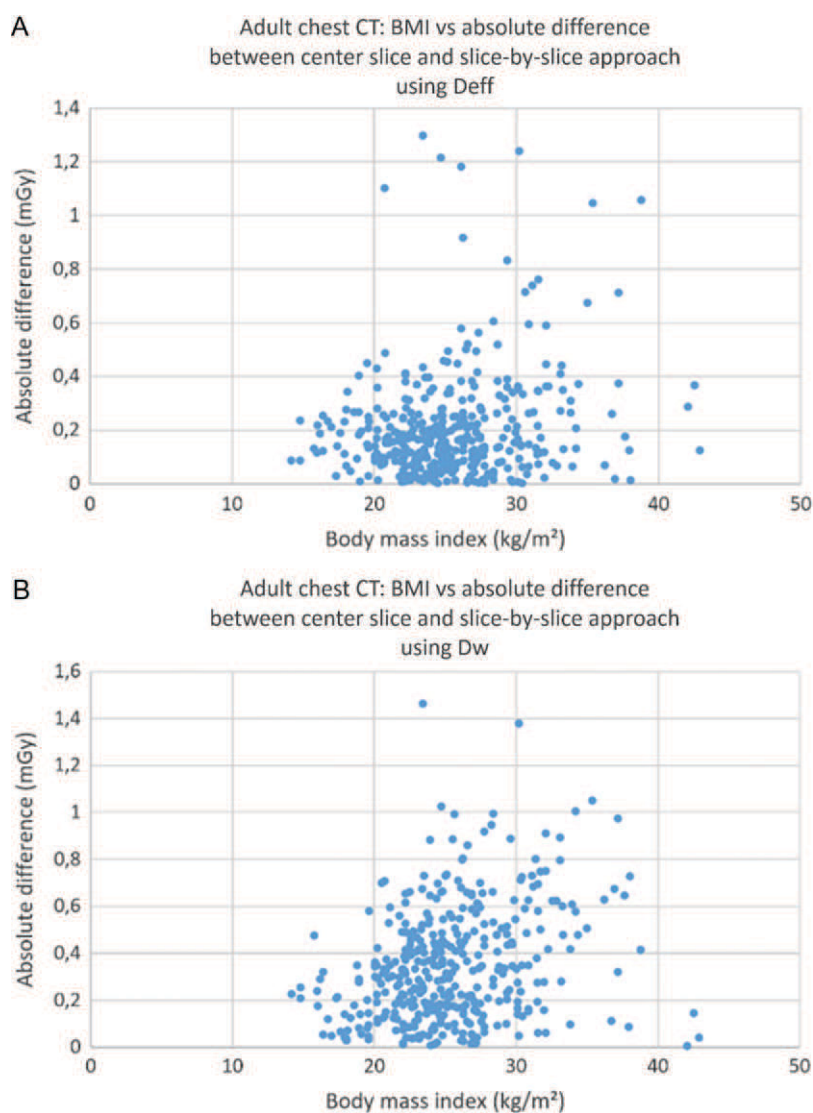


Figure 4. Adult chest CT: correlation of body mass index (BMI, *x*-axis) and the absolute difference per patient between center slice SSDE values and slice-by-slice SSDE values (in mGy) for effective diameter (A) and water-equivalent diameter (B).

without an additional reconstruction with a large field of view one has to be aware that due to the smaller diameter measurements the overall SSDE value will be an overestimation of the true radiation dose in these cases.

Dw had a strong correlation with Deff in adult and pediatric chest and abdominal CT with correlation coefficients of $r = 0.98\text{--}0.99$. However, on average, Deff and Dw of the center slice differed by 2–5% which was more pronounced in chest CT where it led to significantly lower SSDE values

compared to Dw. Our results are in accordance to previous studies^(8, 17) that showed a good correlation between Dw and Deff. Although Dw and Deff can be used to calculate SSDE, Dw is regarded the reference standard⁽⁵⁾ because Deff may lead to inappropriate results, especially in chest CT. The air in the lungs (or in other parts of the body) can lead to a higher central radiation dose which will not be accounted for when using Deff^(5, 7, 15). As Dw is based on attenuation, air within the body is properly included into this patient size metric leading to a

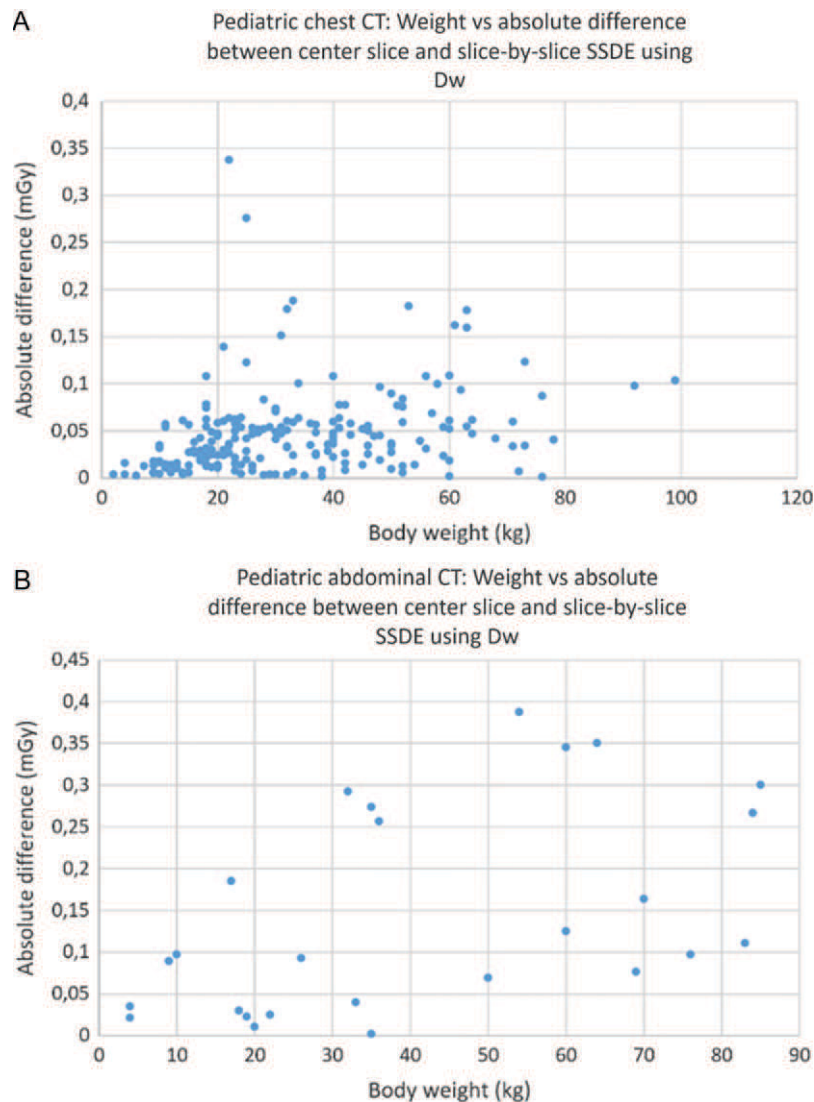


Figure 5. Pediatric chest (A) and abdominal (B) CT: correlation of body weight (x-axis) and the absolute difference per patient between center slice SSDE values and slice-by-slice SSDE values (in mGy) for water-equivalent diameter.

smaller Dw compared to Deff and thus a higher SSDE value.

Our study has limitations. A retrospective study design was used. Most of the included patients were adults that underwent abdominal CT, therefore analysis of CT examinations with the entire body circumference in the field of view could only be performed in these patients. Due to the herein found low mean error between both SSDE methods, the relatively small number of included adult chest CT examinations and pediatric examinations may have influenced our results. Patient's height and weight

were documented by the technician at the time of the CT scan. Inconclusive entries in which the true height and weight at the time of the CT study could not be determined were excluded from this study. BMI is an imperfect descriptor for patient size and may be inaccurate in some patients groups (e.g. pediatric patients, very old patients, short or tall patients or very muscular patients). Therefore patient weight was also used in pediatric patients. Size descriptors that include fat and muscle volume of the patients may be more accurate, however, BMI is commonly used as a descriptor for patient size. To overcome

ACCURACY OF CENTER-SLICE SSDE-CALCULATION

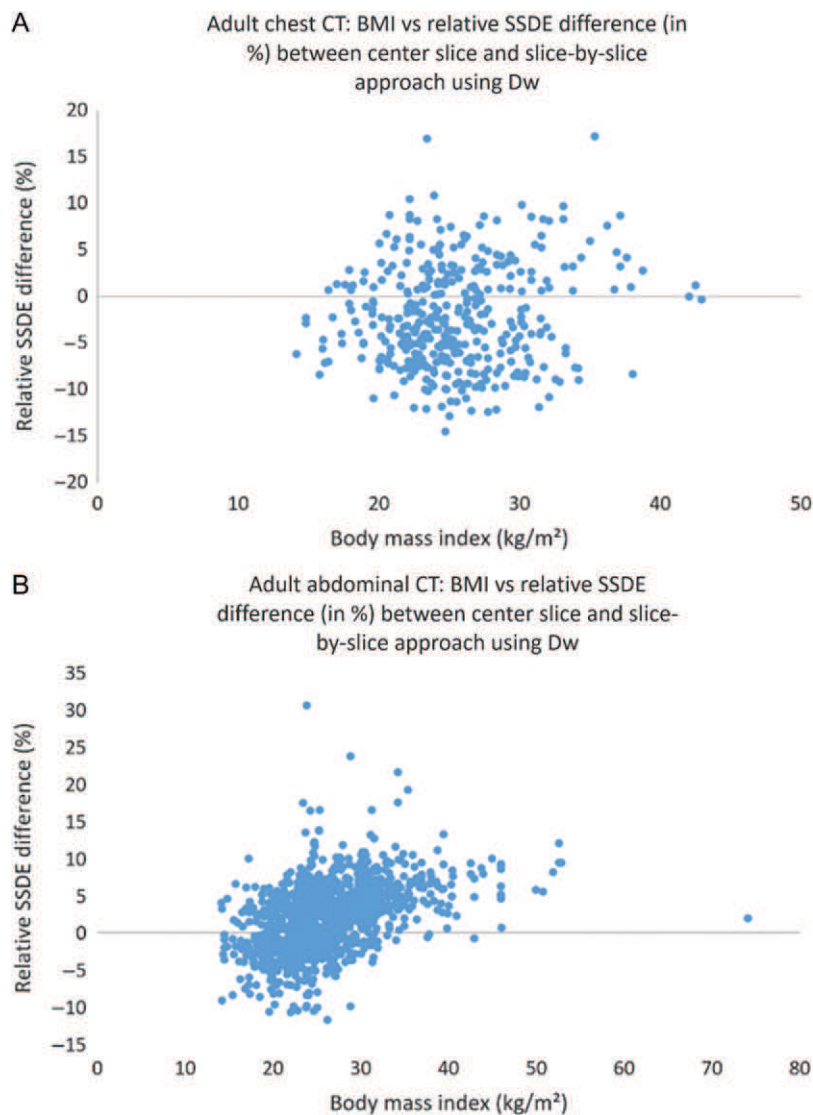


Figure 6. Relative SSDE difference between the center slice approach and the reference standard in adult chest CT (A) and abdominal CT (B). The *x*-axis displays the body mass index and the *y*-axis displays the relative SSDE difference. Negative values mean that the center slice approach overestimated SSDE whereas positive values mean that the center slice approach underestimated SSDE.

this limitation in pediatric patients we also used body weight as a size descriptor, which is in accordance with previous studies⁽¹⁸⁾. All radiation dose values are scanner indicated and we did not perform phantom measurements. The formula used in our study for calculation of the conversion factors was initially obtained for a 32 cm phantom and 120 kVp, however, it is also recommended for other tube voltages by the AAPM^(4, 5). The German Federal Office for Radiation Protection recommends a 32 cm

phantom when performing pediatric abdominal and chest CT⁽²¹⁾, however, other institutions may use a 16 cm phantom and the corresponding formula^(4, 5) for which the results may differ. The herein used automatic method to calculate Dw was not verified using a second method. All diameter calculation were made from the axial CT images and we did not evaluate the accuracy of scout images for SSDE calculation. However, axial images are recommended by the AAPM.

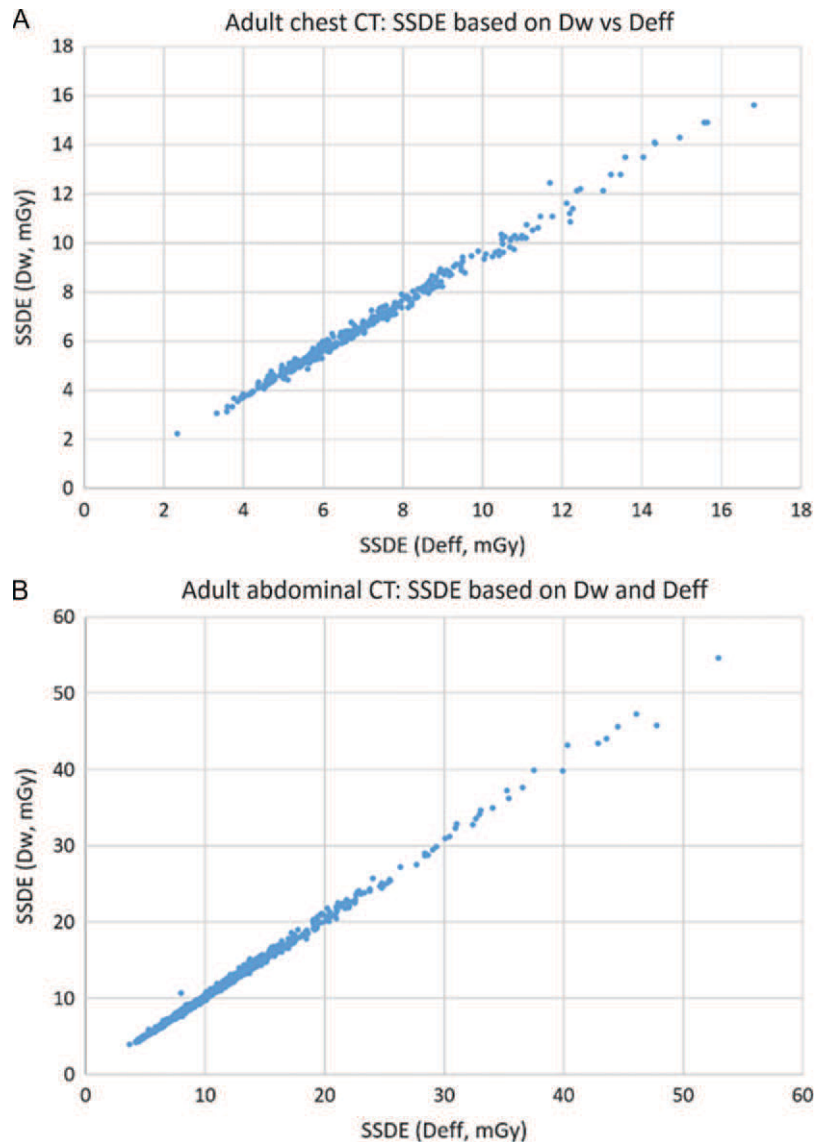


Figure 7. Correlation between SSDE based on water-equivalent diameter and SSDE based on effective diameter in adult chest CT (A) and abdominal CT (B). All values are calculated with all slices of the scan volume.

In conclusion, the center slice SSDE approach led to a mean relative absolute error of 2–5% in pediatric and adult abdominal and chest CT. Dw leads to higher SSDE values compared to Deff in chest CT. The accuracy of the center slice approach was related to patients BMI and weight with a tendency to underestimate SSDE in large patients and overestimate SSDE in small patients. Calculation of Dw from more than just the center slice is beneficial to improve SSDE accuracy, especially in very small and very large patients.

REFERENCES

1. Smith-Bindman, R. *et al.* Radiation doses in consecutive CT examinations from five University of California Medical Centers. *Radiology* **277**(1), 134–141 (2015).
2. Yu, L., Fletcher, J. G., Shiung, M., Thomas, K. B., Matsumoto, J. M., Zingula, S. N. and McCollough, C. H. Radiation dose reduction in pediatric body CT using iterative reconstruction and a novel image-based denoising method. *AJR Am. J. Roentgenol.* **205**(5), 1026–1037 (2015).

ACCURACY OF CENTER-SLICE SSDE-CALCULATION

3. Leng, S., Shiung, M., Duan, X., Yu, L., Zhang, Y. and McCollough, C. H. *Size-specific dose estimates for chest, abdominal, and pelvic CT: effect of inpatient variability in water-equivalent diameter.* *Radiology* **276**(1), 184–190 (2015).
4. The Report of AAPM Taks Group 204. *Size-specific dose estimates (SSDE) in pediatric and adult body CT examinations.* https://www.aapm.org/pubs/reports/RPT_204.pdf. (August 30 2015, date last accessed).
5. The Report of AAPM Task Group 220. *Use of water equivalent diameter for calculating patient size and size-specific dose estimates (SSDE) in CT.* https://www.aapm.org/pubs/reports/RPT_220.pdf. (August 15 2015, date last accessed).
6. Kidoh, M., Utsunomiya, D., Oda, S., Funama, Y., Yuki, H., Nakaura, T., Kai, N., Nozaki, T. and Yamashita, Y. *Validity of the size-specific dose estimate in adults undergoing coronary CT angiography: comparison with the volume CT dose index.* *Int. J. Cardiovasc. Imaging* **31**(Suppl. 2), 205–211 (2015).
7. Ikuta, I., Warden, G. I., Andriole, K. P., Khorasani, R. and Sodickson, A. *Estimating patient dose from x-ray tube output metrics: automated measurement of patient size from CT images enables large-scale size-specific dose estimates.* *Radiology* **270**(2), 472–480 (2014).
8. Gabusi, M., Riccardi, L., Aliberti, C., Vio, S. and Paiusco, M. *Radiation dose in chest CT: assessment of size-specific dose estimates based on water-equivalent correction.* *Phys. Medica PM Int. J. Devoted Appl. Phys. Med. Biol. Off. J. Ital. Assoc. Biomed. Phys. AIFB* **32**(2), 393–397 (2016).
9. Taguchi, N. *et al.* *Using 80 kVp on a 320-row scanner for hepatic multiphase CT reduces the contrast dose by 50% in patients at risk for contrast-induced nephropathy.* *Eur. Radiol.* (2016).
10. Waszczuk, Ł.A., Guziński, M., Czarnecka, A. and Sasiadek, M.J. *Size-specific dose estimates for evaluation of individual patient dose in CT protocol for renal colic.* *AJR Am. J. Roentgenol.* **205**(1), 100–105 (2015).
11. Westra, S. J., Li, X., Gulati, K., Singh, S., Liu, B., Kalra, M. K. and Abbara, S. *Entrance skin dosimetry and size-specific dose estimate from pediatric chest CTA.* *J. Cardiovasc. Comput. Tomogr.* **8**(2), 97–107 (2014).
12. Christner, J. A., Braun, N. N., Jacobsen, M. C., Carter, R. E., Kofler, J. M. and McCollough, C. H. *Size-specific dose estimates for adult patients at CT of the torso.* *Radiology* **265**(3), 841–847 (2012).
13. Imai, R., Miyazaki, O., Horiuchi, T., Kurosawa, H. and Nosaka, S. *Local diagnostic reference level based on size-specific dose estimates: assessment of pediatric abdominal/pelvic computed tomography at a Japanese national children's hospital.* *Pediatr. Radiol.* **45**(3), 345–353 (2015).
14. Boos, J., Meineke, A., Bethge, O. T., Antoch, G. and Kröpil, P. *Dose monitoring in radiology departments: status quo and future perspectives.* *Rofo Fortschr. Geb. Rontgenstr. Nuklearmed.* **188**(5), 443–450 (2016).
15. Cheng, P. M. *Automated estimation of abdominal effective diameter for body size normalization of CT dose.* *J. Digit. Imaging* **26**(3), 406–411 (2013).
16. Larson, D. B., Wang, L. L., Podberesky, D. J. and Goske, M. J. *System for verifiable CT radiation dose optimization based on image quality. Part I. Optimization model.* *Radiology* **269**(1), 167–176 (2013).
17. Karmazyn, B., Ai, H., Klahr, P., Ouyang, F. and Jennings, S. G. *How accurate is size-specific dose estimate in pediatric body CT examinations?* *Pediatr. Radiol.* (2016).
18. Khawaja, R. D., Singh, S., Vettiyil, B., Lim, R., Gee, M., Westra, S. and Kalra, M. K. *Simplifying size-specific radiation dose estimates in pediatric CT.* *AJR Am. J. Roentgenol.* **204**(1), 167–176 (2015).
19. Boos, J., Lanzman, R. S., Heusch, P., Aissa, J., Schleich, C., Thomas, C., Sawicki, L. M., Antoch, G. and Kröpil, P. *Does body mass index outperform body weight as a surrogate parameter in the calculation of size-specific dose estimates in adult body CT?* *Br. J. Radiol.* **89**(1059), 20150734 (2016).
20. Franck, C., Vandevoorde, C., Goethals, I., Smeets, P., Achten, E., Verstraete, K., Thierens, H. and Bacher, K. *The role of Size-Specific Dose Estimate (SSDE) in patient-specific organ dose and cancer risk estimation in paediatric chest and abdominopelvic CT examinations.* *Eur. Radiol.* (2015).
21. German Federal Office for Radiation Protection. *Publication of updated diagnostic reference levels for diagnostic and interventional X-ray examinations.* 15072016. https://www.bfs.de/EN/topics/ion/medicine/diagnostics/reference-values/reference-values.html?jsessionid=CA471437B50A57ED2E79DCBAFEB8A618.1_cid382.



PAPER

Institutional computed tomography diagnostic reference levels based on water-equivalent diameter and size-specific dose estimates

To cite this article: Johannes Boos *et al* 2018 *J. Radiol. Prot.* **38** 536

View the [article online](#) for updates and enhancements.

Institutional computed tomography diagnostic reference levels based on water-equivalent diameter and size-specific dose estimates

Johannes Boos¹, Christoph Thomas¹, Elisabeth Appel^{1,2},
Yan Klosterkemper¹, Christoph Schleich¹, Joel Aissa¹,
Oliver Th Bethge¹, Gerald Antoch¹ and Patric Kröpil¹

¹ University Düsseldorf, Medical Faculty, Department of Diagnostic and Interventional Radiology, D-40225 Düsseldorf, Germany

² Department of Radiology, Beth Israel Deaconess Medical Center, 330 Brookline Ave, Boston, MA 02215, United States of America

E-mail: christoph.schleich@med.uni-duesseldorf.de

Received 8 September 2017, revised 9 December 2017

Accepted for publication 20 December 2017

Published 13 March 2018



CrossMark

Abstract

Size-specific institutional diagnostic reference levels (DRLs) were generated for chest and abdominopelvic computed tomography (CT) based on size-specific dose estimates (SSDEs) and depending on patients' water-equivalent diameter (D_w). 1690 CT examinations were included in the IRB-approved retrospective study. SSDEs based on the mean water-equivalent diameter of the entire scan volume were calculated automatically. SSDEs were analyzed for different patient sizes and institutional DRLs (iDRLs; 75% percentiles) based on D_w and SSDEs were generated. iDRLs were compared to the national DRLs. Mean volumetric computed tomography dose index (CTDI_{vol}), D_w and SSDEs for all 1690 CT examinations were 7.2 ± 4.0 mGy (0.84–47.9 mGy), 29.0 ± 3.4 cm and 8.5 ± 3.8 mGy (1.2–37.7 mGy), respectively. Overall, the mean SSDEs of all CT examinations were higher than the CTDI_{vol} in chest CT, abdominopelvic CT and upper abdominal CT, respectively ($p < 0.001$ for all). There was a strong linear correlation between D_w and SSDEs in chest ($R^2 = 0.66$), abdominopelvic ($R^2 = 0.98$) and upper abdominal CT ($R^2 = 0.96$) allowing for the implementation of size-specific institutional DRLs based on SSDEs and patients' D_w. We generated size-specific, D_w-dependent institutional DRLs based on SSDEs, which allow for easier and more comprehensive analyses of CT radiation exposure. Our results indicate that implementation of SSDEs into national DRLs may be beneficial.

Keywords: institutional computed tomography diagnostic reference level (DRL), size-specific dose estimate (SSDE), abdominopelvic computed tomography, patients water-equivalent diameter (Dw), chest computed tomography

(Some figures may appear in colour only in the online journal)

Introduction

National and institutional diagnostic reference levels (DRLs) are commonly used for quality assurance in radiology departments [1–3]. For national DRLs (nDRLs), a volumetric computed tomography dose index (CTDI_{vol}) and a dose length product (DLP) are provided for a CT scan of a body region and can be used as guidance to review institutional CT radiation application [2, 4, 5].

The frequently used DRL method in which a single CTDI_{vol} and DLP value is provided per anatomic region has three major drawbacks. First, the CTDI_{vol} (and thus the DLP) is not a measurement but a calculated value based on phantom measurements using a 16 cm or 32 cm cylindrical phantom. However, CT radiation exposure is influenced by the patient's size and therefore the size-specific dose estimate (SSDE) concept has been introduced by the American Association of Physicists in Medicine (AAPM) [6, 7]. Initial studies produced institutional DRLs (iDRLs) based on SSDE [8].

Second, nDRLs are provided for an average-sized patient, and patient characteristics such as weight or body mass index (BMI) are necessary to interpret CT dose data from single examinations. This may impede analysis of a questionable CT dose application. Therefore, size-dependent DRLs based on BMI or diameter measurements have been proposed [9, 10].

Third, the currently used CT dose metrics have a very high variability when using automatic exposure control systems. Therefore a large sample size is required to properly analyze CT dose data [11].

SSDEs can be calculated based on the effective diameter (D_{eff}) or the water-equivalent diameter (D_w), the latter being the preferred method. The feasibility of automated assessment of D_w has been shown [12, 13]. While recording the patient's metrics such as weight or BMI may be time consuming, automated assessment of D_w and SSDE allows for a fast and comprehensive method which can enable implementation of size-specific iDRLs.

Therefore, the goal of our study was to produce iDRLs based on SSDEs that depend on patients' D_w, which allow for an easier and more comprehensive analysis of CT dose output compared with DRLs that are tailored to an average-sized patient.

Methods

This retrospective study was approved by the institutional review board. All CT examinations from the three institutional multi-detector CT scanners (Definition Flash with 128 slices, Definition AS + with 128 slices, Definition AS with sliding gantry with 64 slices, Siemens Healthineers, Forchheim, Germany) performed between July 2016 and November 2016 were included. 15370 CT examinations were performed during the study period. Exclusion criteria were pediatric CT examinations, CT protocols that were not assigned to the body regions 'chest', 'abdominopelvic' or 'upper abdomen', and CT examinations with truncated images. All low dose CT protocols were excluded (figure 1). Therefore, 1690 CT examinations (300

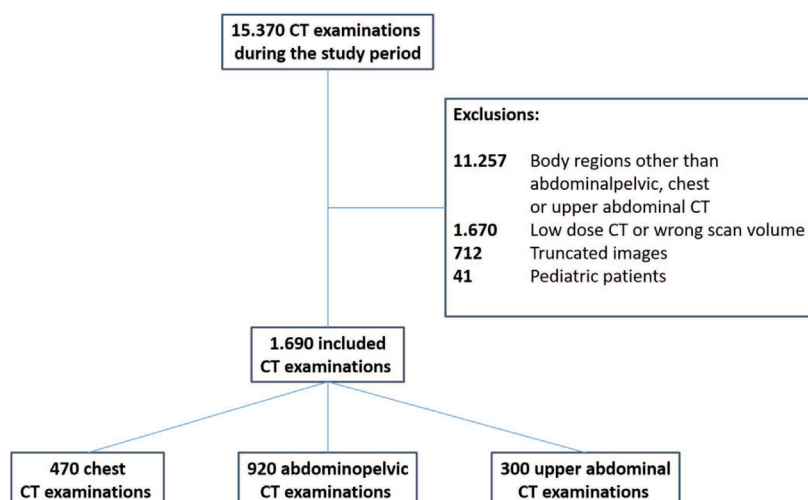


Figure 1. Flowchart of our study population according to the Standards for Reporting Diagnostic Accuracy (STARD) initiative.

upper abdominal CT examinations, 470 chest CT examinations, 920 abdominopelvic CT examinations) were included in the analysis.

CT protocols

CT protocols for chest, upper abdomen and the entire abdomen were included in the study. The scan volume of the institutional standard CT protocols included the upper chest aperture to the base of the diaphragm in chest CT, the lower lungs to the base of the liver in upper abdominal CT and the upper edge of the liver to the symphysis in abdominopelvic CT. The scan volume of upper abdominal CT may vary due to the indication of the examination. CT examinations were performed in spiral mode with or without intravenous contrast material (Omnipaque, GE Healthcare, Munich, Germany) depending on the indication. Automated tube current modulation (CareDose 4D, Siemens Healthineers, Forchheim, Germany) and automated tube voltage selection (CareKV, Siemens Healthineers, Forchheim, Germany) were activated in all examinations. Five different strength levels ('very weak', 'weak', 'average', 'strong' or 'very strong') can be selected when using the CareDose 4D (Siemens Healthineers, Forchheim, Germany). In our institution, the level 'average' is used for all CT scanners and for all body regions. Scan parameters are listed in table 1. Images were reconstructed with a medium level of iterative reconstruction (SAFIRE Level 3, Siemens Healthineers, Forchheim, Germany) when performed on the Definition AS+ or Flash CT scanner and with filtered back projection on the Definition AS (sliding gantry) CT scanner. A 32 cm phantom was used for CTDIvol calculation in all scans.

CT dose monitoring and calculation of water-equivalent diameter and SSDEs

Automated CT dose monitoring based on the Digital Imaging and Communications Radiation Dose Structured Report (DICOM-RDSR) was used to obtain the CT dose data and technical parameters (DoseIntelligence, Pulmokard, Herdecke, Germany) including CTDIvol, DLP, pitch, mean tube current time product, tube voltage, scan length, anatomic region, phantom size and CT protocol [3]. Height and weight of the patient were automatically stored in the

Table 1. CT scan parameters.

	Chest CT (<i>n</i> = 470)	Upper abdominal CT (<i>n</i> = 300)	Abdominopelvic CT (<i>n</i> = 920)
Pitch factor	0.6	0.6	0.6
Number of examinations at a tube voltage (<i>n</i>)			
80 kVp	24	1	0
100 kVp	355	280	824
120 kVp	91	19	94
140 kVp	0	0	2
Single collimation (mm)	0.6	0.6	0.6
Effective tube current time product (mAs) ^a	219 ± 147 (43–557)	217 ± 99 (62–631)	219 ± 81 (80–617)
Tube rotation time (s)	0.3	0.5	0.5
Automated tube current modulation strength level	Average	Average	Average

^a Data provided as mean ± standard deviation, range in parentheses.

DICOM-RDSR at the time of the CT examination if they were available in the electronic patient records. Assignment of CT protocols to body regions (which was necessary for comparison to national DRLs) was performed manually by one radiologist (J B, with four years of experience in radiology).

CT protocols that were assigned to the anatomic region ‘abdominopelvic’ included CT angiography (reference tube current time product (ref. mAs) by institutional SOP, CT Definition Flash and Definition AS+/CT Definition AS with a sliding gantry: 160/220 mAs) as well as non-contrast (ref. mAs 120/150 mAs) or contrast-enhanced routine abdominopelvic CT (ref. mAs. 166/207 mAs). CT protocols that were assigned to the anatomic region ‘chest’ included routine chest CT with (110/140 mAs) or without (ref. mAs 60/140 mAs) contrast medium and CT angiography of the pulmonary arteries (ref. mAs 135/160 mAs). CT protocols that were assigned to the anatomic region ‘upper abdomen’ included liver CT (ref. mAs 166/207 mAs), renal CT (ref. mAs 166/207 mAs), non-contrast adrenal CT (ref. mAs 120/200 mAs), pancreatic CT (ref. mAs 166/207 mAs) and non-contrast (ref. mAs 120/150 mAs) or contrast-enhanced (ref. mAs 166/207 mAs) routine upper abdominal CT.

SSDE calculation was performed automatically for every CT examination after the scan. For SSDE calculation, the entire scan volume was automatically transferred to a post-processing server immediately after the CT examination. Dw from every slice of the CT scan was obtained automatically by using a previously validated self-developed algorithm and the Matlab environment (version R2015, The Mathworks, Natick, MA, [14]). The algorithm consists of different steps. (1) The CT table is removed by using a three-dimensional analysis approach. (2) The image is binarized and a threshold of –144 HU is used to identify air-filled pixels and to detect the outer body circumference. At this step, truncated CT examinations were identified by the analysis of pixels other than air (density of >–144 HU) adjacent to the outer border of the field of view. The number of pixels with >–144 HU at the outer border of the field of view was automatically calculated and examinations with an average number of more than 100 non-air pixels per CT slice were excluded. A small number of 100 pixels per slice was selected to ensure that truncation of the CT examinations did not influence our results. (3) The water-equivalent diameter was calculated according to the AAPM guidelines [6, 7]. The AAPM conversion factor was calculated for each slice using Dw and the formula

provided in Report 204, appendix A [6, 7]. The conversion factor was then multiplied with the CTDIvol of the corresponding slice to obtain the SSDE of the slice. The SSDE of the examination was the mean SSDE of all slices. After the automated calculation of the SSDE with our algorithm, the Dw and SSDE were stored in the institutional CT dose monitoring software (DoseIntelligence, Pulmokard, Herdecke, Germany).

Calculation of iDRLs and data analysis

For assessment of iDRLs, patients with the same Dw were categorized into 1 cm water-equivalent diameter bins and the SSDE per Dw bin was calculated for each body region. Analysis was performed by one radiologist (J B). Dose data was only obtained for a Dw bin when at least five examinations were available (chest: 21–34 cm bins; abdominal: 22–36 cm bins; upper abdominal CT: 23–36 cm bins). As recommended by the International Commission on Radiological Protection, the 75th percentile of the SSDE was regarded as the upper limit of the iDRL and the 25th percentile was chosen as the lower limit [15]. Variability of CTDIvol and SSDEs between different CT protocols assigned to the same body region was evaluated. As current German national DRLs are only provided for CTDIvol (and not as SSDEs) and for an average size patient (defined as 70 ± 3 kg), the CTDIvol of an average size patient as determined by Dw was compared to the nDRLs [16]. The number of CT examinations exceeding the nDRLs and the size-specific iDRL were compared. Paired values were compared using a paired t-test. A chi-squared test was used to compare proportions. Linear regression was used to produce institutional DRLs based on patient Dw. All data is given as mean \pm standard deviation with range or median with interquartile range (IQR). A p -value < 0.05 was considered to indicate statistical significance.

Results

Patient characteristics

1690 CT examinations (300 upper abdominal CT examinations, 470 chest CT examinations, 920 abdominal CT examinations) were included in the study (618 men, 1072 women). Mean patient age was 62.8 ± 14.7 years (range 18–96 years). Weight and height were available in 490/1690 (29.0%) patients (weight 75.5 ± 16.4 kg (42–145 kg), height 171.4 ± 9.3 cm (150–197 cm), BMI 25.6 ± 4.5 kg m⁻² (14.0–45.8 kg m⁻²)). The average water-equivalent diameter was 29.0 ± 3.4 cm (15.9–41.1 cm) (table 2). There was a significant correlation between BMI and Dw ($r = 0.34$, $p < 0.05$).

CT dose parameters

Mean CTDIvol across the three body regions was 7.2 ± 4.0 mGy (0.84–47.3 mGy), mean DLP was 270.1 ± 192.2 mGy cm (11.2–1633.6 mGy cm) and mean SSDE was 8.5 ± 3.8 mGy (1.2–37.7 mGy). CT dose parameters per body region and per Dw bin are listed in tables 2 and 3. SSDEs were significantly higher than CTDIvol in chest CT, abdominopelvic CT and upper abdominal CT (table 2; all $p < 0.0001$).

iDRL

SSDE linearly increased with increasing Dw (figures 2–4). There was a very strong correlation of SSDE and Dw with high coefficients of determination in abdominopelvic CT ($R^2 = 0.98$), in upper abdominal CT ($R^2 = 0.96$) and in chest CT ($R^2 = 0.66$). The high

Table 2. Patient characteristics and computed tomography dose parameters.

	Chest CT	Upper abdominal CT	Abdominopelvic CT
CTDIvol (mGy)	4.6 ± 3.5 (0.8–22.6)	7.9 ± 4.4 (1.9–47.9)	8.3 ± 3.5 (2.7–27.6)
DLP (mGy cm)	147 ± 137 (11–1634)	186 ± 109 (18–7909)	360 ± 191 (26–1308)
SSDE (mGy) ^a	5.7 ± 3.7 (1.3–21.4)	8.7 ± 3.7 (2.8–37.7)	9.8 ± 3.1 (3.8–25.7)
nDRL CTDIvol (mGy)	10	15	15
nDRL DLP (mGy cm)	350	360	700
Age (years)	62.7 ± 15.2 (18.4–96.1)	63.4 ± 13.6 (23.8–90.4)	62.6 ± 14.7 (19.2–90.7)
Water-equivalent diameter (cm)	27.8 ± 3.3 (15.9–37.8)	30.3 ± 3.8 (19.5–41.1)	29.2 ± 3.1 (20.3–39.4)
Weight (kg)	75.2 ± 15.7 (42–128) ^b	77.3 ± 1.8 (44–145) ^c	74.4 ± 15.5 (42–128) ^d
Height (kg)	170.4 ± 9.1 (150–197) ^b	171.1 ± 8.6 (151–190) ^c	172.2 ± 9.9 (155–197) ^d
Body mass index (kg m ⁻²)	25.8 ± 4.2 (16.4–39.5)	26.3 ± 5.2 (17.0–45.8)	25.0 ± 4.0 (14.0–39.5)

^a Based on the mean water-equivalent diameter of the scan volume; CT: computed tomography.

^b Based on 136 available entries of height and weight.

^c Based on 148 available entries of height and weight.

^d Based on 206 available entries of height and weight. Data is given as mean ± standard deviation with range in parenthesis.; nDRL: national diagnostic reference levels.

CTDIvol: volumetric computed tomography dose index; DLP: dose length product; SSDE: size-specific dose estimates.

coefficients of determination in all three body regions demonstrate the feasibility of using Dw and SSDEs to produce size-specific iDRLs when using automated tube current modulation. Median SSDEs increased by 0.5 mGy per additional cm Dw in abdominal and upper abdominal CT and by 0.6 mGy per additional cm Dw in chest CT. The herein found equations of the 50th (figures 2–4) and the 275th SSDE percentile (abdominal: $y = 0.6858x - 8.4256$; chest: $y = 0.5646x - 8.1297$; upper abdominal CT: $y = 0.5131x - 6.0791$) can be implemented into automated CT dose monitoring software to automatically compare patient radiation exposure to the size-specific iDRLs (figures 2–4).

Variability between CT protocols of the same body region

Indication-based CT protocols in upper abdominal CT included pancreatic CT, liver CT, adrenal CT and renal CT with mean SSDE ranging from 8.2 ± 2.8 for renal CT to 15.8 ± 10.9 mGy for adrenal CT. Only two different CT protocols were used in abdominopelvic CT (CT angiography and routine abdominopelvic CT) and in chest CT (CT for pulmonary embolism, routine chest CT). The difference of radiation exposure between the different indication-based CT protocols was small in abdominal and chest CT, respectively (table 4).

Comparison to national diagnostic reference levels

German nDRLs (CTDIvol/DLP) are 10 mGy/350 mGy cm for chest CT, 15 mGy/700 mGy cm for abdominopelvic CT and 15 mGy/360 mGy cm for upper abdominal CT [16]. The mean weight of our study population was higher than the 70 ± 3 kg for which nDRLs are provided (chest CT: 75.2 ± 15.7 kg (range: 42–128 kg); upper abdominal CT: 77.3 ± 1.8 kg

Table 3. Number of patients per water-equivalent diameter bin with corresponding CTDIvol and SSDEs. These bins were used for calculation of size-specific institutional diagnostic reference levels.

Water-equivalent diameter (Dw)	Number of chest CTs	CTDIvol (mGy)	SSDE (mGy)	Number of abdominopelvic CTs	CTDIvol (mGy)	SSDE (mGy)	Number of upper abdominal CTs	
							CTDIvol (mGy)	SSDE (mGy)
21	10	2.3 ± 1.0	3.8 ± 1.7	—	—	—	—	—
22	19	2.5 ± 1.1	4.0 ± 1.8	13	3.9 ± 0.6	6.4 ± 0.9	—	—
23	23	2.6 ± 1.8	4.1 ± 2.8	19	4.8 ± 0.9	7.5 ± 1.4	5	5.5 ± 1.0
24	27	2.6 ± 1.4	3.9 ± 2.2	45	4.9 ± 0.7	7.4 ± 1.1	13	6.2 ± 1.5
25	46	3.0 ± 1.6	4.4 ± 2.4	63	5.3 ± 1.0	7.5 ± 1.5	17	6.0 ± 0.8
26	54	3.5 ± 2.0	4.8 ± 2.8	79	6.0 ± 1.1	8.3 ± 1.5	22	7.2 ± 1.7
27	67	4.0 ± 2.5	5.2 ± 3.4	83	6.7 ± 1.6	8.8 ± 2.1	16	7.4 ± 2.9
28	47	5.5 ± 2.9	6.9 ± 3.8	128	7.3 ± 1.7	9.2 ± 2.1	22	8.1 ± 2.2
29	40	5.2 ± 2.8	6.3 ± 3.4	120	8.0 ± 2.0	9.7 ± 2.3	38	7.4 ± 1.8
30	49	5.8 ± 3.4	6.8 ± 4.0	96	9.2 ± 2.6	10.7 ± 3.0	25	8.9 ± 2.6
31	27	6.5 ± 3.5	7.2 ± 3.9	92	9.9 ± 2.6	11.0 ± 2.9	25	9.8 ± 3.4
32	17	6.1 ± 4.0	6.5 ± 4.4	59	10.6 ± 2.3	11.3 ± 2.4	38	9.0 ± 1.6
33	10	8.2 ± 5.7	8.4 ± 5.9	49	12.4 ± 3.2	12.6 ± 3.3	13	10.3 ± 2.4
34	7	8.1 ± 4.8	8.0 ± 4.7	60	13.5 ± 3.7	13.4 ± 3.6	21	11.0 ± 2.8
35	—	—	—	20	15.7 ± 4.1	14.7 ± 3.8	8	12.0 ± 2.7
36	—	—	—	6	18.1 ± 3.8	16.3 ± 3.5	6	11.5 ± 1.5

— ≤ five patients for the bin and not included in the analysis; CT: computed tomography; SSDE: size-specific dose estimates. All values are given as mean ± standard deviation.

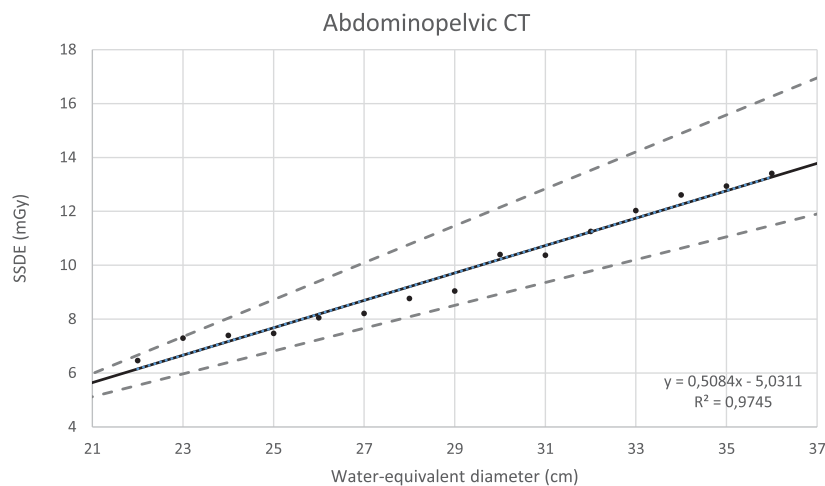


Figure 2. Institutional diagnostic reference levels for abdominopelvic CT examinations. There was a very strong correlation between the water-equivalent diameter and SSDE ($R^2 = 0.98$). The bold line represents the linear regression for which the equation and the coefficient of determination (R^2) are provided (lower right corner). The dashed lines are fitting results of the 75th (upper line) and 25th (lower line) percentile of each bin. The 50th or 75th percentile is commonly used for DRL calculation.

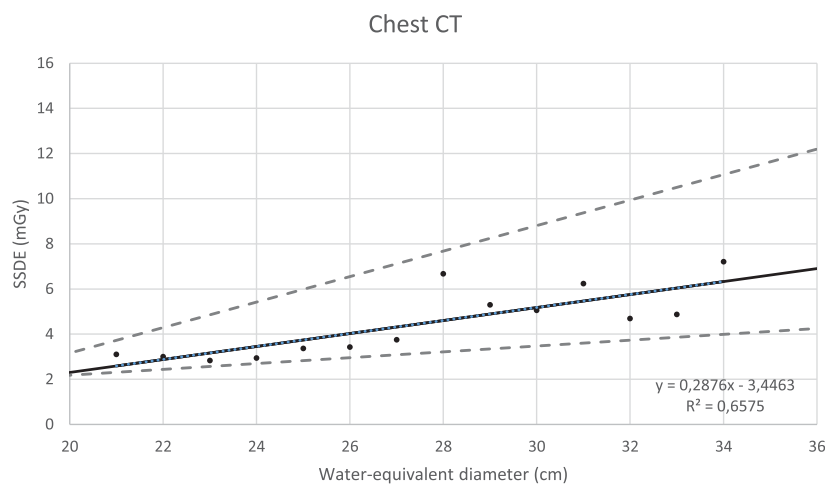


Figure 3. Institutional diagnostic reference levels for chest CT examinations. There was a strong correlation between the water-equivalent diameter and SSDE ($R^2 = 0.66$). The bold line represents the linear regression for which the equation and the coefficient of determination (R^2) are provided (lower right corner). The dashed lines are fitting results of the 75th (upper line) and 25th (lower line) percentile of each bin. The 50th or 75th percentile is commonly used for DRL calculation.

(44–145 kg); abdominopelvic CT: 74.4 ± 15.5 kg (42–128 kg). For the average-size patients in our study as measured by Dw (Dw of 29 cm), mean CTDIvol was lower than the nDRLs ($52.2 \pm 27.7\%$ in chest CT, $53.2 \pm 13.0\%$ in abdominopelvic CT and $40.9 \pm 9.7\%$ in upper abdominal CT). The 75% percentile CTDIvol for an average size patient in this study were

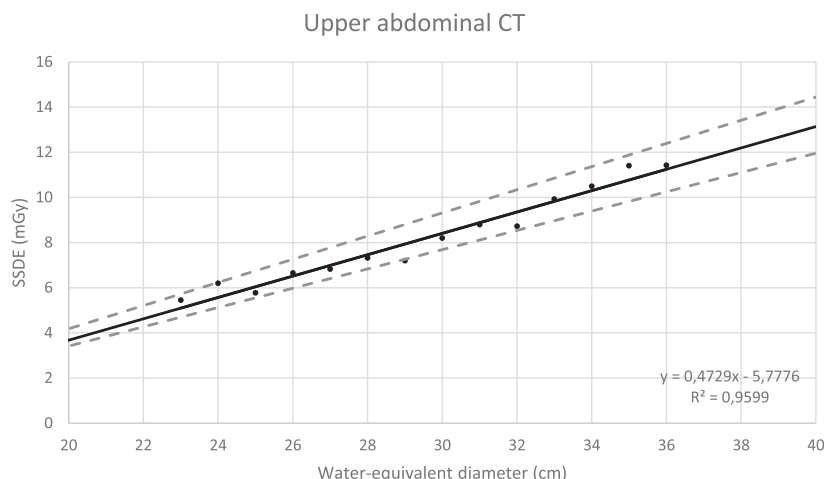


Figure 4. Institutional diagnostic reference levels for upper abdominal CT examinations. There was a very strong correlation between the water-equivalent diameter and SSDE ($R^2 = 0.96$). The bold line represents the linear regression for which the equation and the coefficient of determination (R^2) are provided (lower right corner). The dashed lines are fitting results of the 75th (upper line) and 25th (lower line) percentile of each bin. The 50th or 75th percentile is commonly used for DRL calculation.

Table 4. Variability in volumetric CT dose index (CTDIvol) and size-specific dose estimates (SSDEs) between CT protocols (with at least ten examinations) in upper abdominal, chest and abdominopelvic CT.

	Number of examinations (<i>n</i>)	CTDIvol (mGy)	SSDE (mGy)
<i>Upper abdominal CT</i>			
Routine upper abdominal CT	26	8.8 ± 4.0	9.8 ± 3.3
Renal CT	26	6.9 ± 3.2	8.2 ± 2.8
Liver CT	237	7.7 ± 3.7	8.5 ± 2.8
<i>Chest CT</i>			
Routine chest CT	423	4.6 ± 3.5	5.7 ± 3.7
Pulmonary embolism CT	47	4.8 ± 3–5	5.9 ± 3.8
<i>Abdominopelvic CT</i>			
CT angiography	96	8.2 ± 3.2	9.7 ± 2.7
Routine abdominopelvic CT	824	8.3 ± 3.5	9.8 ± 3.1

CT: computed tomography; CTDIvol: volumetric computed tomography dose index; SSDE: size-specific dose estimates. All values are given as mean ± standard deviation.

73.6% of the nDRL in chest CT, 59.5% in abdominopelvic CT and 42.8% in upper abdominal CT. In 367/1690 (21.7%) of the examinations the iDRLs were exceeded while only in 133/1690 (7.9%) the nDRLs were exceeded ($p < 0.001$).

Discussion

In this study, we implemented and evaluated size-specific institutional DRLs based on SSDEs and patients' Dw that can be used to more accurately and more reliably evaluate CT radiation exposure without the need for additional patient characteristics such as body mass index or weight. We demonstrated that size-specific institutional DRLs allow for a more comprehensive analysis of CT dose data as more outliers can be detected. Of note, institutional CT dose exposure of normal weight patients was lower than national DRLs and SSDEs were larger than scanner-indicated CTDIvol in chest and abdominopelvic CT.

In this study, feasibility of automated assessment of Dw and calculation of SSDE was demonstrated which is in accordance with previous studies [12, 13]. Although weight or BMI may be useful in the calculation of SSDEs [17, 18], automated assessment of Dw seems easier, more reliable and less time consuming. Additionally, we used all slices of each CT scan volume for SSDE calculation, which is more accurate than the previously proposed method of taking the midslice of the scan volume or diameter measurements from positioning radiograph images [6, 7, 13]. We found that automated SSDE calculation based on all slices of the scan volume can be performed in real time in a clinical setting using third-party software; however, the effort is notable and implementation of Dw and SSDEs into the CT scanner software is desirable.

Our automated SSDE assessment was used to implement and evaluate institutional size-specific DRLs. National DRLs are usually provided to enable large-scale analysis of dose data to detect systematic dose application errors but are not suitable for the analysis of single CT examinations without additional patient information. Automated assessment of Dw in combination with DRLs that account for patient size may help to simplify and refine the analysis of CT dose data without the requirement for other size metrics such as height, weight or BMI [19].

We found a strong correlation between Dw and SSDEs in chest, upper abdominal and abdominopelvic CT. This has to be expected as automated tube current modulation and automated tube potential selection were used in all scans. The tube current time product (and thus the CTDIvol) was adapted to the patient attenuation and therefore to the patients' Dw [6, 7]. In contrast to our results, initial studies found no correlation between patient size and SSDE [20]. However, positioning radiograph diameters without attenuation information were used. Two recent studies evaluated size-specific DRLs based on SSDEs and reported a correlation between patient size and SSDEs [10, 22]. Strauss *et al* [10] provided DRL ranges for pediatric chest CT examinations. However, only the lateral diameter from positioning radiograph images and effective diameter were used for size correction, which may lead to considerable errors, especially in chest CT [7, 21]. Kanal *et al* [22] investigated over 1.3 million CT examinations using the American College of Radiology Dose Index Registry (ACR-DIR) and provided size-specific DRLs for ten CT protocols. The DRLs were provided for water-equivalent diameter ranges. However, only positioning radiograph diameter measurements were used, which are regarded as the least accurate method for SSDE calculation [7]. Furthermore, it remains unclear how attenuation measurements were obtained to calculate the water-equivalent diameter [22, 23]. As different measurement techniques may lead to considerable deviations [21] an automated method using all axial CT slices to calculate Dw seems beneficial, especially when DRLs are used to tailor and optimize institutional CT protocols.

More specific DRLs have been introduced in some countries [24, 25], however the updated 2016 German DRLs are still based on body regions [16]. Using body regions for DRL analysis limits the complexity, as only a small number of DRLs are considered.

However, more specific DRLs, e.g. based on CT protocols and patient size, can potentially help to further improve CT dose analysis, particularly in the setting of automated CT dose monitoring. This is reflected in the larger number of dose outliers that was detected with the size-specific DRLs compared with the national DRLs in our study. Although not performed in our study, automated analysis of prior CT examinations using automated CT dose monitoring software to provide size-specific institutional DRLs seems to be feasible and may help to improve CT dose analysis.

SSDEs were larger than CTDI_{vol} in our collective. This is the result of the average Dw of 29 cm, which is smaller than the 32 cm phantom used for CTDI_{vol} calculation. This demonstrates the limitation of using a fixed 32 cm water phantom for CT dose calculation. Mean CTDI_{vol} was significantly smaller than the national DRLs although the mean patient weight was higher in our collective compared with the standard weight for which the nDRLs are provided. Thus, CTDI_{vol} of an average size patient (as determined by Dw) was also smaller than the nDRLs. Although not further investigated in this study, this may be the result of the ongoing radiation dose optimization process in our institution.

Our study has limitations. First, although a large number of patients were included in the study, only a relatively small number of patients per body region and centimeter Dw was available. Results may not be applicable for very small and very large patients, as the limited number did not allow for reliable calculation of iDRLs in these patients. Additionally, scanner-specific limitations such as the maximal tube current time product may influence the SSDEs in these patients.

Second, CT scanners from one vendor were used in this study. Automated tube current modulation differs between vendors and may even differ across scanners of the same vendor. As only one automated exposure device and one strength level was used in our study, the results may not be applicable to other automated exposure devices. Third, we do not use an additional full field-of-view reconstruction in clinical routine as suggested by the AAPM [6, 7]. Therefore, images were truncated in some patients. We used an automated approach that detects air-filled pixels adjacent to the body surface. Patients with a truncated body circumference were excluded from the study. Although image truncation is a common phenomenon, especially in chest CT, where the field-of-view is usually adjusted to the lung parenchyma, truncation may more frequently appear in large patients, which may have influenced our results. Although, recently, conversion factors for truncated images have been published [26], performing an additional full field-of-view reconstruction is preferable.

Conclusion

In conclusion, we produced size-specific institutional DRLs based on SSDEs and patient water-equivalent diameter. The size-specific institutional DRLs can be used to more accurately analyze CT radiation exposure compared with the national DRLs that are provided for a standard size patient. Thus, size-specific DRLs may help to further optimize the radiation dose of CT protocols.

References

- [1] MacGregor K, Li I, Dowdell T and Gray B G 2015 Identifying institutional diagnostic reference levels for CT with radiation dose index monitoring software *Radiology* **276** 507–17
- [2] Ghetti C, Ortenzia O, Palleri F and Sireus M 2016 Definition of local diagnostic reference levels in a radiology department using a dose tracking software *Radiat. Prot. Dosimetry* **175** 38–45

- [3] Boos J *et al* 2016 Cloud-based CT dose monitoring using the DICOM-structured report: fully automated analysis in regard to national diagnostic reference levels *ROFO Fortschr Geb Rontgenstr Nuklearmed.* **188** 288–94
- [4] European Commission. Diagnostic Reference Levels in Thirty—six European Countries. 2015 (<https://ec.europa.eu/energy/sites/ener/files/documents/RP180%20part2.pdf>). Accessed August 15, 2015
- [5] Boos J, Meineke A, Bethge O T, Antoch G and Kröpil P 2016 Dose monitoring in radiology departments: status quo and future perspectives *ROFO Fortschr Geb Rontgenstr Nuklearmed.* **188** 443–50
- [6] The Report of AAPM Taks Group 204. Size-Specific Dose Estimates (SSDE) in Pediatric and Adult Body CT Examinations. (https://aapm.org/pubs/reports/RPT_204.pdf). Accessed August 30, 2015
- [7] The Report of AAPM Task Group 220. Use of Water Equivalent Diameter for Calculating Patient Size and Size-Specific Dose Estimates (SSDE) in CT. (https://aapm.org/pubs/reports/RPT_220.pdf). Accessed August 15, 2015
- [8] Imai R, Miyazaki O, Horiuchi T, Kurosawa H and Nosaka S 2015 Local diagnostic reference level based on size-specific dose estimates: assessment of pediatric abdominal/pelvic computed tomography at a Japanese national children’s hospital *Pediatr. Radiol.* **45** 345–53
- [9] Salat D. Dynamic diagnostic reference level (DDRL). 2014; (http://inis.iaea.org/Search/search.aspx?orig_q=RN:46091438). Accessed December 19, 2016
- [10] Strauss K J *et al* 2017 Pediatric chest CT diagnostic reference ranges: development and application *Radiology* **161**530
- [11] Taylor S, Van Muylem A, Howarth N, Gevenois P A and Tack D 2017 CT dose survey in adults: what sample size for what precision? *Eur. Radiol.* **27** 365–73
- [12] Anam C, Haryanto F, Widita R, Arif I and Dougherty G 2016 Automated calculation of water-equivalent diameter (DW) based on AAPM task group 220 *J. Appl. Clin. Med. Phys.* **17** 6171
- [13] Leng S, Shiung M, Duan X, Yu L, Zhang Y and McCollough C H 2015 Size-specific dose estimates for chest, abdominal, and pelvic CT: effect of inpatient variability in water-equivalent diameter *Radiology* **276** 184–90
- [14] Boos J *et al* 2017 Accuracy of size-specific dose estimate calculation from center slice in computed tomography *Radiat. Prot. Dosimetry* **178** 1–12
- [15] The 2007 Recommendations of the International Commission on Radiological Protection. ICRP publication 103. *Ann ICRP.* 2007;37(2–4):1–332
- [16] German Federal Office for Radiation Protection. Publication of updated diagnostic reference levels for diagnostic and interventional X-ray examinations. Published on 15 July 2016. (<https://bfs.de/>). Accessed November 20, 2016
- [17] Khawaja R D A *et al* 2015 Simplifying size-specific radiation dose estimates in pediatric CT *AJR Am. J. Roentgenol.* **204** 167–76
- [18] Boos J *et al* 2016 Does body mass index outperform body weight as a surrogate parameter in the calculation of size-specific dose estimates in adult body CT? *Br. J. Radiol.* **89** 20150734
- [19] Park Y J *et al* 2012 Automatic tube potential selection with tube current modulation (APSCM) in coronary CT angiography: comparison of image quality and radiation dose with conventional body mass index-based protocol *J. Cardiovasc. Comput. Tomogr.* **6** 184–90
- [20] Christner J A, Braun N N, Jacobsen M C, Carter R E, Kofler J M and McCollough C H 2012 Size-specific dose estimates for adult patients at CT of the torso *Radiology* **265** 841–7
- [21] Gabusi M, Riccardi L, Aliberti C, Vio S and Pausco M 2016 Radiation dose in chest CT: assessment of size-specific dose estimates based on water-equivalent correction *Phys. Medica PM Int. J. Devoted Appl. Phys. Med. Biol. Off J. Ital. Assoc. Biomed. Phys. AIFB* **32** 393–7
- [22] Kanal K M, Butler P F, Sengupta D, Bhargavan-Chatfield M, Coombs L P and Morin R L 2017 US diagnostic reference levels and achievable doses for 10 adult CT examinations *Radiology* **284** 120–33
- [23] Christianson O, Li X, Frush D and Samei E 2012 Automated size-specific CT dose monitoring program: assessing variability in CT dose *Med. Phys.* **39** 7131–9
- [24] Lajunen A 2015 Indication-based diagnostic reference levels for adult CT-examinations in Finland *Radiat. Prot. Dosimetry* **165** 95–7
- [25] Järvinen H *et al* 2015 Indication-based national diagnostic reference levels for paediatric CT: a new approach with proposed values *Radiat. Prot. Dosimetry* **165** 86–90

- [26] Anam C, Haryanto F, Widita R, Arif I and Dougherty G 2016 The size-specific dose estimate (SSDE) for truncated computed tomography images *Radiat. Prot. Dosimetry* **175** 313–20